HIG-69-8

EDDIES IN HAWAIIAN WATERS

By

WILLIAM CHARLES PATZERT

APRIL 1969

Prepared for:

OFFICE OF NAVAL RESEARCH
UNDER CONTRACT NO. NONR-3748(00)

HAWAII INSTITUTE OF GEOPHYSICS
UNIVERSITY OF HAWAII

HIG-69-8

EDDIES IN HAWAIIAN WATERS

By

William Charles Patzert

April 1969

Prepared for

Office of Naval Research
under Contract No. Nonr-3748(06)

Approved by Director

George P. Woollard

Date: 14 April 1969

TABLE OF CONTENTS

Table of Contents iii

Abstract v

INTRODUCTION 1

ATMOSPHERIC AND OCEANIC CLIMATE OF THE HAWAIIAN ISLANDS 3

- Topography of the Hawaiian Islands 3
- Large-Scale Atmospheric Climate 3
- Large-Scale Oceanic Flow 5

HYDROGRAPHY OF THE EDDIES 7

- Location of the Eddies in Time and Space . . . 7
- Shape and Size of the Eddies 7
- Temperature Structure 8
- Salinity Structure 11
- Velocity Field of the Eddies 11
  - Dynamic topography 11
  - Geostrophic volume transports 12
  - Parachute drogue observations 13
  - Other current observations 14
  - Comparison of observed currents with geostrophic calculations 15
- Upwelling and Biological Effects 17
- Tilt of the Eddy Axes 18
- Eddy Lifetime, Movement, and Decay 18
  - Formation 18
  - Movement and decay 19
  - Lifetime 21

THEORETICAL ANALYSIS AND DISCUSSION 23
Dimensional Analysis of the Eddies 23
Geostrophic Eddy Model 27
Energy Model for the Eddies 29
Locally Wind-Driven Eddies 32
Eddies Generated Due to a Flow around Hawaii . 34
Translation of Eddies Due to Variation in Coriolis Parameter 41
Effect of Centrifugal Forces in Eddy Motion . 42
SUMMARY AND CONCLUSIONS 45
ACKNOWLEDGMENTS 48
LITERATURE CITED 49
APPENDIX.
Table 1
Explanation of the Parameters Listed in Table 1
Figures 1 through 71

ABSTRACT

Oceanographic observations near the Hawaiian Islands demonstrate that ocean circulation is extremely variable and is dominated by eddies with diameters ranging from 50 to 150 kilometers. The data from 20 cruises that describe these eddies have been analyzed. Most of the eddies are cyclonic, and have been observed during all seasons. Observations show that the flow in them is nearly geostrophic and volume transports can be as large as 8 million m^3/sec. Although surface flow around them can be in excess of 100 cm/sec, the eddies are relatively shallow in depth and most of the horizontal flow is concentrated in the upper 150 m, above the 20°C isothermal surface. Near the center of the cyclonic eddies, doming of isothermal layers and upwelling take place. The energies of the eddies have been calculated, using a simplified geostrophic model, and the total of individual eddy energies is found to vary from 1×10^{22} ergs for a weak eddy to 5×10^{22} ergs for an intense eddy.

Calculations show that the eddies are not generated by the large-scale flow through the Hawaiian Islands—in the sense of a Kármán vortex stream behind an obstacle. Energy calculations indicate rather that the eddies are driven by strong, local winds blowing through the restricted passage between the islands of Maui and Hawaii. The calculations show that the eddies have a formation time of between 2 and 6 weeks, a value consistent with observations.

INTRODUCTION

The ocean circulation near the Hawaiian Islands is known to be extremely variable and to be dominated by large well-developed eddies. The existence of these eddies was first noted in 1949 by scientists at the Bureau of Commercial Fisheries (BCF) in Honolulu, and reported by McGary (1955) and by Seckel (1955). Subsequently, scientists from the Naval Electronics Laboratory (NEL) in San Diego investigated cyclonic and anticyclonic eddies in the lee of the island of Hawaii during August 1964 and July 1966 (Smith, 1967). More recently, scientists at the University of Hawaii, aboard the R/V TERITU, surveyed some well-defined eddies west of the Hawaiian Islands (Wyrtki et al., 1967).

During the past decade, studies of motions in the size range encountered in the Hawaiian eddies (radius 25-100 km) have been conducted by oceanographers. Particularly pertinent are the studies by Reid et al. (1963) off California, by Austin (1955) in the Gulf of Mexico, by Fuglister (1964) in the Gulf Stream, and by Ichiye (1956) in the Kuroshio Current. These investigators variously suggested a number of generating mechanisms for the eddies, such as meteorological disturbances, the development of an unstable shearing layer into a series of vortices, and flow past a barrier. In addition, as the techniques and observations became more refined, more synoptic features were reported with the accuracy sufficient to formulate plausible hypotheses concerning the role the eddies play in ocean circulation. It is known that energy transfer between the mean motion and its perturbations plays an important role in maintaining and changing ocean circulation. Recently, Webster (1961) and Ichiye (1965) have both suggested that in some areas energy is transferred from fluctuations or eddies to the mean current. This concept is contrary however to statistical theories on turbulence, which predict that energy is transferred from larger to smaller eddies. Before the role of eddies of the scale observed in the Hawaiian waters can be clarified, it will be necessary to understand their nature as well as their behavior.

Such clarification would be useful to two groups operating in Hawaiian waters. The U. S. Navy, in conducting training operations in the lee of the islands, has found that the frequent occurrence and consequent effect of these eddies on the density structure makes long-term prediction of underwater sound-propagation

parameters unsatisfactory (Smith, 1967). Second, scientists at the BCF in Honolulu have suggested that the eddies affect the biological environment and hence local fishing (Barkley in Manar, 1967). Both of these groups have made studies of the eddies, and much of their data will be discussed later in my report.

The objective of this study can be summarized as follows: to collect, compile, and analyze the available data on Hawaiian eddies, presenting a description of them and suggesting some possible generating mechanisms.

The analysis (which begins on page 3) is divided into four sections:

(1) The initial discussion includes the general flow field of the ocean and atmosphere in the Hawaiian area. The effect of the Hawaiian Archipelago on the existing flow of both the ocean and atmosphere is basic to an analysis of the eddies.

(2) The second section presents the existing data concerning the eddies. This synthesis of the available information provides a definite picture of the behavior of Hawaiian eddies.

(3) In the third section, the analytical relationships that govern fluid motion are applied to the observations and discussed. Included is a model of eddy flow as well as calculations of the energies associated with the eddies. These calculations should provide insight into the mechanisms and forces that govern eddy motion in Hawaiian waters.

(4) The final section summarizes the discussions and analyses of the preceding three sections.

ATMOSPHERIC AND OCEANIC CLIMATE OF THE HAWAIIAN ISLANDS

Before eddy formation in Hawaiian waters is discussed, a description of the effect of the island chain's topography on the atmospheric and oceanic circulation is needed.

Topography of the Hawaiian Islands

The profile of the Hawaiian Islands below sea level (Fig. 1) resembles a barrier having two deep openings—the Alenuihaha Channel between Hawaii and Maui and the Kauai Channel between Oahu and Kauai, both of which are deeper than 1500 m—and two much shallower and much narrower openings—the Kaiwi Channel between Oahu and Molokai (sill depth 614 m) and the Pailolo Channel between Molokai and Maui (sill depth 80 m).

Above sea level (Fig. 1), the Hawaiian Islands are a series of vertical obstacles lying in a northwest-southeast direction. The island of Hawaii presents to the trade winds a solid barrier of approximately 120 kilometers. It should be noted that the Alenuihaha Channel is bounded on both sides by mountains which are higher than those bounding both sides of the Kauai Channel.

Large-Scale Atmospheric Climate

According to the atlas of Pilot Charts (U. S. Navy Hydrographic Office, 1945), winds from the northeast, east, and southeast account for 86% of all ships' observations during the year (Fig. 2). These are the trade winds usually blowing through the Hawaiian Archipelago. When averaged on a monthly basis, a well-defined yearly periodicity is evident, the maximum occurring during July (96% of ships' observations), the minimum during December to March (77% of observations). Although the average wind velocity is between 10 and 20 knots, it is not unusual to have velocities of over 20 knots for more than a week.

The maximum thickness of the atmospheric layer in which the trade winds are dominant is of the order of 1800 m (Ramage, 1960). Figure 1 shows that the island of Hawaii is a solid barrier to trade-wind flow and that high mountains on both sides of the Alenuihaha Channel are over 1000 m above the trade-wind layer. The islands

of Kauai, Oahu, Molokai, and Maui may also act as wind barriers, but they are below the maximum height of trade winds.

The effect exerted by these topographic barriers on the atmospheric circulation patterns is demonstrated in a preliminary study (unpublished) of resultant winds in the area of the Hawaiian Islands conducted by the Weather Bureau in Honolulu. Figure 3 is a plot of the mean resultant winds taken from ships' observations over the last fifteen years. The values have been plotted for 10-minute (approximately 18.5 km) squares of latitude and longitude. The resultant wind vectors have been streamlined by the author. An inspection of this chart shows that, even with the smoothing imposed by averaging over a long period, the islands have a marked effect on atmospheric circulation. In the lee of each island, a wind minimum exists. Winds in the channels increase in strength. Figure 3 also shows that this effect is stronger in the Alenuihaha Channel than in the other channels, many of the resultant wind vectors indicating velocities of 20 to 25 knots between Maui and Hawaii. It is highly probable that this increase in wind velocities in the Alenuihaha Channel is due to channeling of the trade-wind flow in the channel by the high mountains on both sides. This situation is analogous to an increase in flow due to the "Venturi effect" of flow through a constricted opening. The topography may also deflect or impose a shear upon the incident trade winds. This can also be clearly seen in the lee of the island of Hawaii. Cyclonic eddies develop to the north; anticyclonic eddies to the south. Atmospheric eddies are also thought to develop in the lee of Oahu and Kauai (Saul Price, personal correspondence); but if they do, they are probably less intense and far more infrequent than the eddies behind Hawaii. The fact that Oahu and Kauai are not as large or as high as Hawaii, as well as the infrequency of occurrence, may possibly explain why no atmospheric eddies are evident in the lee of Oahu and Kauai (Fig. 3).

Since the discussion will center on the ocean eddies in the lee of Hawaii, the atmospheric eddies of the west coast of this island will play an important role in the analysis that follows. Wind observations taken during four R/V TERITU cruises (Figs. 4, 5, 6, and 7) also show the existence of atmospheric eddies in the lee of Hawaii. These atmospheric eddies appear to be permanent features during trade-wind conditions.

Another argument for the existence of atmospheric eddies is the rainfall regime of the Kona (west) coast of Hawaii. Since the Hawaiian Islands lie in the path

of the prevailing northeast trade winds, the rainfall pattern throughout most of the islands shows considerably larger amounts of precipitation in exposed windward areas than in protected leeward areas. Precipitation along the Kona (leeward) coast, however, is atypical of the general Hawaiian pattern in three major respects: (1) Because of the blocking effect of the mountain masses (notably Mauna Loa) on the island of Hawaii, trade-wind showers are never present. (2) Compared to other lee areas in the chain, many of which receive less than 50 cm of rain annually, Kona is relatively wet (150 cm/yr). (3) More rainfall occurs during the summer months than during the winter months, coinciding with maximum trade-wind conditions. The minimum monthly rainfall coincides with the weak trade-wind conditions of the winter months (Taliaferro, 1958 and 1959). This can possibly be explained by noting that the area of maximum rainfall along the Kona coast (Anonymous, 1955) coincides with the convergence zone between the cyclonic and anticyclonic eddies to the west of the island (Fig. 3). The Kona coast rainfall regime is probably the consequence of these quasi-permanent atmospheric eddies offshore.

The general pattern of atmospheric circulation in the region of the Hawaiian Islands is as follows: (1) Trade winds are incident to the archipelago. (2) There is a yearly periodicity in the trade winds with maximum winds during the summer months. (3) The islands act as barriers to trade-wind flow, causing wind minima in the lee of the islands, shear-induced eddies in the lee of Hawaii, and deflection of the winds in the lee of the other islands. (4) Winds in the channels increase in strength due to the "Venturi effect" of flow through a constricted opening.

Large-Scale Oceanic Flow

Until fairly recently, the mean ocean flow through the Hawaiian Islands has been described as approximately 25 cm/sec to the west (U. S. Navy Hydrographic Office, 1947). The North Equatorial Current was thought to be the cause of this flow. In recent investigations, however, Seckel (1962) and Seckel *et al*. (1967) conclude that circulation patterns in the Hawaiian region cannot be generalized into the concept of a steady North Equatorial Current. Seckel further states that the mean geostrophic flow (if it does exist) is small, approximately 10 to 20 cm/sec. Recent coastal current measurements off the Hawaiian Islands (Wyrtki *et al*., 1969) show a net flow to the west in some areas; but the mean velocity is less than 20 cm/sec in most cases. This new evidence suggests that the North Equatorial Current is

not the controlling factor in circulation through the islands.

Figure 3 shows 15-knot winds as a long-term mean in the Hawaiian region. This figure also shows that the winds increase in the channels between the islands. It is possible that the local wind conditions generate a shallow Ekman drift with velocities as large as 50 cm/sec. A strong, locally generated Ekman drift in the channels should be considered in any discussion of eddy formation in Hawaiian waters.

HYDROGRAPHY OF THE EDDIES

The first detailed series of hydrographic stations in the region of the Hawaiian Islands was made on cruises of the R/V HUGH M. SMITH, beginning in 1949 (McGary, 1955). Since that time many such cruises have been made by various organizations, and the data available from 20 cruises that document the hydrographic conditions of the eddies have been studied and analyzed. These data have been summarized in Table 1 (See Appendix). Features concerning the temperature, salinity, and dynamic structure are listed. In the discussion that follows, the various characteristics of Hawaiian eddies will be illustrated by the use of Table 1 and selected figures.

Location of the Eddies in Time and Space

Eddies have been observed at all times of the year (See Table 1). The only failure to locate eddies in the lee of the islands was during Cruise UH-1 (Fig. 8). The dynamic topography 0/500 db shows the existence of an elongated trough situated south of Oahu and stretching east to Hawaii. During the cruise, weak southerly winds prevailed. R. A. Barkley (personal correspondence) has noted the lack of eddy development during slack wind conditions. It seems reasonable to speculate that eddies will always be developed when trade winds are strong.

Most of the eddies studied were in the region to the west of the island of Hawaii. Figure 10 locates the centers of the various eddies listed in Table 1. Eddies have been observed as near to shore as 40 km (Fig. 36) and as far away as 350 km from the islands (Fig. 54). The discussion will center on the situation in the lee of the island of Hawaii. The eddy conditions in this area are well documented, and hydrographic surveys of the Hawaiian region show that the eddies appear more regularly in the lee of this island than in other areas (Fig. 10). Eddies also appear in the lee of Oahu and Kauai (Fig. 59), and the generating mechanism of these eddies is thought to be similar to that of the eddies off Hawaii.

Shape and Size of the Eddies

The eddies range in shape from almost circular (Fig. 52) to the more common elliptical configuration

(Fig. 29). In the analysis and description that follows, an eddy radius ℓ will be used. This eddy radius was calculated on the basis that the area of an ellipse ($A = \pi ab$) equals the area of a circle ($A = \pi \ell^2$). Table 1 lists the values of the half major (a) and half minor (b) axis for each eddy. The eddy radius used in the following discussion is $\sqrt{ab} = \ell$. The values of a and b were measured from plots of either the dynamic topography or the depth of the 20°C isotherm. The procedure of defining and measuring a and b is outlined on pages 27 and 28. Figure 55 shows four observed distributions of dynamic topography and the radius listed in Table 1.

The eccentricity ($e = \frac{\sqrt{a^2 - b^2}}{a}$) of the elliptical eddy pattern ranges from zero to .79. The mean value of the eccentricity is .55. This means that the ratio of the major to the minor axis varies from 1.0 to 1.7, with a mean value of 1.2. The eccentricity of an eddy near the islands is greater than that of an eddy farther away. This is similar to the situation Fuglister (1967) described for a Gulf Stream eddy. In the same manner as Hawaiian eddies, the Gulf Stream eddy exhibited an elliptical shape in its early stages.

The eddy radius ℓ varies from 28 km for a weak eddy near Hawaii to 80 km for a well-developed eddy farther offshore. The mean value of the eddy radius is 59 km. As the eddies age and move away from the islands, they increase in area. Figure 11 illustrates the increase in radius ℓ as the eddies move away from the island of Hawaii.

Temperature Structure

The most characteristic feature of the eddies is the temperature structure. The temperature distribution within the eddies has been measured using a variety of methods. NEL conducted two surveys with a continuously recording thermistor chain. BCF and UH scientists have measured the thermal structure using bathythermographs (BT), reversing thermometers, and continuously recording depth, temperature, and salinity recorders (DTS).

The thermal structure can be related to the flow around the eddies. The cyclonic and anticyclonic rotation appear as a "dome" and a "depression" in the thermal structure. In cyclonic rotation, the heavier water accumulates around the axis of rotation while the lighter is forced to the outside (Defant, 1961). In anticyclonic rotation, the rotation gives rise to an accumulation of the lighter water around the rotational axis. Figure 14

illustrates the "dome" and "depression" structure of an eddy pair as is often observed in the lee of Hawaii.

The magnitude of the thermal doming of the cyclonic eddies is approximately equal to the depression of the anticyclonic eddies in a shallow surface layer (depth 100 m). In depths greater than 100 m, the anticyclonic depression is less pronounced than the cyclonic dome and has a broader horizontal extent. The temperature data collected during Cruise UH-2 illustrates this feature. The distribution of mixed-layer depth (mean depth approximately 50 m in May) shows that the cyclonic dome was situated to the northwest of Hawaii, and the anticyclonic depression to the southwest (Fig. 15). In the 20°C isotherm topography (Fig. 16), the cyclonic dome is more intense and smaller in area than is the anticyclonic depression. The mean depth of the 20°C isotherm in Hawaiian waters is 170 m. The 20°C isotherm is 70 m shallower than the mean level at the center of the cyclonic eddy, whereas the center of the anticyclonic eddy is only 30 m below the mean level. The anticyclonic eddy has a larger area than the cyclonic eddy. In the 15°C isotherm topography (Fig. 17), the cyclonic dome is still 50 m above the surrounding level of the 15°C isotherm, but the anticyclonic depression can no longer be seen. The depth of the 10°C isotherm (Fig. 18) still defines the cyclonic eddy (310 - 340 m), but it gives no indication of the existence of the anticyclonic eddy. These data are typical of the pattern and structure of eddies observed during other cruises, and represent the normal situation of eddy-pair formation as observed in the lee of Hawaii.

The small-scale vertical variation in the temperature structure of the eddies has been discussed by Smith (1967). Using NEL thermistor chain data, he found that most vertical variations in the temperature structure are 7 to 10 m in amplitude, with wavelengths of 1 to 2 kilometers. These variations are masked in an analysis based on isolated hydrostations, but they are small compared to the size of the eddies and to the magnitude of the observed large-scale features.

Table 1 lists the observed depths of the 20°, 15°, and 10°C isotherms at the center and peripheries of the eddies. The peripheries of the eddies are defined as the distances a and b discussed earlier. Also listed, for each of the isotherms, is the difference between the depths at the center and at the periphery. These are designated by $\Delta 20°$, $\Delta 15°$, and $\Delta 10°$. The average value of each of these parameters has been calculated for the cyclonic and anticyclonic eddies and is listed in the following table.

Table 2. Average differences between the depths at the center and on the periphery of all eddies observed for the 20°, 15°, and 10°C isotherms and the mean depth of these isotherms in Hawaiian waters

	Δ20°	Δ15°	Δ10°
Cyclonic	54 m	38 m	27 m
Anticyclonic	24 m	11 m	10 m
Mean depth of the isotherm	170 m	240 m	340 m

The cyclonic eddies influence the thermal structure much more than do the anticyclonic eddies, and they penetrate to greater depths. The anticyclonic eddies seem to be confined to the upper 200 m, since their effect on the temperature structure at 240 m is of the same order as the observed random vertical variations of the temperature structure (Smith, 1967). It should be noted that, for the cyclonic eddies, the magnitude of the 20°C isotherm dome is twice that of the 10°C isotherm. Figures 19 and 20 illustrate the doming of the temperature structure in the cyclonic eddies. The lower limit of doming is from 300 to 400 m. This would suggest that the flow around the cyclonic eddies is restricted to approximately 300 m depth.

The strong doming of the cyclonic eddies indicates that the upwelling associated with the surface divergence must be considerable. Figure 22 illustrates this upwelling effect. The surface divergence is of such intensity that the mixed layer has been completely removed at the center of the eddy. The heavier, cooler water that rises at the center of the cyclonic eddies can be observed at the sea surface (Figs. 23, 24, and 25). The distribution of surface temperature for Cruise UH-3 (Fig. 24) shows the most extreme case observed for an intense cyclonic eddy located near Hawaii. There is a 2°C change in the surface temperature from the center to the periphery of the eddy. The other two figures show more usual situations. The presence of a cyclonic eddy near the island of Hawaii is indicated by a change of surface temperature of 1°C or more. The change in surface temperature across each of the eddies is listed in Table 1.

Salinity Structure

The vertical distribution of salinity in Hawaiian waters is characterized by an increase of salinity to a salinity maximum of 35.1‰ at approximately 150 meters. Figure 27 shows an extreme case where the salinity maximum has risen to the surface near the center of a cyclonic eddy. This indicates an upwelling of the salinity structure of 150 m, completely removing the water of lower salinity in the mixed layer. The salinity at the sea surface was 0.6‰ greater than that of surrounding surface waters due to the strong vertical movement in the center of this cyclonic eddy. Figures 26 and 28 also document the areas of high surface salinity that indicate the presence of cyclonic eddies in the lee of Hawaii. Table 1 lists the change in surface salinity across the eddies observed.

Velocity Field of the Eddies

A variety of methods has been used to measure the surface flow around the eddies. The methods include observations of the paths of parachute drogues, geomagnetic electrokinetograph (GEK) fixes, moored current meters, and geostrophic calculations based on observed dynamic topographies.

Dynamic topography. For the observed mass distribution in the region of the eddies, the dynamic topographies have been calculated and plotted for 14 cruises (Refer to Table 1). The observed range of the dynamic height difference between the center and periphery of an eddy is from 30 dyn cm for a well-developed eddy to 10 dyn cm for a weak eddy. Figure 29 shows an intense cyclonic eddy with a dynamic height difference in excess of 30 dyn cm. The dynamic topography 200/500 db (Fig. 30) still indicates eddy motion, but the dynamic height difference is only 6 dyn cm at this depth. The main flow is contained in the shallow upper layer. Figure 31 illustrates a weak cyclonic and anticyclonic eddy pair with a dynamic height difference of less than 10 dyn cm. The dynamic topography 200/500 db gives no indication of eddy structure (Fig. 32).

Table 1 lists the differences in dynamic height at the center and on the periphery for the various eddies. In the early reports of the Bureau of Commercial Fisheries, the dynamic topographies were calculated relative to 1000 decibars. The University of Hawaii calculations are referenced to 500 decibars. A comparison of the differences in dynamic heights across the eddies when referenced to 1000 db with dynamic heights referenced to

500 db shows virtually no difference and demonstrates that the eddies are shallow features. A comparison of average differences between dynamic heights at the center and on the periphery of all the eddies observed is presented in Table 3.

Table 3. Average differences between the dynamic heights at the center and on the periphery of all eddies observed

University of Hawaii Cruises

Type and (number) of eddies averaged	Average dynamic height difference 0/500 db	200/500 db
Cyclonic (8)	16.0 dyn cm	3.9 dyn cm
Anticyclonic (3)	8.5 dyn cm	2.5 dyn cm

Bureau of Commercial Fisheries Cruises

Type and (number) of eddies averaged	Average dynamic height difference 0/1000 db	200/1000 db
Cyclonic (7)	15.1 dyn cm	4.1 dyn cm
Anticyclonic (2)	9.5 dyn cm	1.5 dyn cm

Since referencing the dynamic calculations to 1000 db and 500 db gives virtually the same results, there is no restriction to using 500 db as the reference level in the eddies. The dynamic calculations show that approximately 75% of the observed dynamic height difference is concentrated in the upper 200 m. This confirms the conclusions based on the temperature and salinity structure that the eddies are shallow and confined to the upper 300 m or less.

Geostrophic volume transports. Wyrtki et al. (1967) calculated the geostrophic volume transports of various eddies during the UH cruises; the results are listed in Table 1 for the respective eddies. The transport varied from 8.0 million m^3/sec for an intense cyclonic eddy surveyed during UH-3 (Fig. 29) to 3.0 million m^3/sec for a weak cyclonic eddy surveyed during UH-12 (Fig. 31).

Parachute drogue observations. During four cruises (CHARLES H. GILBERT 64, 68 I, 68 II, and UH-17) parachute drogues were released in eddies and their trajectories plotted. Figures 49, 40, 41, and 46 show, respectively, the paths of these drogues plotted together with the depth of the 20°C isotherm during the period of drogue observations. The 20°C isotherm was chosen because its topography closely resembles the dynamic topography of the sea surface. All four eddies are cyclonic, as shown by the thermal doming and counterclockwise path of the drogues. During cruises GILBERT 68 I and 68 II, the same eddy was observed for nine days. The average speed of each drogue is also shown in the figures.

These average speeds have been plotted as function of the eddy radius (Figs. 42 and 43). Since the observations from GILBERT 68 I and 68 II describe the same eddy, they are plotted together (Fig. 43). The average drogue speeds from GILBERT 64 and UH-17 are of the same magnitude; they also are plotted together (Fig. 42). The observations from GILBERT 64 show an increase of speed outward from the center of the eddy to a distance of 60 kilometers. As indicated on the same plot, one of the drogues was set deep (600 m). It is difficult to state whether the speed of this deep drogue was indicative of deep flow or was influenced by the drag on the line that connected the drogue to the surface. The UH-17 drogues had average speeds of over 60 cm/sec at distances of from 75 to 90 km from the center of the eddy. The drogue speeds did not decrease with distance from the eddy center, because the eddy was located very close to Hawaii and all the north-flowing water had to pass between the center of the eddy and Hawaii. Also included in Figures 42 and 43 are the velocity distributions of a Rankine vortex, which has a velocity proportional to radius in an inner region and to radius^{-1} in an outer region (Lamb, 1945). The observed average speeds are similar to the Rankine distribution in that the speeds increase linearly to distances of 50 to 60 km from the center of the eddies.

The average speeds of the drogues were used to calculate a period of revolution for each eddy. The period of revolution and the observed difference in depth of the 20°C isotherm for each eddy are listed in Table 4.

Table 4. Period of revolution of cyclonic eddies calculated from drogue observations compared to the observed difference between the depths of the 20°C isotherm at the center and on the periphery of the eddy

Cruise	Period of Revolution	Δ20° (m)
GILBERT 68 I	4.4 days	70
GILBERT 68 II	3.7 days	70
GILBERT 64	6.1 days	40
UH-17	7.3 days	30

Table 4 shows that the period of revolution of an eddy is inversely proportional to the doming of the 20°C isotherm. The doming of the 20°C isotherm during GILBERT 68 I and 68 II was approximately twice the magnitude of the doming during GILBERT 64 and UH-17. The average speed of the drogues during GILBERT 68 I and 68 II (Figs. 40 and 41) was 95 cm/sec. The average speed of the drogues during GILBERT 64 and UH-17 (Figs. 49 and 46) was less than half this value, 45 cm/sec. The response of the 20°C isotherm seems to be linearly related to the intensity of the flow around the eddy. This fact will be more fully developed later in the analysis.

Other current observations. NEL observations (Smith, 1967) include direct current measurements for the eddy pair illustrated in Figure 14. The near-surface currents are the strongest and range from 20 to 75 cm/sec. The current decreases with depth in all areas except one. In the area of eddy convergence (zone between the cyclonic and anticyclonic eddies), velocities of greater than 60 cm/sec persist to depths of 200 meters. This is not an unusual situation for the zone of convergence between the eddy pair. An inspection of Figures 8, 12, and 67 shows that this feature, a strong flow to the east, often appears in the dynamic topographies of this area. The dynamic topographies 200/500 db indicate that the flow between the eddy pair persists to 200 m (Figs. 9, 13, and 68). This onshore current splits into north- and south-flowing currents when it approaches the coast of Hawaii. Over a period of a week in 1965, BCF scientists measured this divergence of the onshore current with drogues (unpublished BCF data). The coastal currents along the Kona (west) coast of Hawaii seem to be controlled by the relative positions of the eddy pair. It is reasonable to assume that, as the eddies form and move to the west, the position of the divergence of the coastal currents and

the intensity of the coastal flow will change.

Calculations of currents from GEK fixes in cyclonic eddies observed during UH-16 and -17 (Figs. 69 and 45) show the strong cyclonic circulation and give the magnitude of the surface currents. Similar measurements were made by the BCF (McGary, 1955; Seckel, 1955) and confirm the cyclonic flow.

Comparison of observed currents with geostrophic calculations. A comparison of average drogue speeds, currents calculated from GEK fixes, and geostrophic current calculations based on observed dynamic topography shows the cyclonic eddies to be in near geostrophic balance. In Table 5, the average drogue speeds from UH-17 (Fig. 46) and currents calculated from GEK fixes from UH-16 and -17 (Figs. 69 and 45) are compared to the geostrophic current calculations based on the observed dynamic topography 0/500 dt (Figs. 67 and 44).

Table 5. Comparison of average drogue speeds, currents calculated from GEK fixes, and geostrophic current calculations

Cruise	Geostrophic speed (cm/sec)	GEK speed (cm/sec)	Average drogue speed (cm/sec)
UH-16	48 - 64	45 - 70	none
UH-17	55	48	57

The drogue speeds and geostrophic speeds for UH-17 show excellent agreement. The calculations for UH-16 show that the range of the geostrophic and GEK speeds are of the same order. This comparison of the geostrophic, GEK, and drogue speeds shows that the eddies are in near geostrophic balance.

The average individual drogue speeds for the eddies surveyed during Cruises GILBERT 64, 68 I, 68 II, and UH-17 have been plotted as a function of eddy radius (Figs. 42 and 43). Also included in these figures are the geostrophic velocity distributions calculated from a model of eddy flow that is discussed on pages 27 through 29. The proposed geostrophic distribution shows general agreement with the average drogue speeds.

Recent coastal current measurements (Wyrtki et al., 1969) show that most coastal circulation in the vicinity

of the Hawaiian Islands is dominated by tides. In the lee of Hawaii and in the Alenuihaha Channel (Refer to Table 6) the coastal currents are atypical of this pattern in that the observations show steady flows that can be attributed to eddy circulation. During Cruise UH-16, a meter moored 3.3 km offshore from Keahole Point, Hawaii (position A, Fig. 46) measured a northerly current with an average speed of 19 cm/sec. Comparison with Figure 67 shows that the flow was the result of a cyclonic eddy located at that time to the west of Hawaii. Two months later another meter was moored offshore from Upolu Point, Hawaii (position B, Fig. 46). The resultant speed was 51.5 cm/sec to the northeast. During the next month, a meter moored in the Alenuihaha Channel south of Maui, recorded a strong flow to the west with a resultant speed of 50 cm/sec. These three observations are in accordance with the flow indicated by the dynamic topography 0/500 db of Figures 67 and 44. The strong circulation of the cyclonic eddy that forms to the west of Hawaii is the cause of this coastal flow. During 1968, the measurements at Upolu and Keahole points were repeated (Refer to Table 6). At Keahole Point, the flow was again northerly at 15 cm/sec. Although the Upolu Point meter recorded northerly flow again, the resultant speed was only 7.5 cm/sec. These observations show that coastal circulation in this area can be dominated by the eddies and that resultant speeds can be as high as 50 cm/sec for several weeks.

Table 6. Moored current meter observations in the region of eddy formations (Wyrtki et al., 1969)

Location	Date	Resultant Direction	Resultant Speed
Keahole Pt., Hawaii Position A	Apr. 30-May 21, 1967	33°	19.0 cm/sec
Upolu Pt., Hawaii Position B	July 22-Aug. 12, 1967	27°	51.5 cm/sec
Kiakeana Pt., Maui Position C	Aug. 12-Aug. 22, 1967	279°	50.0 cm/sec
Upolu Pt., Hawaii Position B	Aug. 2-Sept. 8, 1968	56°	7.5 cm/sec
Keahole Pt., Hawaii Position A	Aug. 4-Sept. 10, 1968	349°	15.0 cm/sec

Upwelling and Biological Effects

The frequent occurrence of high salinity and low temperature at the sea surface in the lee of Hawaii is the result of divergent motion. This divergence and the associated upwelling which can cause enrichment of surface layers may have significant biological effects. Although few biological and chemical data exist concerning this problem, some observations are worth discussing.

In the early stages of formation, the cyclonic eddies must exhibit upward motion to attain hydrostatic equilibrium. In the cyclonic eddy observed during Cruise UH-3, the 20°C isotherm was raised 120 m above its mean level (Table 1). If the formation time of this eddy was two weeks, the average vertical velocity during this period would have been 10^{-2} cm/sec. This is a large vertical velocity and suggests considerable enrichment of the surface waters with deeper waters.

Eddies that move away from the islands do not exhibit the high salinity and low temperature at the sea surface which are commonly found in nearshore eddies, suggesting that the upwelling occurs chiefly during formation.

The cyclonic eddies could affect the biologic balance in two general ways: enrichment of the surface layers (euphotic zone) with nutrient-rich subsurface waters, and entrainment of organisms such as littoral larvae into the circulation. In the early 1950's, the BCF in Honolulu investigated the effect of eddies on the dissolved oxygen and inorganic phosphate concentrations in Hawaiian waters (McGary, 1955). No enrichment that could be attributed to the eddies was noted. The vertical distribution of inorganic phosphate is characterized by less than 1.0 µg at/l above 200 m depth (0.4 µg at/l at the surface). The 3.0 µg at/l level is found at depths greater than 450 m (McGary, 1955). To enrich the euphotic zone, the nutrient-rich waters found below 300 m would have to be raised to depths of 100 m or above. McGary's (1955) findings are consistent with observations that show a relatively shallow flow around the eddies. The intensity of the observed flow could conceivably cause considerable upwelling, but only in a relatively shallow layer and over the short time span during the formation. Thus, enrichment of the euphotic zone is minimal.

Analyses of zooplankton by King and Hida (1954) indicated that there were slight maxima of zooplankton near the cyclonic eddies. Their data also showed other

maxima that could not be attributed to any hydrographic features. The effect that cyclonic eddies have on the biologic community in Hawaiian waters is unresolved and deserves further consideration. If this problem is approached in the future, the fact that the depth of significant nutrients in Hawaiian waters is below the level of the main eddy flow should be recognized. This fact would suggest that enrichment of the euphotic zone and the resulting biological response are small.

Tilt of the Eddy Axes

Smith (1967) states that the cyclonic eddy surveyed during the first phase of U.S.S. MARYSVILLE Cruise 36 appeared asymmetric about a vertical center. The axis of the dome slanted eastward. Ten days later, as the eddy moved away from the islands, the eddy was resurveyed. Smith noted that the dome structure was better developed and symmetric about a vertical center. Since the NEL analysis is based on the continuously recording thermistor chain data, the resolution of the features is greater than that of the BCF or UH cruises. The data from the BCF and UH cruises suggest that the eddies translate as a column. If the eddies are asymmetrical with depth, the tilt is within the resolution of the hydrographic stations, approximately 20 kilometers.

Eddy Lifetime, Movement, and Decay

Because of the large number of cruises required to track an eddy over a period of many months, the most difficult questions concerning the eddies relate to the time parameters. Nonetheless, a consideration of the observations concerning eddy formation, movement, and decay provide insight into the time parameters pertinent to Hawaiian eddies.

Formation. It is reasonable to speculate that the data from Cruise UH-12 shows a young eddy in the early stages of formation. During moderate trade-wind conditions, the area west of Hawaii was intensely surveyed. During the first part of the cruise, no large eddy or thermal dome was found. There was a rather weak depression in the 20°C isotherm (Fig. 36). In the northern part of the area, a shallow, summer mixed layer had formed (Fig. 35). In the center of the anticyclonic eddy, the mixed layer is very deep. Only on the last day of the operation was a small eddy discovered to the west of the Alenuihaha Channel. This eddy seemed to be in a very early stage of development since it was not apparent either in the surface temperature and salinity distributions

or in the topographies of the 15° and 10°C isotherms (Figs. 33, 34, 37, and 38).

During the last two days of this cruise, six parachute drogues were released in the Alenuihaha Channel (Fig. 39). These drogues showed a very irregular drift pattern. In general, the drift was to the south toward the island of Hawaii, but considerable oscillations were superimposed. It could be assumed that these oscillations were of a tidal character, but the data are not adequate to demonstrate this. Drogues drifted only 8 to 16 km during the entire period, although individual drogue speeds were as high as 50 cm/sec.

The behavior of the drogues is not consistent with the theory of flow around Hawaii as the cause of eddy formation. The hydrographic data show a weak eddy that could be in the early stages of formation, yet no strong flow through the channel appears. Figure 6 shows the cyclonic pattern of the winds in the area of the weak eddy. Wind speeds were steady and strong (15 to 20 knots) during the period of this cruise. It would appear that the only source available to drive the "young" eddy was the wind shear.

Barkley (Manar, 1967) estimates the formation time of the eddies to be approximately 10 to 15 days. Barkley (1966) also states that the eddy observed during January and February, 1966 (TOWNSEND CROMWELL Cruise 22) had a residence time of at least 1 month and possibly 2 months in the lee of Hawaii. He further states that, since the eddy showed no signs either of dissipation or growth during the interval, it was nearly stationary throughout the duration of the cruise. According to Barkley's observations and the discussion of the weak eddy observed during UH-12, the time needed to form an eddy is probably of the order of 1 week for a weak eddy to a month or more for the case of intense eddy development.

Movement and decay. Three BCF cruises (GILBERT 64, 68, and 72) were planned specifically to measure eddy movement. NEL Cruise 29 monitored the movement of a cyclonic eddy in the lee of Hawaii. The procedure for these four cruises was the same. An initial survey of the temperature structure was made; later, the same general area was resurveyed. A shift in the temperature structure indicated eddy movement. The observations show that the eddies move away from Hawaii in a westerly or northwesterly direction.

The temperature data from NEL Cruise 29 also show this westerly movement. The temperature structure in the lee of Hawaii was surveyed with a towed thermistor chain

from August 17 to 24, 1964 (Fig. 47). A strong cyclonic eddy was located 140 km west of Hawaii; and, 130 km farther west, a weaker cyclonic eddy was evident in the thermal structure. Part of the same area was resurveyed during August 28 - September 3, 1964 (Fig. 48). At that time, ten days after the first survey, the strong eddy had moved 37 km to the west. Nearshore, the temperature structure indicated that a cyclonic eddy was developing to the northwest and that an anticyclonic eddy was evident to the southwest. The net observed speed of the strong cyclonic eddy was 3.7 km/day to the west.

During GILBERT Cruise 64, a cyclonic eddy south of Oahu translated to the west and seemed to decay into a group of smaller cyclonic eddies. From April 9 - 11, 1963, the original cyclonic eddy (Fig. 49) was surveyed using BT and drogue data. The area was resurveyed during April 12 - 14, 1963 (Fig. 50), and the center of the eddy had translated 30 km in three days. The net speed was 10 km/day to the northwest. About ten days later (April 24 - 29, 1963) this area was surveyed for the third time. A series of small, shallow cyclonic eddies had replaced the larger cyclonic eddy (Fig. 51). Unfortunately, observations made during the third survey (Fig. 51) did not cover a large enough area to include the central region of the eddy as it was observed during the first cruise (Fig. 49). Nonetheless, it is reasonable to assume that this is the pattern of eddy decay since it is consistent with the classical statistical theories of turbulence that predict a decay from larger to smaller eddies. An inspection of the three plots of the 20°C isotherm suggests that the eddy pattern was becoming more irregular with time.

The observed temperature structure during GILBERT 68 I and II monitored a cyclonic eddy 150 km west of Hawaii (Figs. 40 and 41). The center of the eddy had shifted 15 km to the northwest in 3.5 days. This gives a net speed of 4.5 km/day.

GILBERT Cruise 72 monitored the movement of an intense cyclonic eddy with BT observations. During Phase I (April 15 - 20, 1964), the eddy was surveyed twice (Figs. 52 and 53). The movement was 15 km in three days (5 km/day). The entire leeward area was resurveyed (Fig. 54) a month later (May 16 - 23, 1964). The thermal structure showed an intense cyclonic eddy 80 km to the northwest of the eddy noted during Phase I. It is reasonable to assume that this was the same eddy as it seems unlikely that an eddy of the intensity found during Phase I could have dissipated over a period of only one month. This eddy would have translated 80 km to the northwest in 28 days. The net average speed would have been

3 km/day. This value is consistent with the other observations.

Table 7. Net observed speed and direction of eddy movement

Cruise	Net observed Speed (km/day)	Net observed Direction
GILBERT 64	10.0 (11.6 cm/sec)	NW
GILBERT 68	4.5 (5.2 cm/sec)	NW
GILBERT 72 I	5.0 (5.8 cm/sec)	W
GILBERT 72 II	3.0 (3.5 cm/sec)	NW
MARYSVILLE 29	3.7 (4.3 cm/sec)	W

The average net observed speed for the observations listed in Table 7 is 5.2 km/day (6.0 cm/sec). The eddies move away from Hawaii in a westerly direction and then apparently move to the northwest, parallel to the archipelago. This movement of the eddies is shown in Figure 10.

Lifetime. Figure 10 shows that the eddies can maintain their identity as far as 350 km from Hawaii. If their translation away from the islands is of the order of 5.2 km/day (See Table 7), they must have lifetimes in excess of 65 days.

Although a complete time series of the growth, movement, and decay of an eddy does not exist, a discussion of three surveys of the same area over a 3-month period (UH-12, MARYSVILLE 36, and UH-14) provides some insight into eddy lifetimes. The weak cyclonic eddy surveyed during UH-12 was apparently a young eddy in the early stages of formation (Fig. 31). One month later, NEL scientists surveyed a large, intense eddy pair west of Hawaii (Fig. 14). If the cyclonic eddy was the same eddy that was developing during UH-12, it had traveled 70 km to the south in 60 days (1.2 km/day). The fact that this eddy moved slowly into the lee of Hawaii (south) is consistent with Barkley's (1966) observation of an eddy that showed little movement in this same area. On this basis it is reasonable to assume that this eddy was the same eddy that was surveyed during UH-12. Twenty-five days later, the data from UH-14 shows a cyclonic eddy 150 km northwest of the cyclonic eddy investigated by NEL (Fig. 59). If this was the same eddy, it had moved at an average net speed of 6 km/day to the northwest (See Fig. 10). This is consistent with the observed eddy movements

listed in Table 7. This time series seems probable and gives the eddy a lifetime of 3 months or more.

THEORETICAL ANALYSIS AND DISCUSSION

The generation of eddies in the lee of the Hawaiian Islands has been ascribed by previous investigators [McGary, 1955 and Barkley (Manar, 1967)] to the same cause: the flow around and through the islands. To generate eddies behind a barrier, a strong flow is necessary. Recent investigations by Seckel (1962), Seckel *et al*. (1967) and Wyrtki *et al*. (1969) conclude that the circulation through the Hawaiian Islands cannot be generalized into the concept of a steady flow to the west. The main flow of the North Equatorial Current is apparently situated to the south of the Hawaiian Islands. The wind observations in the previous discussion provide a well-documented mechanism to drive eddies. In the analysis that follows, pro and con points of view will be discussed, mainly from the standpoint of energy considerations.

Dimensional Analysis of the Eddies

A dimensional analysis of the equations of motion should give some measure of the forces acting and giving rise to the eddies. Assuming an incompressible ocean of density ρ, the horizontal equations are

$$\frac{\partial u}{\partial t} + \nabla\cdot(uV) + w\frac{\partial u}{\partial z} - fv = -\frac{1}{\rho}\frac{\partial p}{\partial x} + A_h\nabla^2 u + \frac{1}{\rho}\frac{\partial \tau_x}{\partial z} \quad (1)$$

$$\frac{\partial v}{\partial t} + \nabla\cdot(vV) + w\frac{\partial v}{\partial z} + fu = -\frac{1}{\rho}\frac{\partial p}{\partial y} + A_h\nabla^2 v + \frac{1}{\rho}\frac{\partial \tau_y}{\partial z} \quad (2)$$

Here u and v are the eastward (x) and northward (y) components of the horizontal velocity V, ∇ is the horizontal gradient operator, ∇^2 is the horizontal Laplace operator, w the upward (z) velocity component, f the Coriolis parameter, p the pressure, A_h the coefficient of lateral eddy viscosity (assumed constant), and τ_x and τ_y the horizontal components of the wind stress. The eddies are assumed to be hydrostatically balanced. Thus

$$\frac{dp}{\rho} = gdz \quad , \qquad (3)$$

where g is the acceleration due to gravity. The pressure gradient terms can be expressed in terms of the dynamic topography $\left\{\frac{1}{\rho}\frac{\partial p}{\partial x,y} = \frac{\partial \Delta D}{\partial x,y}\right\}$. These terms can also be expressed as $g\frac{\partial \Delta h}{\partial x,y}$, where Δh is the surface topography of the eddy.

Equations (1) and (2) can be expressed in terms of scale factors that are characteristic of Hawaiian eddies. These scale factors are

$x,y = L\,x',y'$	$L = 10^7$ cm (typical eddy diameter)
$z = D\,z'$	$D = 2\times10^4$ cm (typical eddy depth, 200 m)
$t = T\,t'$	$T = 1.3 - 10\times10^5$ sec (characteristic time varies from the inertial period at 20° latitude, 35 hr, to the estimated formation time of an eddy, 10 days)
$u,v = V\,u',v'$	$V = 50$ cm/sec (typical eddy velocity)
$w = W\,w'$	$W = 10^{-2}$ (highest estimate of vertical velocity)
$f = f_o\,f'$	$f_o = 5\times10^{-5}$ sec^{-1} (f at 20° latitude)
$\Delta h = \Delta h_o \Delta h'$	$\Delta h_o = 20$ cm (typical observed difference in surface topography across an eddy)
$\tau_{x,y} = \tau_o \tau'_{x,y}$	$\tau_o = 4 - 10$ gr/cm sec^2 (winds of from 20 to 37 knots as discussed by Deacon and Webb, 1962)
	$A_h = 10^5 - 10^7$ cm^2/sec (lateral eddy viscosity).

Since the eddies are assumed to be symmetrical and f = constant, equations (1) and (2) have the same form. The scaled form of the horizontal equations of motion is

$$\frac{V}{T}\frac{\partial u'}{\partial t'} + \frac{V^2}{L}\nabla'\cdot(u'V') + \frac{WV}{L}\left(w'\frac{\partial u'}{\partial z'}\right) - f_o V f'v' =$$

(a) (b) (c) (d)

$$-\frac{g\Delta h_o}{L}\frac{\partial \Delta h'}{\partial x'} + \frac{A_h V}{L^2}\nabla'^2 u' + \frac{\tau_o}{\rho D}\frac{\partial \tau'_x}{\partial z'} \qquad (4)$$

(e) (f) (g)

Calculating the magnitude of terms (a) - (g):

(a) time-dependent inertial term = 3.8×10^{-4} - 5.0×10^{-5} (T = 35 hr - 10 days)

(b) curvature inertial term = 2.5×10^{-4}

(c) vertical inertial term = 2.5×10^{-5}

(d) Coriolis term = 2.5×10^{-3}

(e) pressure-gradient term = 2.0×10^{-3}

(f) horizontal viscous term = 5.0×10^{-8} - 5.0×10^{-6} ($A_h = 10^5$ - 10^7 cm^2/sec)

(g) wind-stress term = 2 - 5×10^{-4} (τ_o = 4 - 10 gr/cm sec).

A comparison of the magnitudes of the above scaled terms gives a measure of the relative importance of the individual terms in the governing equations of motion. An inspection of terms (a) through (g) shows that the two dominant forces are (d) and (e), i.e., the Coriolis and pressure-gradient forces. These forces are larger than the other forces by a factor of almost ten.

The next most important forces are the time-dependent (a) and curvature (b) inertial terms and the wind-stress term (g). The time-dependent inertial term becomes important only at periods of less than 10 days. If the period of inertial oscillations (35 hrs at 20° latitude) is used as the characteristic time parameter, this term has the third-largest magnitude. At high wind speeds the wind-stress term can be a controlling factor in eddy flow.

The remaining terms, vertical inertial (c) and horizontal viscous (f), have the smallest values. The magnitude of W used in the calculation is 10^{-2} cm/sec. This

value overestimates the relative importance of the term, because the upwelling is probably not a continuous feature in eddy flow. It should be noted that varying the value of A_h from 10^5 to 10^7 cm^2/sec does not make the horizontal viscous term comparable to the other terms. The vertical inertial and horizontal viscous forces seem to be of least importance.

By dividing the inertial scale factor (V^2/L) by the scale factors of terms (d), (e), and (f), three nondimensional ratios are defined. These are

Reynolds number (Re) (5)

$$= \frac{V^2/L}{A_h V/L^2} = \frac{V\,L}{A_h} = 5000 - 50 \quad (A_h = 10^5 - 10^7 \text{ cm}^2/\text{sec})$$

$$\text{Froude number (Fr)} = \frac{V^2/L}{g\Delta h_o/L} = \frac{V^2}{g\Delta h_o} = .12$$

$$\text{Rossby number (Ro)} = \frac{V^2/L}{f_o\,V} = \frac{V}{L\,f_o} = .10$$

The Reynolds number is here used in terms of a coefficient of lateral eddy viscosity, and not in terms of the coefficient of molecular viscosity. Since the Reynolds number is the ratio of the inertial force to the viscous force, its numerical value in any specific case is a measure of the relative importance of these forces. The value of Re ranges from 5000 ($A_h = 10^5$) to 50 ($A_h = 10^7$), which shows that the inertial forces are dominant. The value of the Reynolds number will be discussed in more detail later in the analysis.

Froude's number is the ratio of inertial force to gravitational force. Fr = .12 means that the gravitational force has an influence almost ten times the magnitude of the inertial force. The Rossby number is the ratio of the inertial force to Coriolis force. Since Ro = .10 is small, the Coriolis effect is a dominant force in eddy motion. The dimensional analysis of the governing equations shows that two forces are of primary importance in an analysis of the eddies: the Coriolis and pressure-gradient forces.

Since the Reynolds number is large (Re = 50 - 5000) and the Rossby number is small (Ro = .10), the Coriolis force is much larger than either the viscous or inertial forces. If the wind-stress term (g) in equation (4) is assumed to be small, the two remaining forces are Coriolis and pressure-gradient (gravitational) forces. Because geostrophic motion is the balance of these two forces, the Froude number must be equal to the Rossby number for geostrophic flow in Hawaiian eddies. Since Fr = .12 and Ro = .10, the dimensional analysis shows that Hawaiian eddies should be in near geostrophic balance in the absence of strong winds.

Geostrophic Eddy Model

In the analysis that follows, it is assumed that the eddies are geostrophically balanced. This assumption is based on the comparison of average drogue speeds and currents calculated from GEK fixes with geostrophic current calculations as well as on the dimensional analysis. The geostrophic eddy model will be used to calculate the order of magnitude of the eddy energies.

The equation of geostrophic motion in polar coordinates if $f\,c = \frac{1}{\rho}\frac{\partial p}{\partial r}$, where c is the tangential velocity. The influence of centrifugal forces will also be considered in cyclonic and anticyclonic eddy motion (See pages 42 to 44). The eddies are assumed to be rotationally symmetrical; thus, variations in the θ direction are zero. The geostrophic equation can be expressed in terms of the dynamic-height anomaly ΔD. The geostrophic velocity field of the eddies is now defined as

$$c = \frac{\partial \Delta D}{f \partial r} \quad . \tag{6}$$

Figure 55 shows observed normalized dynamic heights plotted as a function of eddy radius. The assumed distribution,

$$\Delta D = D_o\, e^{-r^2/\ell^2} \quad \text{(Gaussian distribution)}, \tag{7}$$

agrees remarkably well with the observed distributions

from various UH cruises. D_o is the observed difference in dynamic topography between the center and the periphery of an eddy and r is the distance from the eddy center. Since most of the eddies were elliptical in shape, the half major (a) and minor (b) axes were measured for each eddy. They are defined as the distance from the center where D_o has been diminished by 62.5%. From the plots of the dynamic topographies 0/500 db, a and b were measured for each eddy. For those eddies where dynamic topographies were not available, the topography of the 20°C isotherm was used to measure a and b. The eddy radius (ℓ) was calculated on the principle that the area of an ellipse ($A = \pi ab$) equals the area of a circle ($A = \pi \ell^2$). Thus, the eddy radius used in the following analysis is $\sqrt{ab} = \ell$. Although the method of definition and measurement is somewhat arbitrary, it provides a consistent method of defining eddy size. The energies calculated from these parameters are only used to make order-of-magnitude comparison. The horizontal geostrophic flow is assumed to be a function of the Gaussian distribution of dynamic topography. Substituting equation (7) into equation (6),

$$c = -\frac{2D_o\, r}{f\ell^2}\, e^{-r^2/\ell^2} \qquad (8)$$

gives the surface flow of the eddies.

Figure 56 shows the geostrophic velocity distributions between stations 70 and 71, Cruise UH-14, as a function of depth. Also included in this figure are three assumed distributions: linear [$v = v_o(1 - z/d)$]; exponential ($v = v_o e^{-z/d}$); and Gaussian ($v = v_o e^{-z^2/d^2}$). The Gaussian distribution fits the observed distribution best. The model will assume that the geostrophic velocity is a Gaussian function of depth. An inspection of the three proposed functions shows that any one of the three would not give markedly different results in the calculations that follow. There is some justification for the Gaussian distribution in that flow around the eddies is shallow and concentrated in the upper 200 meters. The three-dimensional model of geostrophic flow now has the form

$$c = -\frac{2D_o\, r}{f\,\ell^2}\, e^{-r^2/\ell^2}\, e^{-z^2/d^2} \qquad (9)$$

and the resulting geostrophic velocity distribution as a function of radius and depth is shown in Figure 57. A comparison of this model distribution and the geostrophic distribution plotted in Figure 58 shows general agreement. The cyclonic eddy surveyed during UH-14 is located on the right side of Figure 58.

Energy Model for the Eddies

Using the above model of velocity and dynamic-height distributions in the eddies, it is possible to calculate the kinetic and potential energies contained in individual eddies.

The kinetic energy is

$$K.E. = \iiint_V \frac{\rho c^2}{2}\, dV \quad . \tag{10}$$

Substituting equation (9) in equation (10), the kinetic energy is

$$K.E. = \frac{2\rho D_o^2}{f^2 \ell^4} \int_0^\infty \int_0^\infty \int_0^{2\pi} r^3 e^{-2r^2/\ell^2}\, e^{-2z^2/d^2}\, d\theta\, dz\, dr \quad . \tag{11}$$

Integrating over the volume of the eddy,

$$K.E. = \frac{\rho D_o \pi^{3/2} d}{f^2 4\sqrt{2}} \quad . \tag{12}$$

The potential energy can be expressed as

$$P.E. = \iiint_V \rho \Delta D\, dV \quad . \tag{13}$$

Substituting equation (7) in equation (13) and assuming ΔD has a Gaussian distribution with depth (e^{-z^2/d^2}), the

potential energy is

$$P.E. = \rho D_o \int_0^{\infty}\int_0^{\infty}\int_0^{2\pi} r\, e^{-r^2/\ell^2}\, e^{-z^2/d^2}\, d\theta dz dr \quad . \tag{14}$$

Integrating over the volume of the eddy,

$$P.E. = \frac{\rho D_o \pi^{3/2} \ell^2 d}{2} \tag{15}$$

The ratio of potential to kinetic energy (P.E./K.E.) is $\frac{f^2 \ell^2 2\sqrt{2}}{D_o}$. The total energy is simply the sum of the potential and kinetic energies. The derived relationships can be simplified further by introducing $D_o = g\Delta h$. Δh is the difference in surface topography across an eddy. The relationships used to calculate the energies become:

$$K.E. = \frac{\rho \Delta h^2 \pi^{3/2} g^2 d}{f^2 4\sqrt{2}} \tag{16}$$

$$P.E. = \frac{\rho \Delta h \pi^{3/2} \ell^2 g d}{2} \tag{17}$$

$$P.E./K.E. = \frac{f^2 \ell^2 2\sqrt{2}}{\Delta h g} \tag{18}$$

$$T.E. = K.E. + P.E. \tag{19}$$

Both kinetic and potential energy are directly proportional to d, a measure of eddy depth. The potential energy is directly proportional to Δh, while the kinetic energy is proportional to Δh^2. Potential energy varies as ℓ^2, a measure of eddy area. Kinetic energy is inversely proportional to f^2, the Coriolis parameter squared. The ratio of potential to kinetic energy in this

simplified model is a function of latitude (Coriolis parameter f), difference in surface topography (Δh), and the eddy radius (ℓ).

The variables in equations (16) - (19) are Δh, f, ℓ, and d. The Coriolis parameter f equals 5×10^{-5} (20° latitude). The values of ℓ and Δh_o are taken from the observations and are listed in Table 1. The value of d, a measure of eddy depth, is the only parameter that has to be determined.

The surface velocity is decreased by 62.5% at the depth d. Table 3 shows that approximately 75% of the average dynamic height difference is concentrated in the upper 200 meters. The geostrophic surface velocity is decreased by 75% at this level. Since it is assumed that the geostrophic velocity in the eddies is a Gaussian function of depth (Eqn. 9), the surface velocity is decreased by 62.5% at approximately 170 meters. Based on the observed average distribution of dynamic height in the eddies, d = 170 m is used to calculate the kinetic and potential energies. This value, 170 m, is also the mean depth of the 20°C isotherm in Hawaiian waters and can be thought of as a boundary for a two-layer model of Hawaiian eddies.

The data for some eddies do not include dynamic calculations, because the eddies were surveyed for temperature structure only. Figure 21 shows the observed change in the depth of the 20°C isotherm from the eddy center to the periphery versus the observed difference in surface topography across the eddy (Δh) for various eddies observed during the UH cruises. The two parameters are linearly related by the relationship $3.35 \Delta h$ (cm) = $\Delta 20°$ (m). This relationship applies only to moderate eddies with $\Delta h < 20$ cm. At higher Δh, the linear relationship does not apply. This relationship has been used to calculate the difference in surface topography across the eddies that were surveyed for thermal structure only. These values of Δh will be used to calculate the energies of the compound eddies.

Table 1 lists the potential, kinetic, and total energies for all the eddies. The calculated range of energies are as follows:

kinetic energy	.07 to .60x10^{22} ergs
potential energy	.42 to 5.67x10^{22} ergs
total energy	.49 to 6.27x10^{22} ergs

The largest energies are for the eddy surveyed during

Cruise UH-3. This was a very intense eddy with a difference in surface topography in excess of 30 cm. The lowest energies are for the weak eddy surveyed during Cruise UH-12. The most intense eddy observed has a total energy thirteen times that of the weak eddy. The majority of the eddies have a total energy of from 2 to 5×10^{22} ergs.

Ichiye (1956) calculated the kinetic energy of an eddy in the Kuroshio Current region. This energy varied between .39 and 2.06×10^{22} ergs over a period of many months. This agrees in order of magnitude with the kinetic energies calculated from the geostrophic model for Hawaiian eddies ($.07 - .60 \times 10^{22}$ ergs). The Kuroshio eddy was larger than the usual Hawaiian eddies; therefore, a larger kinetic energy is to be expected.

The ratio of potential to kinetic energy has been calculated for all the eddies listed in Table 1. For the cyclonic eddies, the ratio varies from 5 to 40. Most of the eddies have a ratio of from 15 to 30 with the average ratio equal to 24.

Locally Wind-Driven Eddies

The existence of strong winds in the channel between Maui and Hawaii and the existence of atmospheric eddies in the lee of Hawaii have been pointed out. It is reasonable to assume that energy is added to the ocean eddy by the winds. A consideration of the energy that is added to an eddy by the wind shear provides some insight into the possibility of locally wind-driven eddies and the time needed to generate them. According to Sverdrup *et al.* (1942), the energy equation, neglecting the dissipation term, can be expressed as

$$\frac{d(T.E.)_e}{dt} = \iint_{Area} v_o \tau_o \, dA \qquad (20)$$

where

v_o = surface speed of ocean

τ_o = wind stress at sea surface

$(T.E.)_e$ = total energy of an eddy

A = surface area (6.7×10^{13} cm^2) acted on by

wind stress. If v_o and τ_o act in the same direction and are taken as averages over the time Δt, equation (20) can be expressed as

$$(T.E.)_e = v_o \tau_o A \Delta t, \quad \text{or} \quad \Delta t = \frac{(T.E.)_e}{v_o \tau_o A} \tag{21}$$

This defines a time Δt needed to generate an energy $(T.E.)_e$ when a wind stress τ_o is exerted over an area A with a surface speed v_o. $(T.E.)_e$, v_o, and τ_o are considered to vary within the following limits:

v_o = 30 - 60 cm/sec (one-half of the observed eddy speeds shown in Figs. 42 and 43)

τ_o = 5 - 10 gr/cm/sec^2 (winds of from 26 - 37 knots; Deacon and Webb, 1962)

$(T.E.)_e$ = 2 - 5x10^{22} ergs (total eddy energies calculated from equation 19).

The wind stress is assumed to act as a torque having the same direction and location as the surface speed of the eddy. Figures 70 and 71 show that this assumption is valid. In both figures, the winds show a cyclonic pattern and are approximately parallel to the dynamic topography 0/500 db of well-developed cyclonic eddies. Although the winds show a cyclonic pattern, the strongest winds (above 25 knots) are found only around the northern half of the eddy. Since the wind stress used in equation (21) is directly proportional to the square of the wind speed (Deacon and Webb, 1962), wind stresses of from 5 to 10 gr/cm/sec^2 are found only around the northern half of the eddies. The area of the eddy where the wind stress is exerted will be taken as 6.7x10^{13} cm^2, half the average observed eddy area. This area is indicated in Figure 70 and in Figure 71 by a shaded half-circle.

Using the above values, three values of time of eddy formation, Δt, have been calculated, as shown in Table 8.

Table 8. Time required to add the energy $(T.E.)_e$ to an eddy, given a surface wind stress (τ_o) and an ocean surface speed (v_o)

Δt (days)	τ_o (gr/cm/sec^2)	v_o (cm/sec)	$(T.E.)_e$ (ergs)
58	5.0 (26 knots)	30	5×10^{22}
18	7.5 (31 knots)	45	3.5×10^{22}
6	10.0 (37 knots)	60	2×10^{22}

The maximum time of 58 days would apply to an intense eddy generated by the smallest wind stress. The minimum time of 6 days would apply to a weak eddy generated by the highest wind stress. An inspection of Table 8 shows that, to generate the energies listed, the winds must be 26 knots for 58 days or 37 knots for 6 days. Although these wind speeds and durations might seem excessive, there is some evidence that such wind conditions do exist in this area. Even with the smoothing imposed by averaging the winds over a long period, Figure 3 shows resultant wind vectors of 25 knots between Maui and Hawaii (Alenuihaha Channel). This suggests that winds of 26 knots could possibly be continuous for 58 days. Figures 4, 5, 6, and 7 all show wind vectors of 30 knots or more in the area of eddy flow. It seems possible that the wind jet in the Alenuihaha Channel (discussed on page 4) could be as high as 37 knots for 6 days.

The estimates, discussed earlier, of the formation time of an eddy were of the order of 1 week for a weak eddy to a month or more for an intense eddy. The calculated values in Table 8 are consistent with the estimates and observations discussed earlier. Although the dissipation term was neglected in the above calculations, it is quite evident that the local winds add considerable energy to the eddies.

Eddies Generated Due to a Flow around Hawaii

McGary (1955) proposed that the generation of eddies in the lee of Hawaii is due to a flow around the island. Barkley (Manar, 1967) suggested that, as the eddies grow, alternate detachment and movement to the west occurs. If a steady current passes through the Hawaiian Archipelago, this "wake stream" could be a possible explanation or mechanism for eddy generation.

This phenomenon was treated analytically by Theodore von Kármán (1911-1912) and bears his name, the Kármán vortex trail. The Kármán model applies to a small-scale flow and does not include Coriolis force. An application of the Kármán solution to Hawaiian eddies is questionable because of the effect of Coriolis force and the large scale of the eddies; nevertheless, this theory has value in that it provides a comparison between the laboratory vortex trail and the ocean vortex trail.

A brief discussion of the phenomenon and Kármán's solution will provide the relationships that will be used to compare Hawaiian eddies to the analytical solution. As a bluff cylindrical body is brought from rest to a constant speed at right angles to its axis, a vortex pair formed through separation at either side will first grow symmetrically. Eventually, one vortex will tend to overbalance the other and pass off into the wake. As the second continues to become larger, a third will form in the place of the first, and a process of alternate formation and detachment is thus ultimately established.

Kármán showed that a trail of irrotational vortices will move stably through a fluid only if the ratio of lateral to longitudinal spacing is 0.28 (Fig. 60). As was shown by Strouhal (1878), the phenomenon is an inertial rather than a viscous one. The frequency of separation (ν) relative to the diameter (D) and the speed (U) of the body (i.e., the Strouhal number $\nu D/U$) for a rigid cylinder maintains a magnitude of about 0.2 over a wide range of Reynolds number.

Some of the characteristics of the actual flow model which could not be foreseen from an irrotational model have been discussed by Rouse (1963). Only over an intermediate range of the Reynolds number (Re = 100 - 500) does anything like an orderly vortex trail appear in the wake of a cylindrical body. At very low Reynolds numbers the viscous action is so great in comparison with the inertia of the flow that separation does not occur. At higher Reynolds numbers (of the order of 50) the vortex pair forms, but remains symmetrical; and, only at still higher values do asymmetry and alternate detachment occur (Re = 100 - 500).

Laboratory measurements (Wille and Timme, 1957) of the Kármán vortex trail show that the eddies move away from the cylinder at approximately eight-tenths of the speed of the flow around the cylinder.

The analytical and laboratory flow models can be compared to the situation in the lee of Hawaii using the four criteria outlined above: (a) ratio of lateral to

longitudinal eddy spacing, (b) frequency of separation of the eddies, (c) Reynolds number, and (d) translation speeds of the eddies away from Hawaii. A comparison of these four parameters should give a measure of how applicable the concept of flow past a cylinder is to the eddies found in the lee of Hawaii.

The Reynolds number used by Kármán (UD/μ) is dependent on the constant speed of the body U, the diameter of the cylinder D, and the coefficient of molecular viscosity μ. The values used for the ocean are the diameter of Hawaii, 150 km ($D = 1.5 \times 10^7$ cm); the assumed speed of flow around the island, 20 cm/sec; and a coefficient of lateral eddy viscosity (A_h) varying from 10^5 to 10^7. The Reynolds number for the Hawaiian eddies is now dependent on the A_h used. If A_h equals $2 - 4 \times 10^6$ cm^2/sec, then Re = 150 - 75. These Reynolds numbers are consistent with the requirements for an eddy pair forming and moving away from Hawaii. Although the comparison between the Reynolds number for the analytical and ocean models is approximate, there is qualitative agreement if A_h is $2 - 4 \times 10^6$ cm^2/sec.

The frequency of separation (0.2 U/D) can be calculated in the same manner. Using U = 20 cm/sec, the period between successive separations ($T = 1/\nu$) is equal to 40 days. A flow of 50 cm/sec gives a period of 16 days. The observations of the rate of eddy formation and separation are not adequate to distinguish between periods of 16 and 40 days. Although there are only a few observations of this parameter for Hawaiian eddies, the time needed to generate Hawaiian eddies is thought to be of the order of a week to a month or more.

The next comparison concerns the ratio of lateral to longitudinal spacing (Fig. 60). The lateral spacing between centers of the cyclonic and anticyclonic eddies (2b) has been measured in Figures 12, 14, 31, 48, and 67. If the direction of movement is to the west, the observed value of b is approximately 40 kilometers. This means that, to satisfy Kármán's solution, the spacing between successive eddies of the same type should equal 284 kilometers. There are only a few observations that show the existence of more than one eddy of the same type at any one time downstream of Hawaii; on the basis of these few cases Barkley (Manar, 1967) estimates that the distance between eddies of the same type is about 220 kilometers. Figure 47 shows two cyclonic eddies west of Hawaii. The spacing between these eddies is 150 kilometers. This does not discount the Kármán model when we consider ocean flow. As the eddies progress downstream, the individual eddies

are subject to three distinct effects. First, the eddies increase in area (Fig. 11) and, second, the circulation diminishes through viscous action (Figs. 49, 50, and 51); both of these effects have been observed. Third, the slight disturbances invariably present in any ocean flow gradually produce an additional departure from the original geometry of the pattern.

The final comparison will be of the speed with which the eddies move away from Hawaii. Laboratory measurements (Wille and Timme, 1957) of the Kármán vortex trail show that the speed at which the eddies move away from the cylinder is approximately eight-tenths of the speed of flow around the cylinder. Observations of the speed at which Hawaiian eddies move to the west range from 3.5 to 11.6 cm/sec. If these speeds are consistent with the laboratory studies, the flow incident to Hawaii must be of the order of 4 to 15 cm/sec.

For the Kármán model to apply to the eddies generated in the lee of Hawaii, a steady flow to the west around Hawaii must exist. However, observations show that in these latitudes the North Equatorial Current is not steady. Still, it is possible that a shallow, trade-wind drift through the islands could provide the flow necessary for a "wake-stream" phenomenon.

Observations of the depth of the mixed layer in the Alenuihaha Channel between Maui and Hawaii show evidence for a westward flow (Figs. 61 and 62). The mixed layer is deeper in the north and shallower in the south, indicating flow to the west in a two-layer model. However, this feature does not appear in the data of all the cruises studied; and an examination of the hydrographic structure of the situation surveyed during UH-16 shows that the flow through the Alenuihaha Channel is not large enough to be consistent with the Kármán theory.

During Cruise UH-16, the search for the eddy was conducted during moderate to strong trade winds (Fig. 7). The surface temperature showed strong advection of cooler water through the Alenuihaha Channel (Fig. 63). This tongue of surface water extended in the same direction as the strong winds in the channel. The depth of the mixed layer was shallow, in accordance with conditions at the beginning of the heating season, and weakly indicated the presence of the thermal dome (Fig. 61). The tilt of the mixed layer in the channel indicated advection to the west.

The depth of the isothermal layers (Figs. 64, 65, and 66) showed an elongated dome stretching from the Alenuihaha Channel west. The circulation around the dome

was cyclonic. Geostrophic transport to the west, relative to 500 db, in its northern portions (Fig. 67, line AB) was 6.0 million m^3/sec. The transport to the northeast (Fig. 67, line BC) was 7.8 million m^3/sec. Measurements with the GEK confirmed the cyclonic circulation in the southwestern area of the Alenuihaha Channel (Fig. 69).

The data show an elongated cyclonic eddy to the northwest and an anticyclonic eddy to the southwest of Hawaii. The depths of the isothermal layers (Figs. 64, 65, and 66) indicate that the structure was more irregular nearer the channel. The depth of the 20° and 15°C isotherms can be interpreted as being due to a weak eddy beginning to form south of Maui. The topography of the 10°C isotherm reveals the intense eddy to the west and gives no indication of the new eddy assumed to be forming south of Maui. The dynamic topography 0/500 db (Fig. 67) can be interpreted in a similar manner. This interpretation of the hydrographic data suggests a wake stream in the lee of Hawaii.

If the eddies are generated by the flow to the west around Hawaii, the flow through the Alenuihaha Channel is the only source that can drive the cyclonic eddies. Figures 63 and 67 show westward flow through this channel. The difference in dynamic topography 0/500 db across the channel (4 dyn cm) indicates a geostrophic surface speed of 20 cm/sec to the west. If the volume transport is simply given by u z y, where u is the mean velocity of the layer of flow (u = 10 cm/sec, assuming a linear decrease in the surface speed), z is the depth of the flow (z = 500 m), and y is the width of the channel (L = 40 km), the geostrophic volume transport was 2 million m^3/sec.

It is possible that a shallow, wind-induced flow in the channel and around the south side of Hawaii provides the flow that drives the eddies. Since the island of Hawaii presents a solid barrier of 120 km to the trade-wind flow, the ocean flow induced by the increase in wind around the island could drive the eddies. To carry this reasoning one step further, it is also possible that the cyclonic eddies are much more intense than the anti-cyclonic eddies due to the wind jet through the Alenuihaha Channel. If a shallow, strong flow of 50 cm/sec as recorded by the moored current meter south of Maui (Refer to page 16) is assumed to extend across the channel in the upper 100 m, the volume transport is again 2 million m^3/sec.

The above estimates of the channel transport are large and do not necessarily represent the usual observed conditions in this channel. Drogues released in this

channel did not move to the west during a period when an eddy was apparently forming. (Refer to Fig. 39 and page 19).

Two records from current meters moored at the north point of Hawaii (Table 6 and Fig. 46) also demonstrate that flow at this position is usually to the north, and controlled by the eddies rather than by the strong local winds.

A comparison of the calculated total energy of the cyclonic eddies with the kinetic energy through a section across the Alenuihaha Channel is one method for calculating whether these eddies are generated by the flow around Hawaii. The assumption to be examined is that the only source of energy for the cyclonic eddies is the advection of kinetic energy by the channel flow.

The kinetic energy of the flow in the channel $(K.E.)_c$ is simply

$$(K.E.)_c = \iiint_{\text{Volume}} \frac{\rho u^2}{2} \, dx \, dy \, dz \quad . \qquad (22)$$

Since $dx = u \, dt$, and assuming $u = u_o e^{-z^2/d^2}$, equation (22) becomes

$$(K.E.)_c = \frac{\rho}{2} \int_0^{\infty} \int_0^{L} \int_0^{\Delta t} u_o^3 e^{-3z^2/d^2} \, dt \, dy \, dz \quad . \qquad (23)$$

Equation (23) is the kinetic energy advected through a section across the Alenuihaha Channel over a given time period. This is integrated to

$$(K.E.)_c = \frac{u_o^3 \, L \, \Delta t \, d\sqrt{\pi}}{4\sqrt{3}} \quad . \qquad (24)$$

If the advection of kinetic energy through the channel is the only source of energy available to drive the eddies, equation (24) should balance the total eddy energies calculated in the section on the energy model for the eddies (See pages 29 to 32). Thus,

$$(T.E.)_e = (K.E.)_c = \frac{u_o^3 \, L \, \Delta t \, d\sqrt{\pi}}{4\sqrt{3}} \quad , \qquad (25)$$

where $(T.E.)_e$ is the total energy of a given eddy. The parameter Δt is the time needed for the advection of energy through the Alenuihaha Channel to form an eddy, assuming that all the energy of the channel flow is used in the generation of the eddy. Obviously, some of this energy will be dissipated through viscous action and some will flow past Hawaii, not into the eddies. This means that Δt is an underestimate of the time needed to generate an eddy.

Observed values for the Alenuihaha Channel to be substituted in equation (25) are

L = 40 km (width of Alenuihaha Channel),

d = 200 km (depth where surface speed has decreased by 62.5%),

u_o = 30 cm/sec (assumed speed of surface current).

These values yield a mass transport of 2 million m^3/sec to the west through the channel, which is consistent with the observations discussed previously. The calculated total energies of an eddy are 1×10^{22} ergs for a weak eddy and 5×10^{22} ergs for an intense eddy. Using the above values, the time needed for the channel flow to form an eddy is 210 days (approximately 7 months) for a weak eddy and 1050 days (approximately 3 years) for an intense eddy.

A Δt of larger than two months is inconsistent with the observations. The above calculation shows that, for the observed mass transport (2 million m^3/sec) and the estimated times of eddy formation (less than 2 months), the advection of kinetic energy through the channel cannot supply enough energy to generate an eddy. If the energies lost due to dissipation and due to the flow past the island are considered, it is clear that the eddies are not driven by the flow through the Alenuihaha Channel.

A final argument can be presented against the Kármán analogy. One of the major characteristics of the Kármán vortex trail is the fact that the speed with which the eddies move away from the cylinder (Hawaii) is approximately eight-tenths of the speed of the flow past the cylinder (Wille and Timme, 1957). If the situation in the lee of Hawaii is a Kármán vortex trail, the incident flow

would need to be much larger than the observed flow discussed previously. If the flow was indeed that large, the eddies must move to the west at speeds much larger than the observed speeds, which are 3.5 - 11.6 cm/sec. Although the flow around Hawaii undoubtedly influences the formation of eddies in the lee of the island, Hawaiian eddies cannot be explained as a Kármán vortex trail.

Translation of Eddies Due to Variation in Coriolis Parameter

Warren (1967) noted that rings of current (eddies) have a tendency to move through an environment at rest due to meridional variation in Coriolis parameter. He developed first order formulas for displacement speeds as applied to eddy shapes (circles) constant in time. Baroclinicity is included in the sense that large vertical shear in the basic horizontal velocity is emphasized.

In the case of a symmetric, cyclonic eddy with a diameter of 100 km (2° latitude), the variation in Coriolis parameter will cause a translation to the west. The trajectory of a particle of water flowing around the eddy cannot be stationary, for, as the particle moves northward (increasing Coriolis parameter), the cyclonic curvature of its trajectory must decrease. As the particle moves southward (decreasing Coriolis parameter), the cyclonic curvature must increase. Thus, the particle must, after every circuit of the eddy, find itself west of its starting position; and, therefore the eddy must move westward. The rate of net westward displacement will be independent of depth, and the eddies will translate as a column.

Warren's expression for the rate of westward displacement is $\frac{1}{2}\beta R^2$. R is the eddy radius and β is the variation of Coriolis parameter with latitude. Substituting values applicable to Hawaiian eddies, R = 50 - 100 km and $\beta = 2.0 \times 10^{-13}$ $cm^{-1} sec^{-1}$, the net rate of westward displacement varies from 2.5 to 10.0 cm/sec. The observed westward drift of Hawaiian eddies is from 3.5 to 11.6 cm/sec.

Warren considers his application of this relationship to Gulf Stream eddies as tenuous. When applied to Hawaiian eddies, the same caution should be exercised. The majority of the Hawaiian eddies studied were not circular (a condition for Warren's solution) but elliptical. Advective effects may in fact be dominant in westward displacement of Hawaiian eddies.

Effect of Centrifugal Forces in Eddy Motion

The dimensional analysis showed that the curvature inertial term is of secondary importance in eddy flow. In the geostrophic calculation of the flow around the eddies (Fig. 57), the effect of the curvature (centrifugal forces) is ignored. A simplified model of an eddy that includes curvature shows the effect of the centrifugal forces in eddy motion.

In the case of a circular eddy with concentric isobars with their centers at r = 0, the eddy is rotationally symmetrical and is governed by the following equation (polar coordinates):

$$\frac{c^2}{r} + fc - \frac{1}{\rho}\frac{\partial p}{\partial r} = 0 \qquad (26)$$

where c is tangential velocity. This equation governs circular motion, parallel to the isobars, with a balance among centrifugal, Coriolis, and pressure-gradient forces.

The solutions of equation (26) are

$$c = -\frac{fr}{2} \pm \sqrt{\frac{f^2r^2}{4} + \frac{r}{\rho}\frac{\partial p}{\partial r}} \quad . \qquad (27)$$

An inspection of equation (27) shows that, when $\partial p/\partial r$ is positive (a low), the square root can never become imaginary, so that all values of pressure gradient are permissible. Where equation (26) is valid, there is no theoretical restriction on the magnitude of the pressure gradient for a cyclonic eddy (a low). However, when $\partial p/\partial r$ is negative (a high), it is possible for the square root to become imaginary. The resulting complex value for c has no physical meaning and must be excluded from the consideration. The condition that c be real is

$$\left|\frac{1}{\rho}\frac{\partial p}{\partial r}\right| \leq \frac{f^2r}{4} \qquad \text{(Hess, 1959).} \qquad (28)$$

Consequently, in an anticyclonic eddy the magnitude of the pressure gradient may not exceed a certain value determined largely by the latitude and distance from the center.

This theoretical restriction for the anticyclonic eddies can be applied to the observed distribution of $\partial p/\partial r$ of Hawaiian eddies. Since $\frac{1}{\rho}\frac{\partial p}{\partial r} = \frac{\partial \Delta D}{\partial r}$, and the observed distribution of dynamic height can be approximated by equation (7) ($\Delta D = D_o e^{-r^2/\ell^2}$), the theoretical restriction for anticyclonic eddies in Hawaiian waters (Eq. 28) can be expressed as

$$e^{-r^2/\ell^2} \geq \frac{f^2 \ell^2}{\beta \Delta h g}, \qquad (29)$$

where $D_o = g\Delta h$ (Δh being the change in surface topography from the center to the periphery of an eddy). The values used to calculate the right-hand term in equation (29) are

$f = 5\times10^{-5}$ sec^{-1} (Coriolis parameter at 20° latitude),

$\ell = 6\times10^{6}$ cm (60 km, average observed anticyclonic eddy radius), and

$\Delta h = 10 - 20$ cm (assumed range of surface topography across the anticyclonic eddies).

The right-hand term has been calculated for three values of Δh and is listed in Table 10. Table 9 lists the value of e^{-r^2/ℓ^2} at 10-km intervals from the center of an eddy.

Table 9.

e^{-r^2/ℓ^2} (ℓ = 60 km) as a function of radius (r)

r	10	20	30	40	50	60	70	80	90	100	Km
e^{-r^2/ℓ^2}	.97	.90	.78	.64	.50	.37	.26	.17	.10	.06	

Table 10. Theoretical restriction imposed on anticyclonic eddies by including the centrifugal forces for various surface topographies

Δh(cm)	$\frac{f^2 \ell^2}{8 \Delta h \ g}$	Radius where solution becomes imaginary
10	1.12	real for all r
15	.84	< 25 km
20	.56	< 45 km

The condition that the solution of equation (27) is not imaginary will be met if the middle column in Table 10 is larger or equal to e^{-r^2/ℓ^2} listed in Table 9. For the assumed values of Δh listed in Table 10, the anticyclonic eddies have real solutions for all r if Δh is 10 cm or less; but, when Δh equals 15 and 20 cm, the solution becomes imaginary at radius values of less than 25 and 45 km, respectively.

This is the explanation of the fact that anticyclonic eddies never exhibit the intensity of cyclonic eddies (Refer to Table 3). While cyclonic eddies can maintain large Δh, the anticyclonic eddies must adjust the distribution of dynamic height to satisfy condition (22).

It would be interesting to compare the magnitude of the geostrophic flow with the magnitude of the flow that includes the centrifugal force, but unfortunately current measurements for the anticyclonic eddies do not exist. The difference in current speed between the eddy pairs would be an excellent gauge of the relative importance of the centrifugal forces. Current measurements in the cyclonic eddies suggest that these eddies are in near geostrophic balance. Centrifugal forces would decrease the maximum velocity in a cyclonic eddy by approximately 20%. Since this is near the accuracy of the GEK fixes and drogue measurements, it is difficult to gauge the effect of the centrifugal forces.

SUMMARY AND CONCLUSIONS

Cyclonic and anticyclonic eddies with diameters from 50 to 150 km have been observed during all seasons in the lee of the Hawaiian Islands. The data from 20 cruises describing these eddies have been analyzed. The majority of the eddies surveyed were cyclonic and were located to the west of Hawaii. Eddy formation has also been observed in the lee of Kauai and Oahu, but not with the same regularity as in the lee of Hawaii. Consequently, this study mainly considered eddy formation in the lee of the island of Hawaii.

The most characteristic feature of the cyclonic and anticyclonic eddy pair that develops in the lee of Hawaii is the temperature structure. The cyclonic eddies are characterized by intense doming of the temperature structure, whereas anticyclonic eddies appear as less intense depressions. Although the doming of the thermal structure and associated surface divergence of the cyclonic eddies can be very intense in the upper 200 m, the process is relatively shallow and is generally confined to the upper 300 to 400 meters. These observations are consistent with dynamic height calculations which show that 500 m is an acceptable reference level in the eddies. Approximately 75% of the observed dynamic height difference is concentrated in the upper 200 m, characterizing the eddies as shallow features.

The surface flow of the eddies has been measured using parachute drogues, GEK fixes, and moored current meters. Surface velocities of 100 cm/sec have been measured in the cyclonic eddies. A comparison of observed currents with geostrophic calculations demonstrates that the eddies are in near geostrophic balance.

The formation time of the eddies has been estimated to be approximately two weeks for a weak eddy to a month for a more intense eddy. The eddies have been observed to translate to the west at an average speed of 6.0 cm/sec. A possible explanation of this drift is the tendency of eddies to move through an environment at rest due to meridional variation in Coriolis parameter (Warren, 1967). It is also possible that a weak, large-scale flow to the west due to the trade-wind drift causes the eddies to drift. The eddies have lifetimes of two months or more in the lee of the islands before they decay or disappear.

Some of the analytical relationships that govern eddy motions of this scale have been applied to the observations. The kinetic, potential, and total energies of the eddies have been calculated using a model that assumes geostrophic eddy flow. The total eddy energies varied from 1×10^{22} ergs for weak eddies to 5×10^{22} ergs for intense eddy development. The ratio of the potential to kinetic energy was also calculated for each eddy and always showed a large excess of potential energy in the eddies. The average value of this ratio was 24.

The observations on the eddies developing to the west of Hawaii suggest two different generating mechanisms:

(1) Eddies generated by the flow past a barrier in the sense of a Kármán vortex trail, and

(2) Wind-induced eddies due to the cyclonic and anticyclonic shear of the winds observed behind Hawaii.

Although many of the characteristics of these eddies show qualitative agreement with the Kármán model, the strong, steady flow necessary to generate eddies of that intensity has not been observed in this area. Calculations of the energy added to the eddies by the existing local winds, especially by the wind jet through the Alenuihaha Channel, show that this is the most probable explanation of eddy generation.

The observations and analysis can be summarized by the following intuitive argument: If the oceanic eddies are locally generated by the cyclonic and anticyclonic shear of the winds leeward of Hawaii and by the strong winds in the Alenuihaha Channel, the flow of the surface layer of the ocean during periods of strong winds and small pressure gradients could be described as an Ekman drift. The dimensional analysis of the governing equations shows that the Coriolis and wind-stress forces causing Ekman flow are dominant during eddy formation, when pressure gradients are small. If the Ekman drift had a cyclonic pattern, the surface layer would be strongly divergent because the transport would be away from the center of the eddy. For anticyclonic Ekman drift, the surface layer would be convergent. In addition to the wind jet observed in the Alenuihaha Channel, cyclonic and anticyclonic eddies have been observed in the atmosphere in the lee of Hawaii. The surface divergence would explain the high salinity and low temperature found at the sea surface near the center of the cyclonic eddies. The surface divergence and associated upwelling cause a doming of the thermocline and the associated density structure as deep as 300 meters. The potential energy of

an eddy is directly proportional to the doming of the density structure or equivalent to the change in dynamic topography across an eddy. Consequently, the longer the duration and the larger the magnitude of the winds, the more potential energy will be accumulated in an eddy. The large potential energies calculated for fully-developed eddies can be accounted for by the input of energy from the strong winds observed in the Alenuihaha Channel.

As soon as the wind diminishes or the eddy moves away from the area of strongest winds in the Alenuihaha Channel, the surface divergence and associated upwelling will cease. This is consistent with observations, since eddies that drift to the west and away from the strong wind field do not exhibit high salinity and low temperature at the sea surface near their centers. The analysis shows that the motion will be nearly geostrophic if the wind-stress is small.

It is assumed that the large excess of potential energy that is common to eddies observed to the west of Hawaii is generated by local wind conditions. This potential energy is converted to kinetic energy at some later time when the winds have a lesser effect. The analysis shows that flow will be nearly geostrophic during this period. The kinetic energy contained in the geostrophic flow is then dissipated through viscous effects and replaced by conversion of potential into kinetic energy. During this period the eddy slowly decreases in intensity, as the thermal structure weakens and the circulation becomes slower. The calculated excess of potential energy that is common to all the eddies should be able to sustain the eddy flow for a considerable time. This is consistent with observations that show that eddies have a lifetime in excess of two months in the lee of Hawaii.

ACKNOWLEDGMENTS

I wish to thank Dr. R. Barkley of the Bureau of Commercial Fisheries in Honolulu and the U.S. Naval Electronics Laboratory in San Diego for making available much of their data concerning Hawaiian eddies. Without their cooperation, this study would have been much less comprehensive.

I am grateful to Professors K. Wyrtki, V. Brock, and B. Gallagher for their suggestions, criticisms, and encouragement during the course of this work.

This study was supported by the Office of Naval Research under Contract Nonr-3748(06).

LITERATURE CITED

Anonymous, 1955, Average Monthly Rainfall Maps, Meteorology Department of Pineapple Research Institute and Experiment Station, Hawaiian Sugar Planters Association in cooperation with U.S. Weather Bureau, 14 p.

Austin, G. B., 1955, Oceanographic survey of the Gulf of Mexico, Trans. of Am. Geophys. Union, Vol. 36, No. 5, p. 885-892.

Deacon, E. L. and E. K. Webb, 1962, Drag coefficients of the sea surface, in: The Sea, Volume 1, M. N. Hill Editor, John Wiley and Sons, New York, p. 57-66.

Defant, Albert, 1961, Physical Oceanography, Volume I, New York, The Macmillan Company, p. 465-475.

Fuglister, F. C., 1964, Gulf Stream '60, Progress in Oceanography, Vol. 1, Pergamon Press, p. 265-373.

Fuglister, F. C., 1967, Cyclonic eddies formed from meanders of the Gulf Stream, Paper presented before the American Geophysical Union in April 1967, unpublished.

Hess, Seymour L., 1959, Introduction to Theoretical Meteorology, New York, Holt, Rinehart and Winston, Inc., p. 180-186.

Ichiye, T., 1956, On the behavior of the vortex in the polar front region (Hydrography of the polar front region, I), Oceanography Mag., Vol. 7, No. 2, p. 115-132.

Ichiye, T., 1965, Dynamics of Gulf Stream meanders, Lamont Geological Observatory Report, Tech. Rep. CU-1706-3, CU-266(48)-13 and CU-2663-20, 90 p.

Kârmân, T. von, 1911-12, Veberden Mechanismus des Widerstandes den ein bewegter Körper in einer Flüssigkeit erfährt, Göttinger Nachrichten.

King, Joseph E. and T. S. Hida, 1954, Variation in zooplankton abundance in Hawaiian waters, 1950-52, U.S. Fish and Wildlife Service, Spec. Sci. Rep.: Fish. No. 118, 66 p., 16 figs.

Lamb, H., 1945, Hydrodynamics, Sixth Edition, New York, Dover Publications.

Manar, Thomas A., 1967, Progress in 1965-66 at the Bureau of Commercial Fisheries Biological Laboratory, Honolulu, U.S. Fish and Wildlife Service, Circ. 274, 51 p.

McGary, James W., 1955, Mid-Pacific Oceanography, Part VI, Hawaiian Offshore Waters, December 1949 - November 1951, U.S. Fish and Wildlife Service, Spec. Sci. Rep.: Fish. No. 152, 138 p.

Ramage, C. S., 1960, Notes on the meteorology of the tropical Pacific and Southeast Asia, Air Force Surveys in Geophysics No. 126, Project 8641, Task 86415, Bedford, Mass.

Reid, J. L., R. A. Schwartzlose, and D. M. Brown, 1963, Direct measurements of a small eddy of Northern Baja California, J. Mar. Res., Vol. 21, No. 3, p. 203-218.

Rouse, Hunter, 1963, On the role of eddies in fluid motion, Am. Scientist, Vol. 51, No. 3, p. 285-314.

Seckel, G. R., 1955, Mid-Pacific Oceanography, Part VII, Hawaiian Offshore Waters, September 1952 - August 1953, U.S. Fish and Wildlife Service, Spec. Sci. Rep.: Fish. No. 164, 250 p.

Seckel, G. R., 1962, Atlas of the Oceanographic Climate of the Hawaiian Region, U.S. Fish and Wildlife Service, Fish. Bull. 193, Vol. 193, p. 371-427.

Seckel, G. R., R. L. Charnell and D. W. K. Au, 1967, The Trade Wind Zone Oceanography Pilot Study, Parts I - VI: TOWNSEND CROMWELL Cruises 1 - 6, 8 - 17, and 21, February 1964 to January 1966, U.S. Fish and Wildlife Service, Spec. Sci. Rep.: Fish. No. 552 to 557, 422 p.

Smith, Edward L., 1967, Migration and temperature structure of eddies on the leeward side of the Hawaiian Islands, U.S. Navy Electronics Laboratory Report, 19 p.

Strouhal, V., 1878, Veber eine besondere Art der Tonerregung, Annalen der Physik und Chemie, 5.

Sverdrup, H. V., M. W. Johnson and R. H. Fleming, 1942, The Oceans, New York, Prentice-Hall, Inc., p. 486-489.

Taliaferro, William J., 1958, Kona Rainfall, Hawaii Water Authority Report, 43 p.

Taliaferro, William J., 1959, Supplement to Kona rainfall, Hawaii Water Authority Report, 20 p.

U.S. Navy Hydrographic Office, 1945, Atlas of Monthly Pilot Charts of North Atlantic and Pacific Oceans, H.O. Pub. No. 560, 12 charts.

U.S. Navy Hydrographic Office, 1947, Current Atlas of the northeast Pacific, H.O. Pub. No. 570, 12 charts.

Warren, Bruce A., 1967, Notes on translatory movement of rings of current with application to Gulf Stream eddies, Deep-Sea Res., Vol. 14, No. 5, p. 505-524.

Webster, T. F., 1961, The effect of meanders on the kinetic energy balance of the Gulf Stream, Tellus Vol. 13, p. 392-401.

Wille, R. and A. Timme, 1957, Uber das Verhalten von Wirbelstraben, Schiffbautechnische Gesellschaft, Berlin, Jahrbuch V. 51, p. 215-221.

Wyrtki, Klaus, J. B. Burks, R. C. Latham and Wm. Patzert, 1967, Oceanographic Observations during 1965-1967 in the Hawaiian Archipelago, Hawaii Institute of Geophysics Report No. HIG-67-15, 150 p.

Wyrtki, K., V. Graefe, and W. C. Patzert, 1969, Current Observations in the Hawaiian Archipelago, Hawaii Institute of Geophysics, unpublished.

APPENDIX.

Table 1

Explanation of the Parameters Listed in Table 1

Figures 1 through 71

Table 1.

	Cruise	Date	Data	Eddy Type	Code	Half Major Axis a (km)	Half Minor Axis b (km)	Eccentricity e	Radius r (km)	Area (km^2) $\pi \times 10^{-3}$	DEPTH OF ISOTHE Center 20°C	15°C	10°C
1.	R/V HUGH M. SMITH 1	Dec. 13-21, 1949	Hydrocasts, BT	C	1	84	75	.45	79	19.6	122	208	
2.	R/V HUGH M. SMITH 13	July 14-31, 1951	Hydrocasts, BT	C	2a	77	70	.42	73	16.7	137		
				C	2b	86	79	.40	83	21.6	93	153	
3.	R/V HUGH M. SMITH 13	Oct. 23 - Nov. 2, 1951	Hydrocasts, BT, GEK	C	3	90	67	.67	75	17.6	110	172	
4.	R/V HUGH M. SMITH 17	Sept., 1952	Hydrocasts, BT	C	4a	70	67	.29	68	14.5	86	189	
				A	4b	55	35	.72	45	6.3	183	247	
5.	R/V HUGH M. SMITH 20	March, 1953	Hydrocasts, BT, GEK	C	5a	62	50	.60	56	9.8	143	226	
				A	5b	74	60	.58	68	14.5	180	254	
				C	5c				80	20.1	107	200	
6.	R/V HUGH M. SMITH 21	Aug., 1953	Hydrocasts, BT, GEK	C	6a				73	16.7	122	220	
				A	6b				65	22.9	214	260	
				C	6c				83	21.6	110	198	
7.	R/V CHARLES H. GILBERT 64	Apr. 9-14, 1963	BT, drogues	C	7a				65	13.3	100	180	
		Apr. 24-29,1963	BT	C	7b				28	2.5	120	220	
				C	7b				22	1.5	130	220	
8.	R/V CHARLES H. GILBERT 66	Aug. 21-24,1963	BT, drogues	C	8a				67	14.1	80	180	
		Aug. 26-29,1963	BT, drogues	C	8b				67	14.1	80	190	
9.	R/V CHARLES H. GILBERT 72	Apr. 14-21,1964	BT	C	9a				73	16.7	130		
		May 16-23, 1964	BT	C	9b				75	17.7	120		
10.	U.S.S. MARYS-VILLE 29	Aug. 17-24,1964	Thermistor chain	C	10a				58	10.6			
		Aug. 26 - Sept. 3, 1964		C	10b				65	13.9			
11.	UB-1	Mar. 18-24,1965	Hydrocasts, BT	C	11								
12.	UB-2	May 18-24, 1965	Hydrocasts, BT	C	12a	65	46	.69	54	9.2	100	200	310
				A	12b	65	55	.54	60	11.3	200	250	350
13.	UB-3	July 19-23,1965	Hydrocasts, BT	C	13	73	55	.66	63	12.5	40	160	280
14.	R/V TOWNSEND CROMWELL 22	Feb. 10-22,1966	BT, DTS	C	14a						50		
		Feb. 23 - Mar. 5, 1966		C	14b								
				A	14c								
15.	UB-12	Apr. 26 - May 5, 1966	BT, DTS, drogues	C	15a	28	28	0	28	2.5	120	230	330
				A	15b	73	44	.79	56	9.8	190	260	350
16.	U.S.S. MARYS-VILLE 36	July 4-13, 1966	Thermistor chain	C	16a				67	14.1	100	190	
				A	16b				75	17.7	220		
17.	UB-14	July 26 - Aug. 6, 1966	BT, DTS	C	17a	73	57	.62	65	13.3	120	190	300
				C	17b	46	28	.42	36	4.1	150	220	310
				C	17c	73	55	.66	63	12.5	110	210	320
18.	UB-15	Oct. 18-21,1966	BT, DTS	C	18						150		
19.	UB-16	Apr. 26 - May 6, 1967	BT, DTS, GEK	C	19a	90	73	.59	81	20.6	90	180	270
				A	19b	55	55	0	55	9.5	160	230	320
20.	UB-17	June 12-20,1967	BT, DTS, GEK, drogues	C	20	73	44	.78	56	10.6	100	180	280

*Calculated, using $3.35 \Delta h(cm) = \Delta 20^{\circ}$ (m)

RMS IN METERS Periphery 20°C	15°C	10°C	Δ20° (m)	Δ15° (m)	Δ10° (m)	Δh(cm) 0/1000 (dt)	Δh(cm) 200/1000 (dt)	ΔT_s °C	ΔS_s ‰	Distance from Hawaii (km)	K.E. ergs x 10^{21}	P.E. ergs x 10^{22}	P.E./K.E.	T.E. ergs x 10^{22}	Observed Geostrophic Vol. Transport Millions m^3/sec
150	223		30	15		14	8	+ .3	- .6	190	1.07	3.51	32	3.62	
200			63			10	2		0	92	.74	2.84	38	2.91	
153	186		60	33		24	8		- .2	208	3.14	6.48	20	6.79	
180	218		70	36		14	4	+ .2	- .2	130	1.30	4.59	35	4.62	
159	244		73	55		20	4	+1.5	- .2	175	2.34	4.48	19	4.71	
171	244		12	3		5	0	-1.0	0	73	.18	.54	29	.55	
183	250		40	24		10	0	+ .3	0	73	.74	1.67	22	1.74	
183	254		3	0		14	4	0	+ .2	203	1.07	2.53	24	2.64	
171	257		64	57		14	4	+ .5	- .4	275	.92	3.01	32	3.10	
						0/500	200/500								
168	242		46	22		12	5	- .1	+ .8	205	.79	2.50	32	2.58	
165	229		49	31		10	4	0	-1.0	280	.47	2.42	51	2.47	
160	206		50	8		14	6	- .1	0	350	.92	3.24	35	3.33	
140	220		40	40		11*				257	.61*	1.69	28*	1.75*	
150	220		30	0		8*				309	.30*	.21*	7*	.24*	
150	220		20	0		5*				255	.14*	.08*	6*	.09*	
150	240		70	60		19*				147	2.25*	3.82*	17*	4.05*	
150	220		70	30		19*				170	2.11*	3.58*	17*	3.75*	
180			50			24*				260	2.70*	3.40*	13*	3.67*	
160			40			16*				330	1.20*	2.13*	18*	2.25*	
						14*				140	1.22*	2.11*	17*	2.23*	
						11*				177	.76*	2.38*	27*	2.15*	
170	240	340	70	40	30	00	4	+ .4	- .4	60	3.12	3.26	10	3.57	7.0
170	240	340	30	10	10	10	2	+ .2	0	140	.66	1.71	26	1.78	3.4
160	240	340	120	80	60	30	6	+2.0	- .6	130	5.97	5.67	9	6.27	8.0
175			125												
160	250	340	40	20	10	10	2	+ .6	0	30	.74	.42	5	.49	3.0
170	250	340	20	10	10	6	2	+ .2	0	135	.24	.59	37	.92	6.0
170	220		70	30		19*				130	2.35*	4.06*	17*	4.30*	
190			30			8*				240	.35*	1.76*	50*	2.00*	
170	240	330	50	30	30	16	4	0	0	165	1.40	2.64	19	2.78	7.0
160	230	330	10	10	20	6	2	- .2	0	55	.50	.58	11	.63	
150	230	330	40	20	10	6	2	+ .4	- .2	55	.50	1.78	35	1.83	3.3
160			10												
140	220	310	50	40	40	16	4	+1.0	- .6	200	1.40	4.11	29	4.25	6.0
140	220	310	20	10	10	8	2	0	+ .1	53	.47	1.28	27	1.33	
130	200	310	30	50	30	10	0	+1.2	- .3	87	.70	1.06	24	1.76	3.4

An explanation of the parameters listed from left to right in Table 1 follows:

(a) Cruise: The data from these cruises were analyzed.

(b) Date: The periods of operation for each cruise.

(c) Data: Hydrocasts (Nansen casts), BT (bathythermographs), GEK (geomagnetic electrokinetograph fixes), drogues (paths of parachute drogues), DTS (continuously recording depth, temperature and salinity recorder) and thermistor chain (continuously recording towed thermistor chain developed by Naval Electronics Laboratory, San Diego).

(d) Eddy type: C (cyclonic eddy) or A (anticyclonic eddy).

(e) Code: Number that is referred to Figure 10 for the positions of the individual eddies observed.

(f) a and b: Half major and minor axes of the elliptical pattern of an eddy. Refer to pages 7 and 8 for a further explanation.

(g) e: eccentricity of the eddy, $e = \frac{\sqrt{a^2 - b^2}}{a}$.

(h) ℓ: The characteristic eddy radius (ℓ) was calculated on the principle that the area of an ellipse ($A = \pi ab$) equals the area of a circle ($A = \pi \ell^2$). The eddy radius is simply $\ell = \sqrt{ab}$.

(i) Area: Eddy area equals $\pi \ell^2$.

(j) Observed depths of the 20°C, 15°C, and 10°C isotherms at the center and periphery of each eddy.

(k) $\Delta 20°$, $\Delta 15°$, and $\Delta 10°$: The difference between the depths of the respective isotherms at the eddy center and periphery.

(l) h: Change in surface topography from the center to the periphery of the eddy. Since hydrostatic balance is assumed,

$(\frac{dp}{\rho} = \Delta D = g\Delta h)$; Δh is simply $\frac{\Delta D}{g}$.

(m) ΔT_s: Change in surface temperature from the center to the periphery of the eddy as measured from the center out.

(n) ΔS_s: Change in surface salinity from the center to the periphery of the eddy as measured from the center out.

(o) Distance from Hawaii: Cyclonic eddies are measured from the north point of Hawaii and anti-cyclonic eddies are measured from the south point of Hawaii.

(p) K.E.: Kinetic energy as calculated from equation (16).

(q) P.E.: Potential energy as calculated from equation (17).

(r) P.E./K.E.: Ratio of potential to kinetic energy as calculated from equation (18).

(s) T.E.: Total energy equals the sum of the kinetic and potential energies.

(t) Observed geostrophic volume transports: These transports are taken from Hawaii Institute of Geophysics Report HIG-67-15 (Wyrtki et al., 1967).

(u) d: A measure of the depth of flow (see Fig. 56) calculated according to equation (9).

BLANK PAGE

Figures 1 through 71

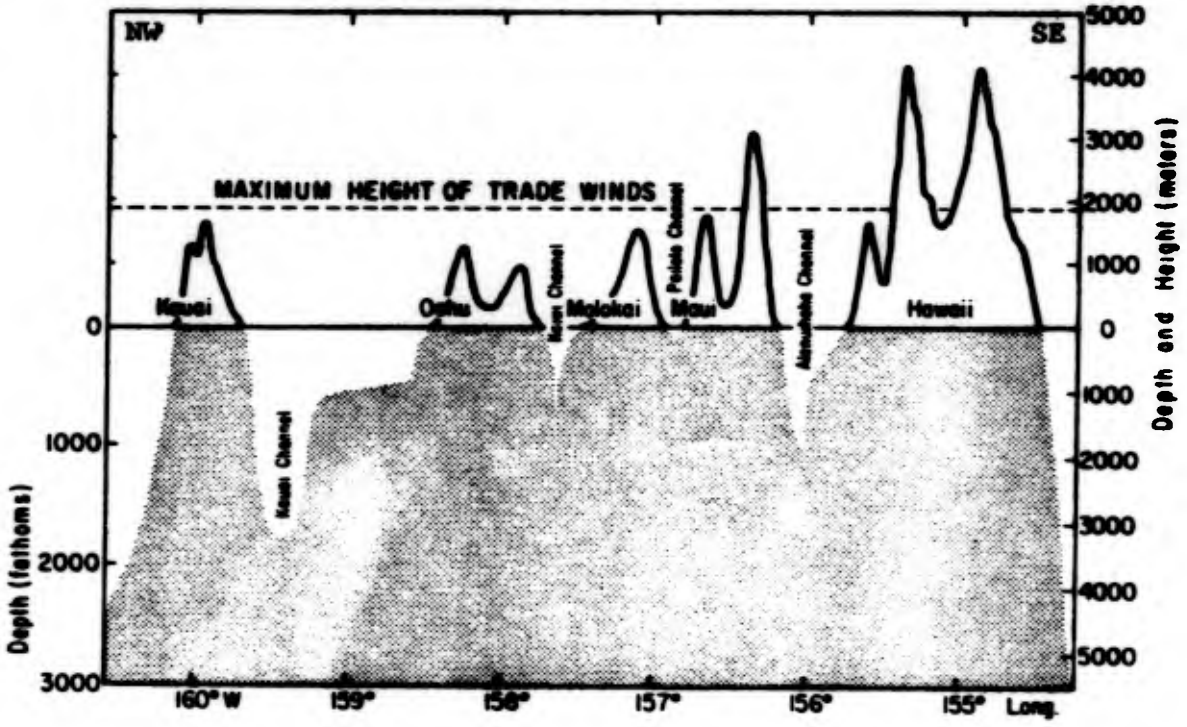

Figure 1. A southeast to northwest cross section of the Hawaiian Archipelago above and below sea level. The location of the maximum height of the northeast trade winds (1800 m) shows that the islands are a series of vertical obstacles that penetrate the trade-wind layer.

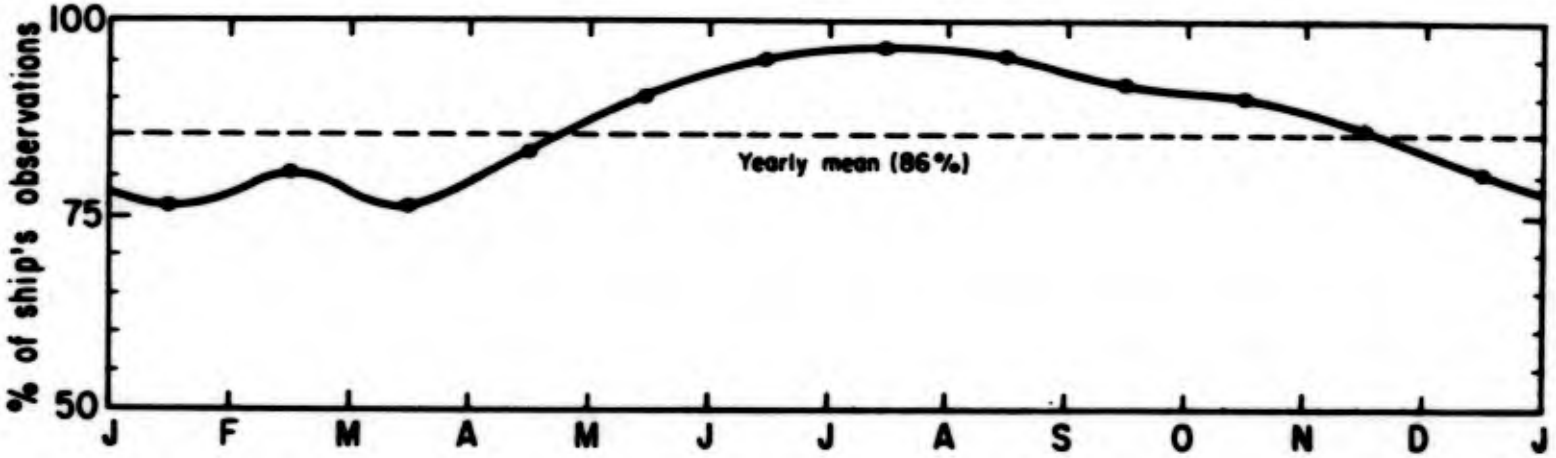

Figure 2. Percentage of ship's observations of winds that were reported for the directions NE, E or SE for the 5° squares between 15°N and 25°N latitude at 150°W to 155°W longitude plotted as monthly averages. The wind data are based on the U.S. Navy Hydrographic Office Pilot Charts (H.O. 560) averaged for monthly periods. The three components (NE, E, and SE) represent trade winds incident to the Hawaiian Archipelago.

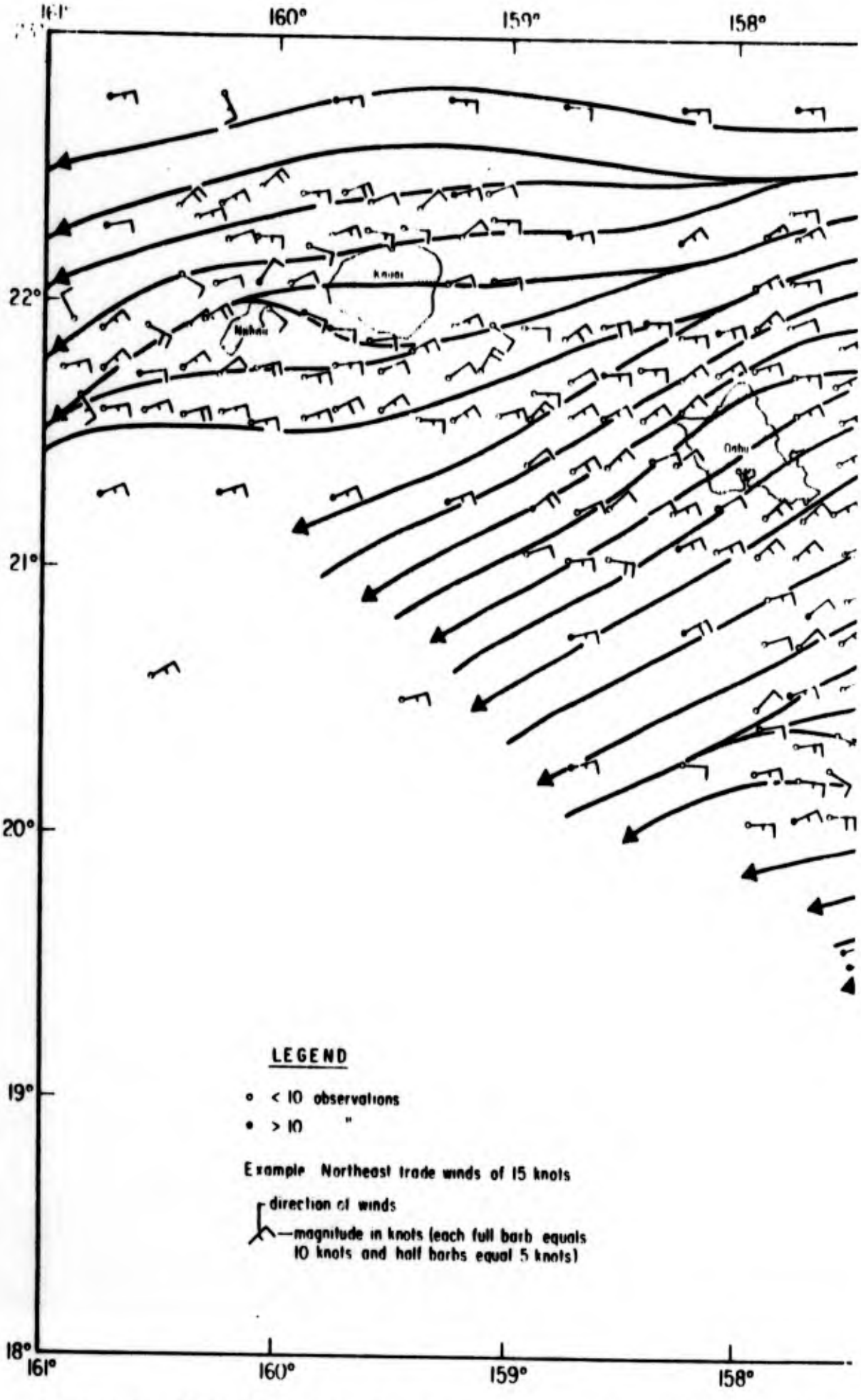

Figure 3. Resultant wind vectors and streamlines over the Sciences Services Administration Weather Bureau,

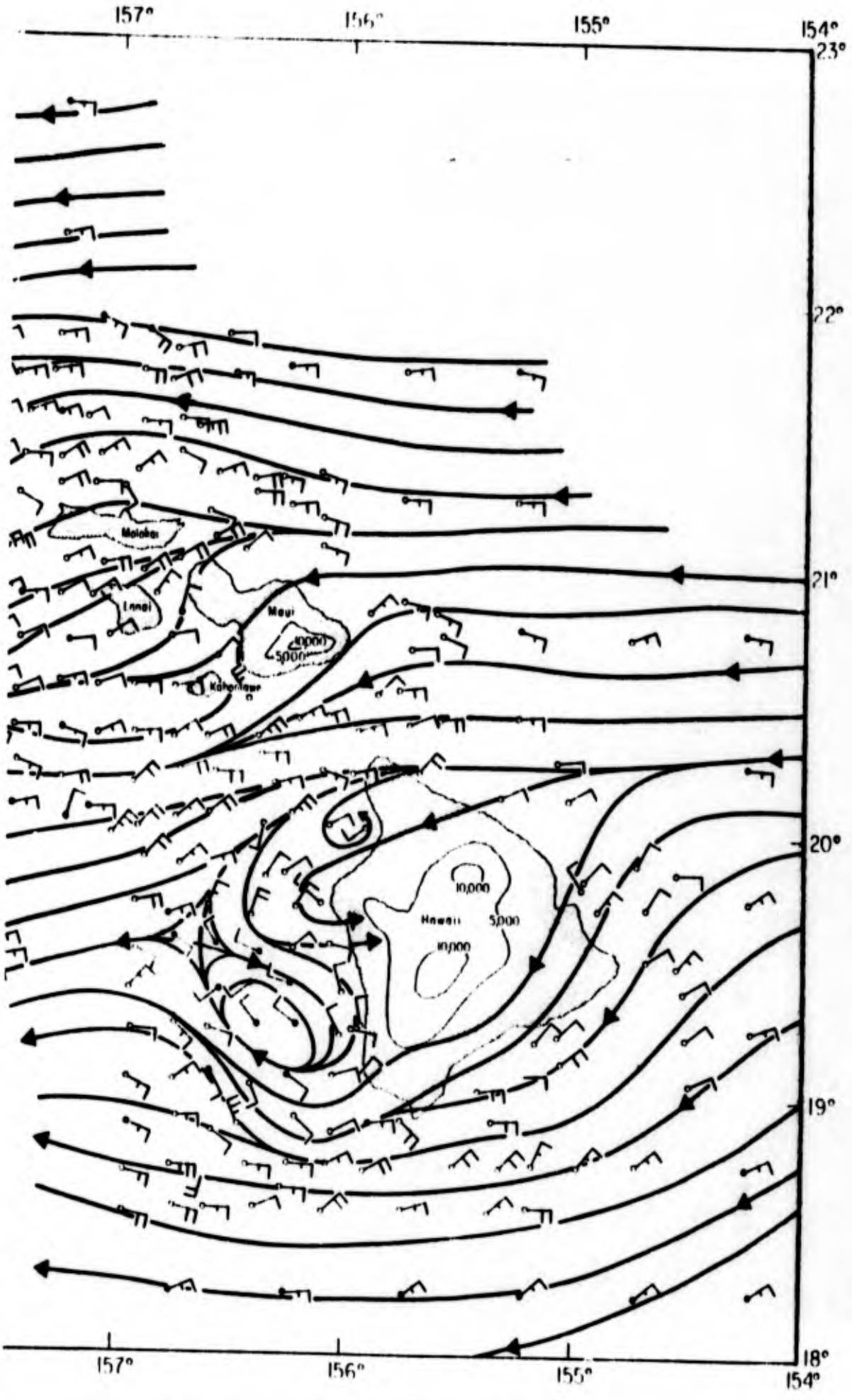

Hawaiian waters (according to unpublished data from Environmental Honolulu, 1968).

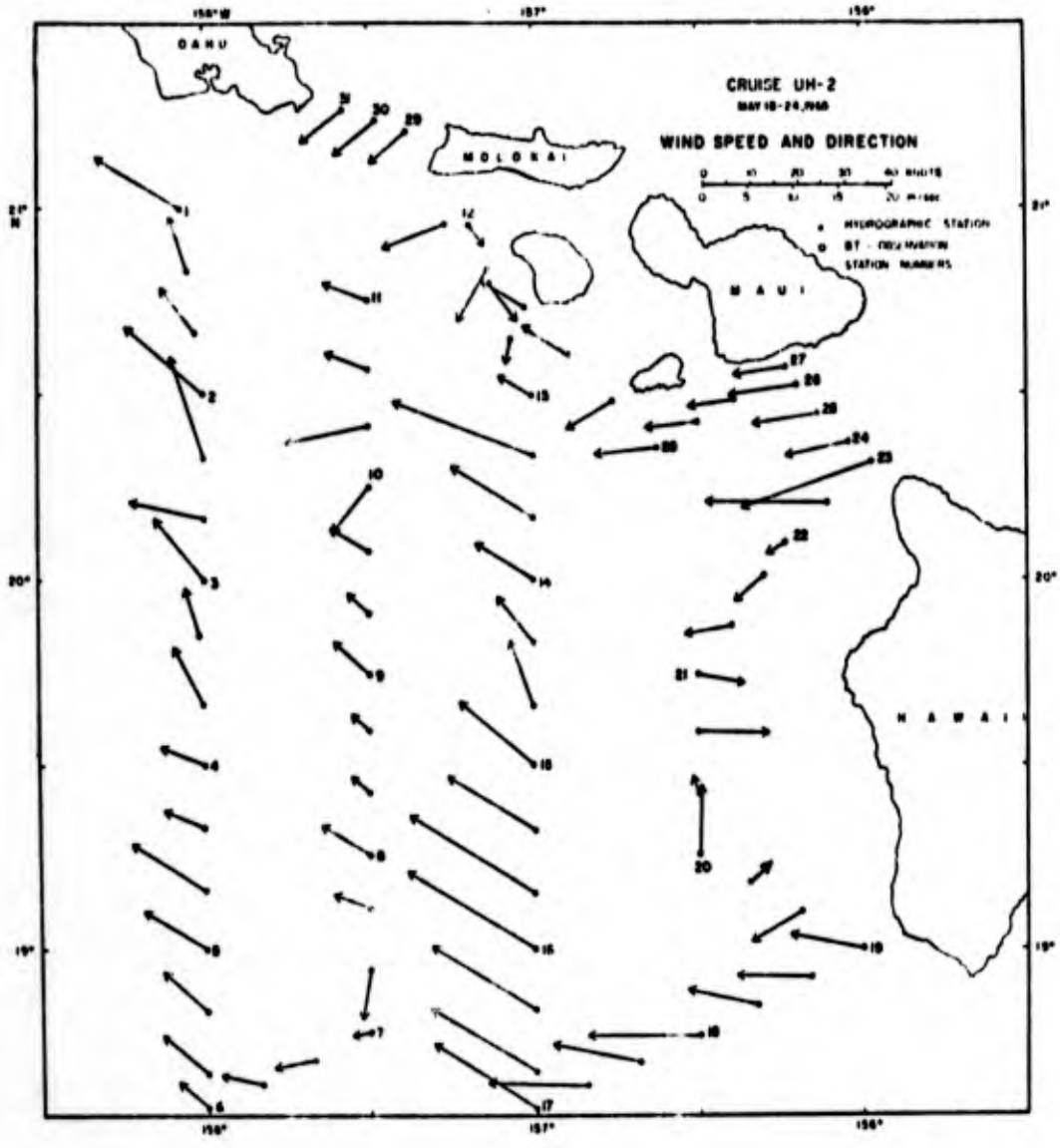

Figure 4. Wind speed and direction from Cruise UH-2, May 18 - 24, 1965.

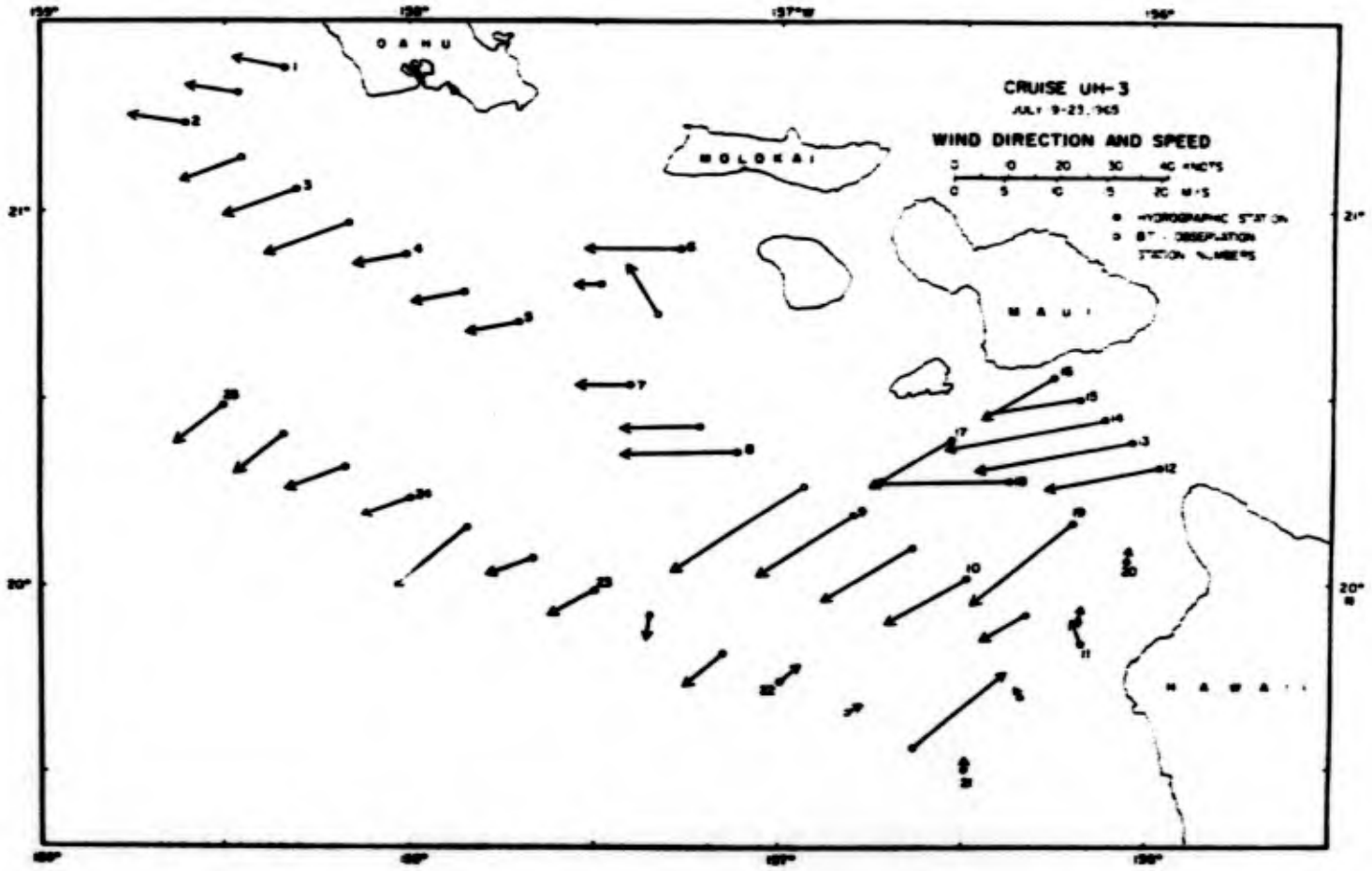

Figure 5. Wind speed and direction from Cruise UH-3, July 19 - 23, 1965.

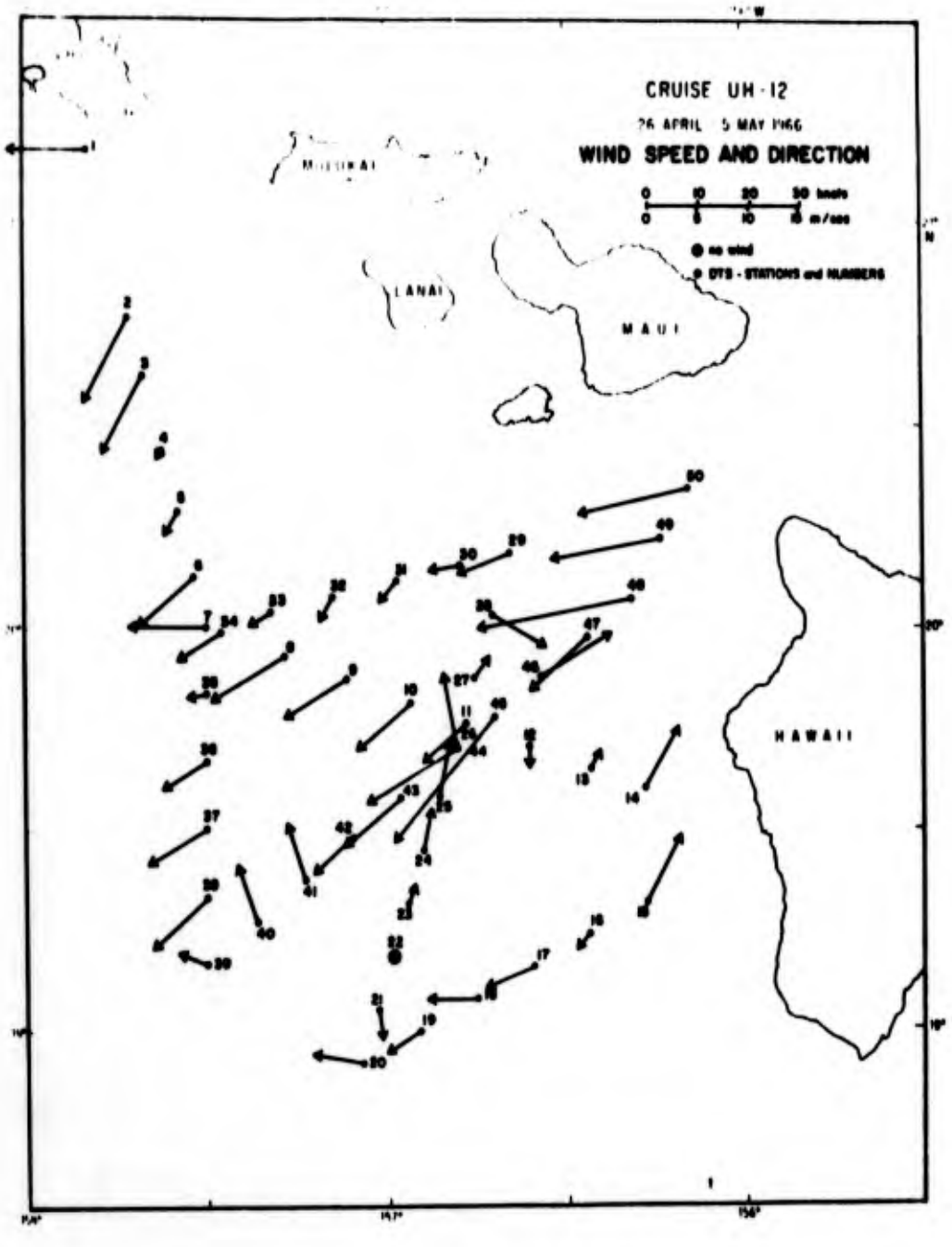

Figure 6. Wind speed and direction from Cruise UH-12, April 26 - May 5, 1966.

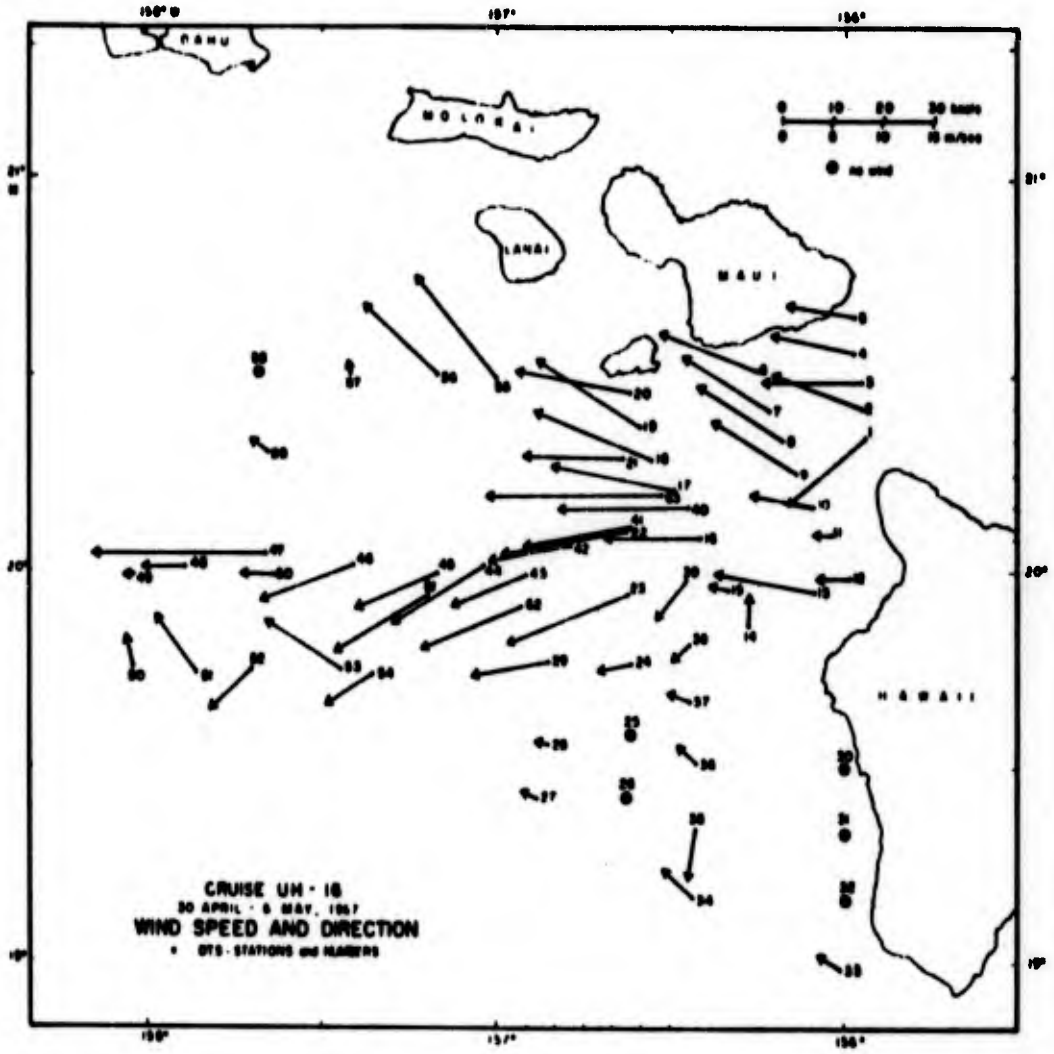

Figure 7. Wind speed and direction from Cruise UH-16, April 30 - May 6, 1967.

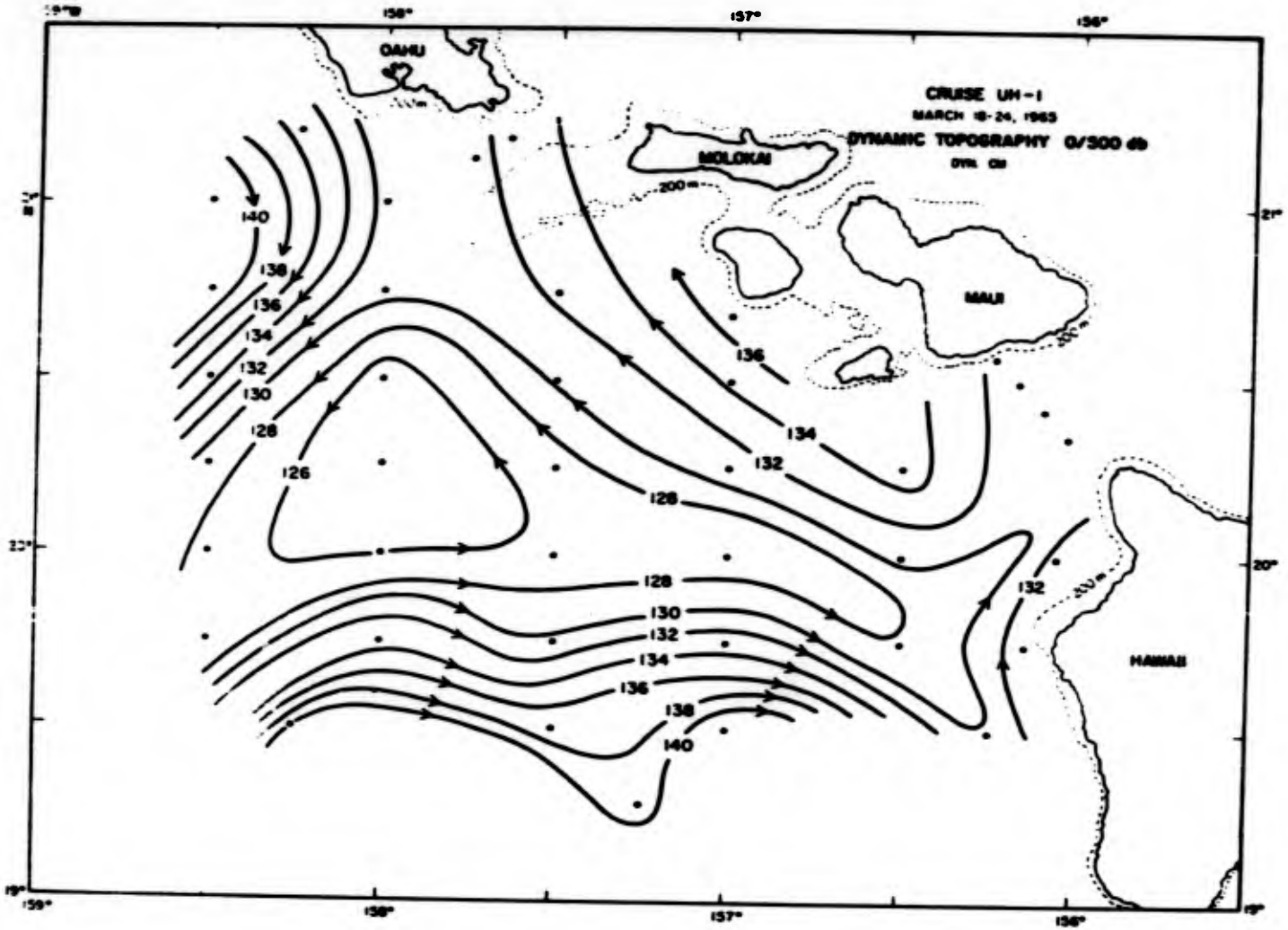

Figure 8. Dynamic topography 0/500 db from Cruise UH-1, March 18 - 24, 1965.

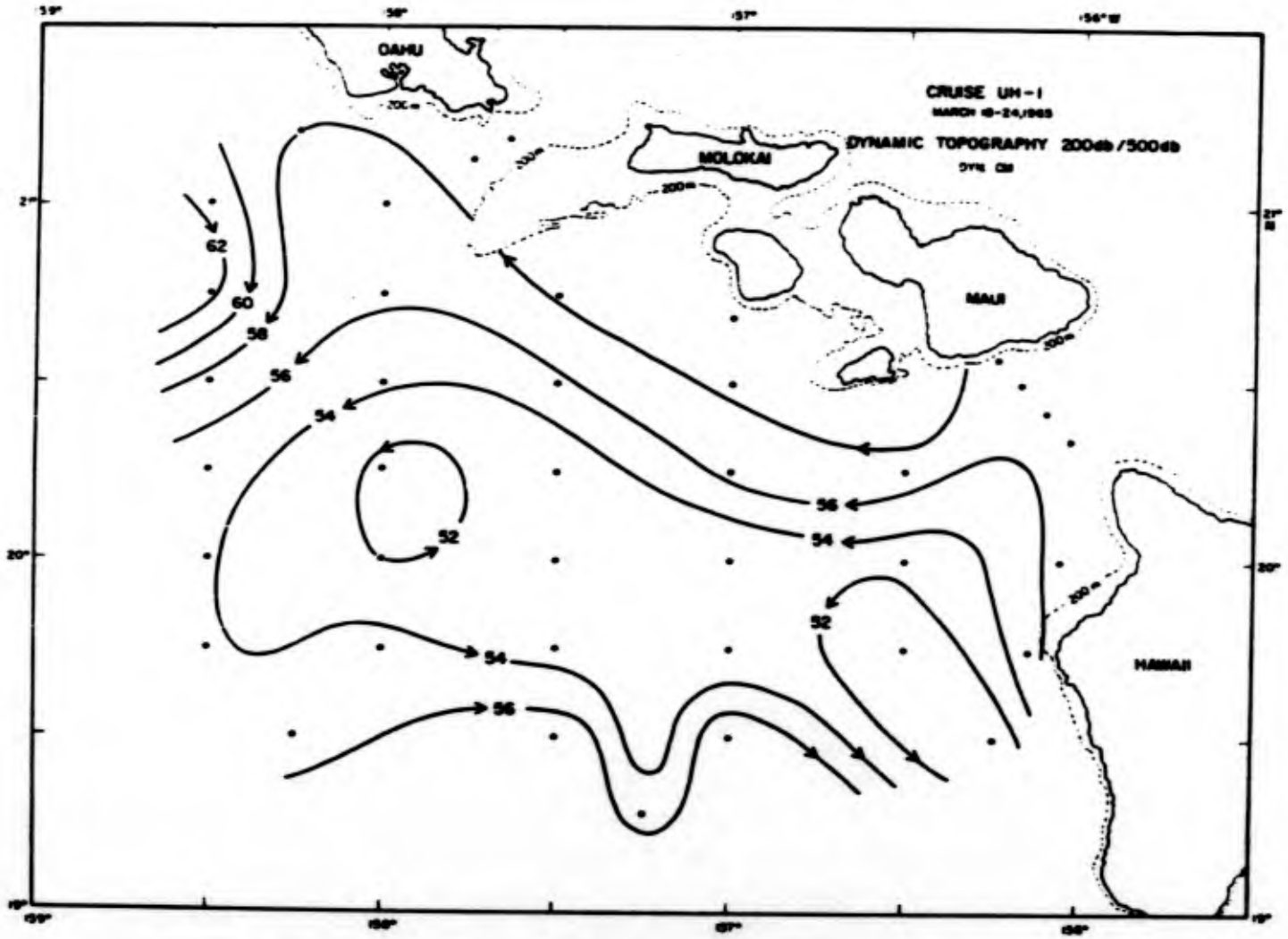

Figure 9. Dynamic topography 200/500 db from Cruise UH-1, March 18 - 24, 1965.

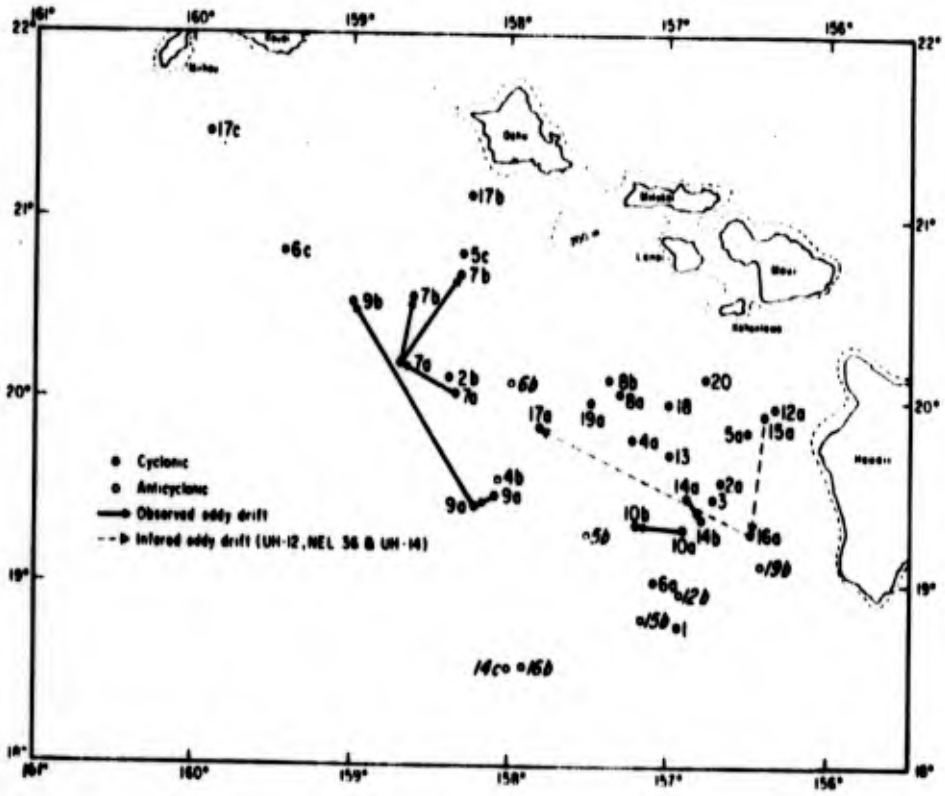

Figure 10. Location and drift of eddies in the lee of the Hawaiian Islands. The positions represent the centers of the eddies and the numbers represent cruises as listed in Table 1.

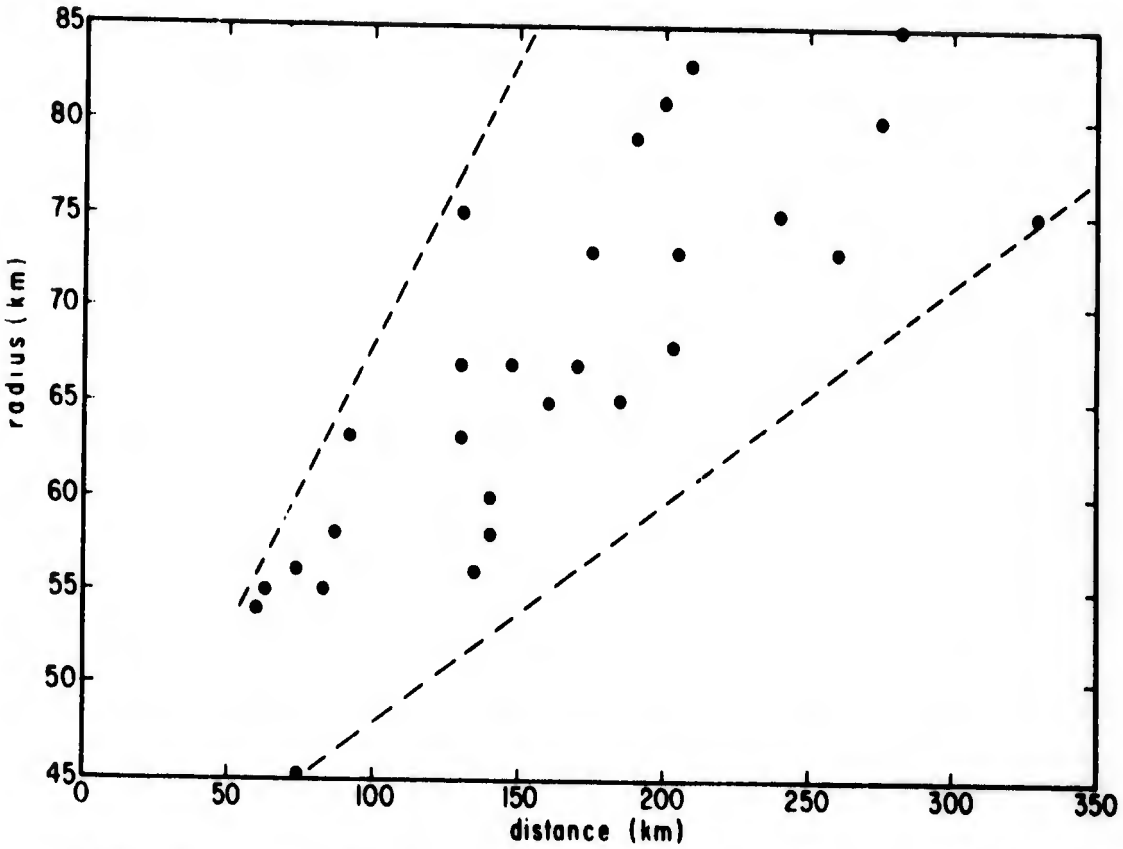

Figure 11. Observed eddy radius versus the distance of the center of the eddy from Island of Hawaii.

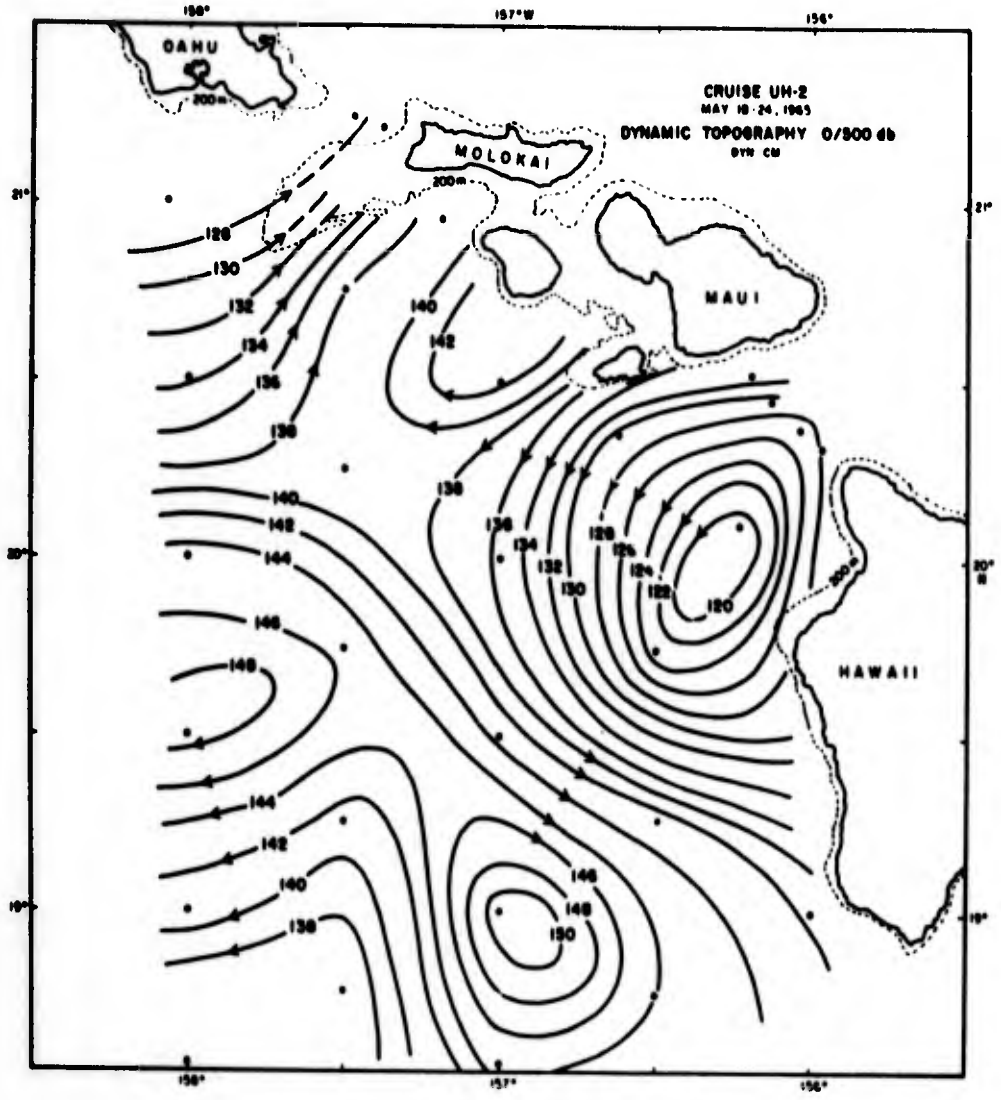

Figure 12. Dynamic topography 0/500 db from Cruise UH-2, May 18 - 24, 1965.

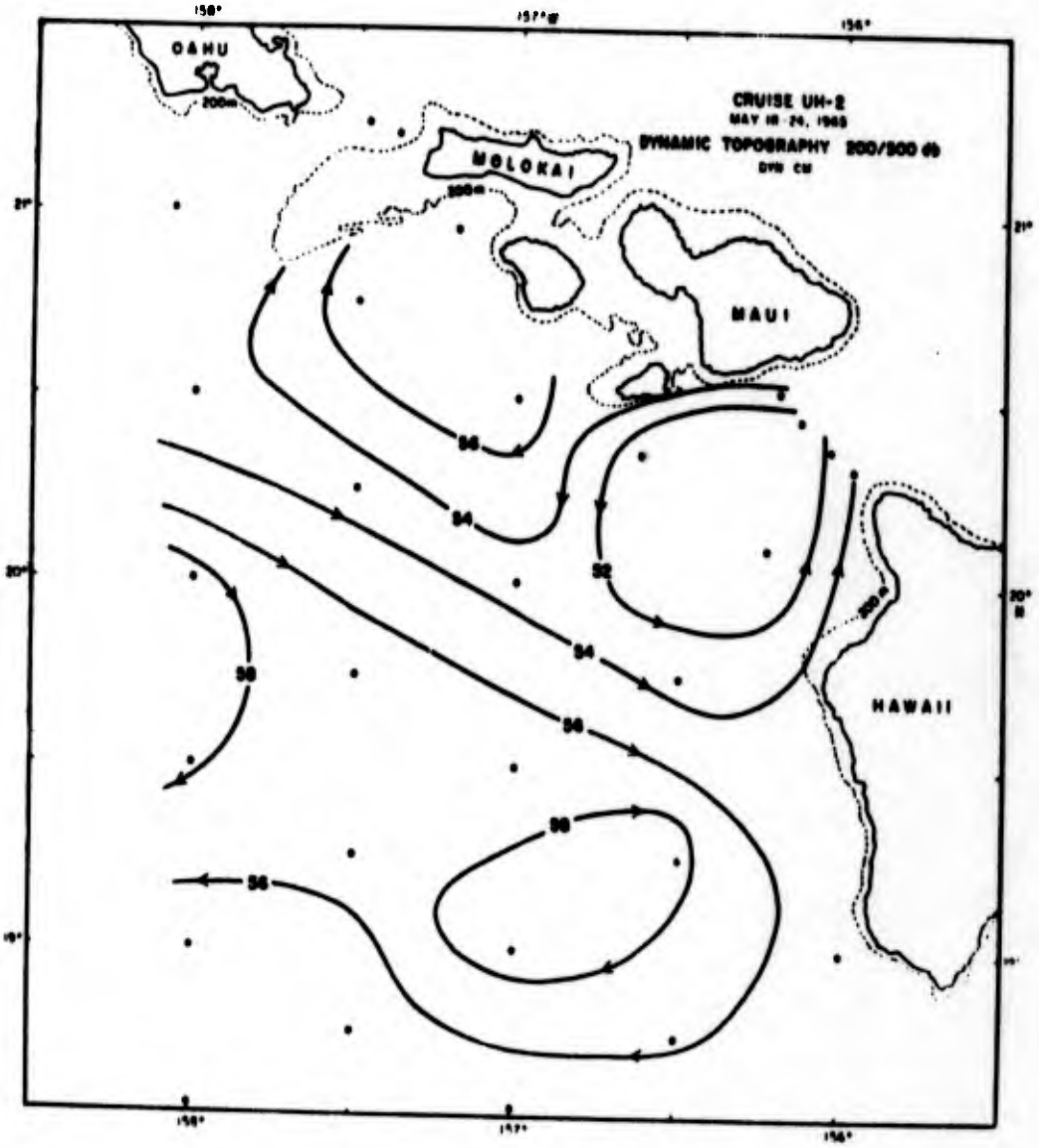

Figure 13. Dynamic topography 200/500 db from Cruise UH-2, May 18 - 24, 1965.

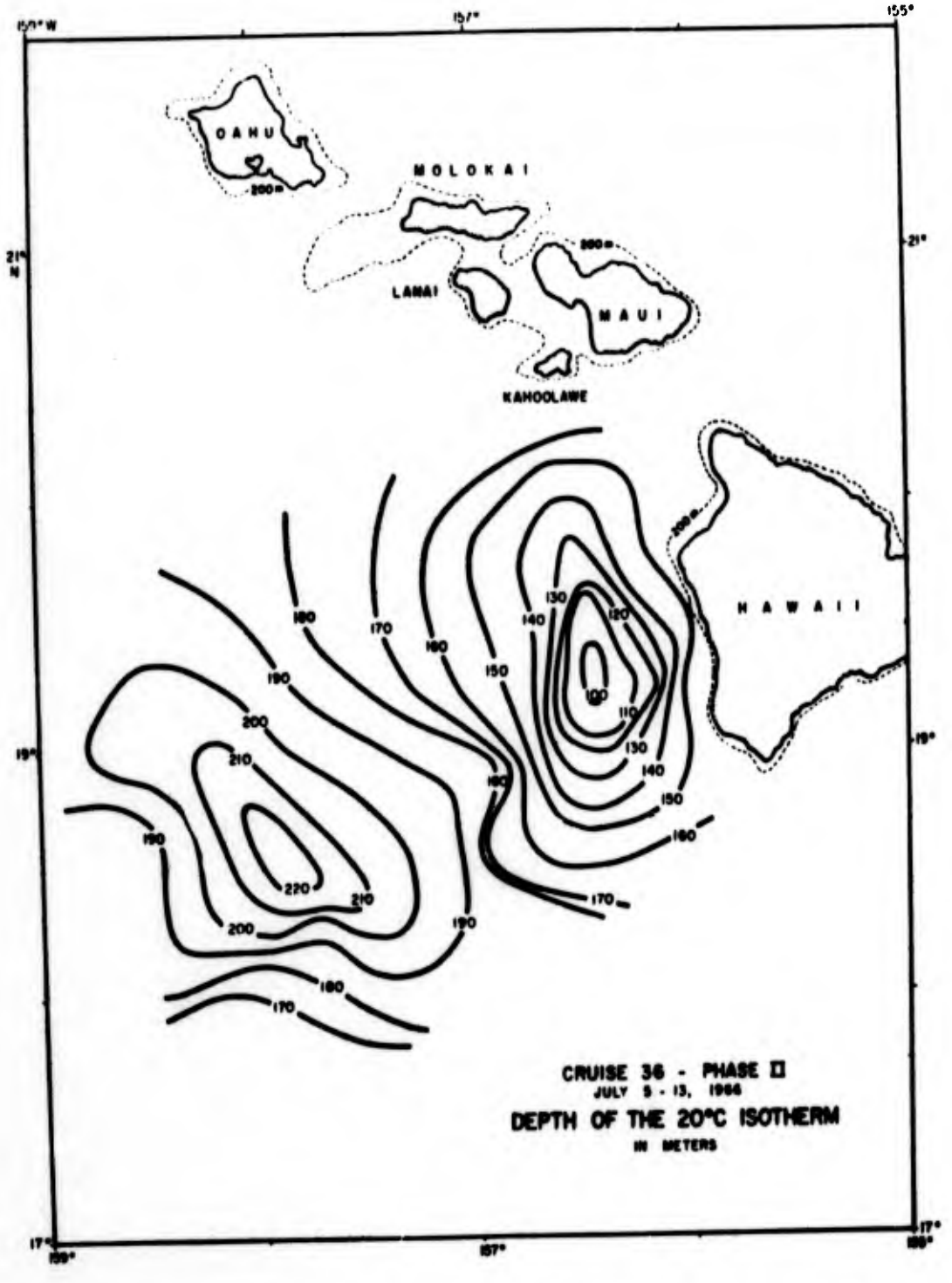

Figure 14. Depth of the 20°C isotherm from U.S.S. MARYSVILLE Cruise 36, Phase II, July 5 - 13, 1966.

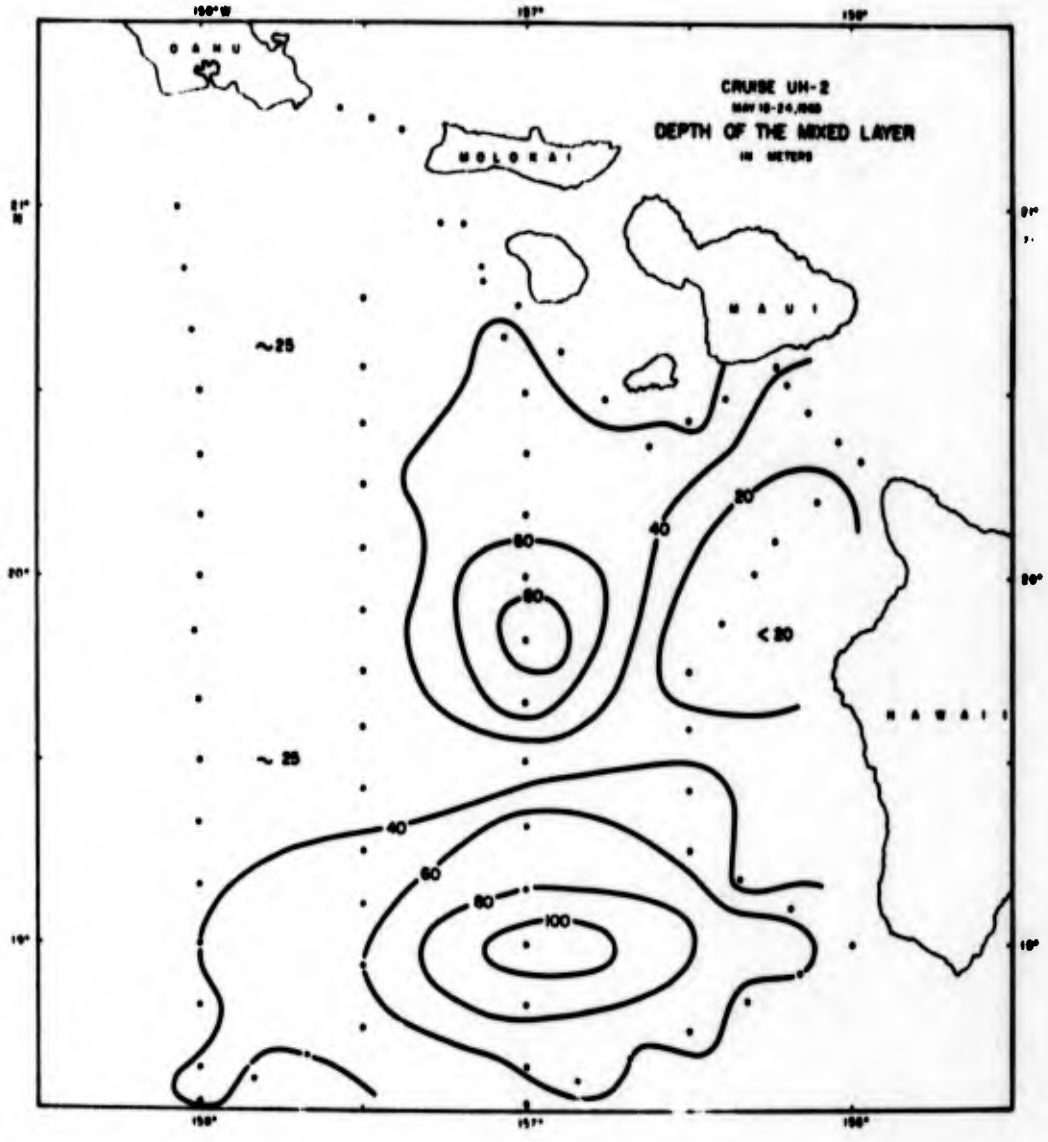

Figure 15. Depth of the mixed layer from Cruise UH-2, May 18 - 24, 1965.

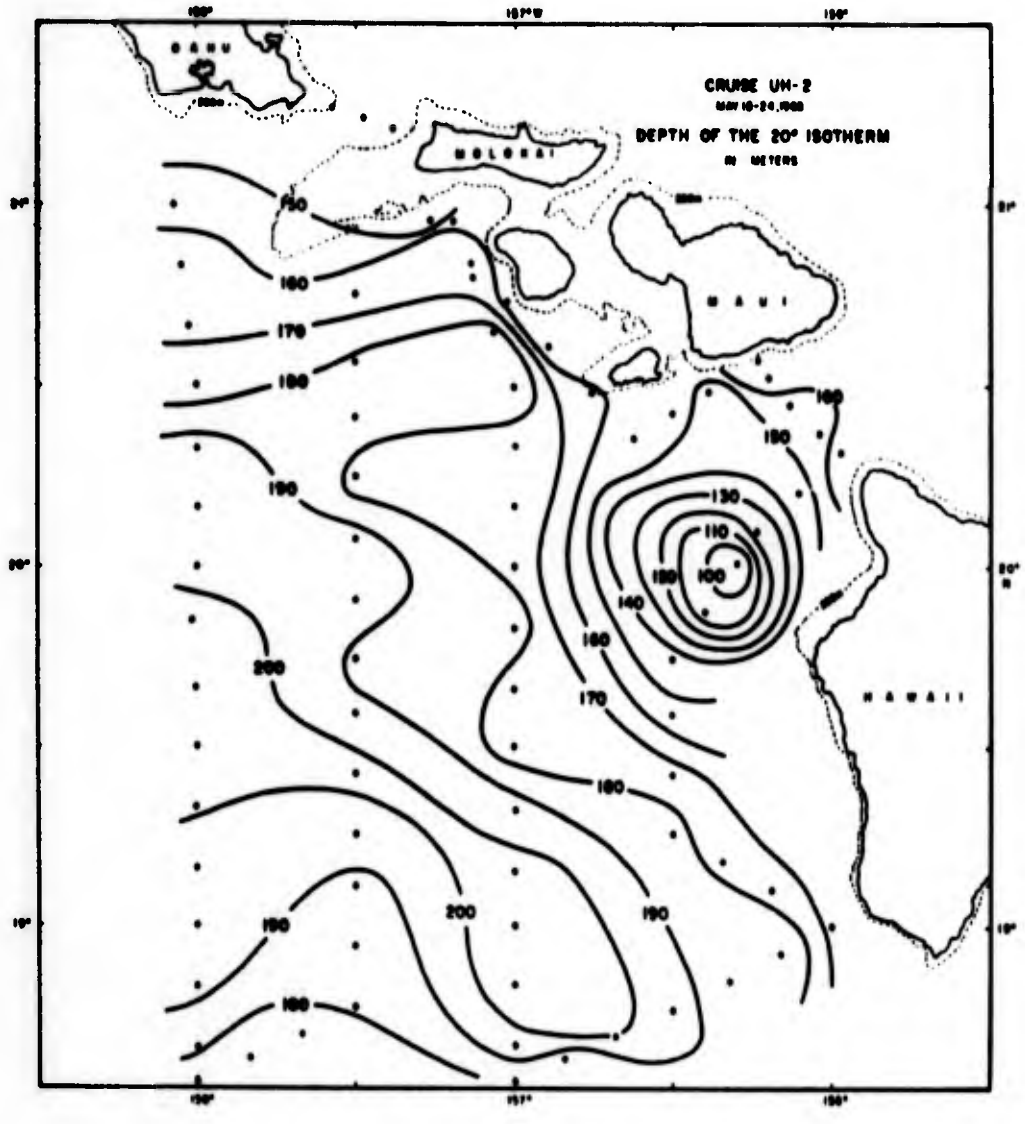

Figure 16. Depth of the 20°C isotherm from Cruise UH-2, May 18 - 24, 1965.

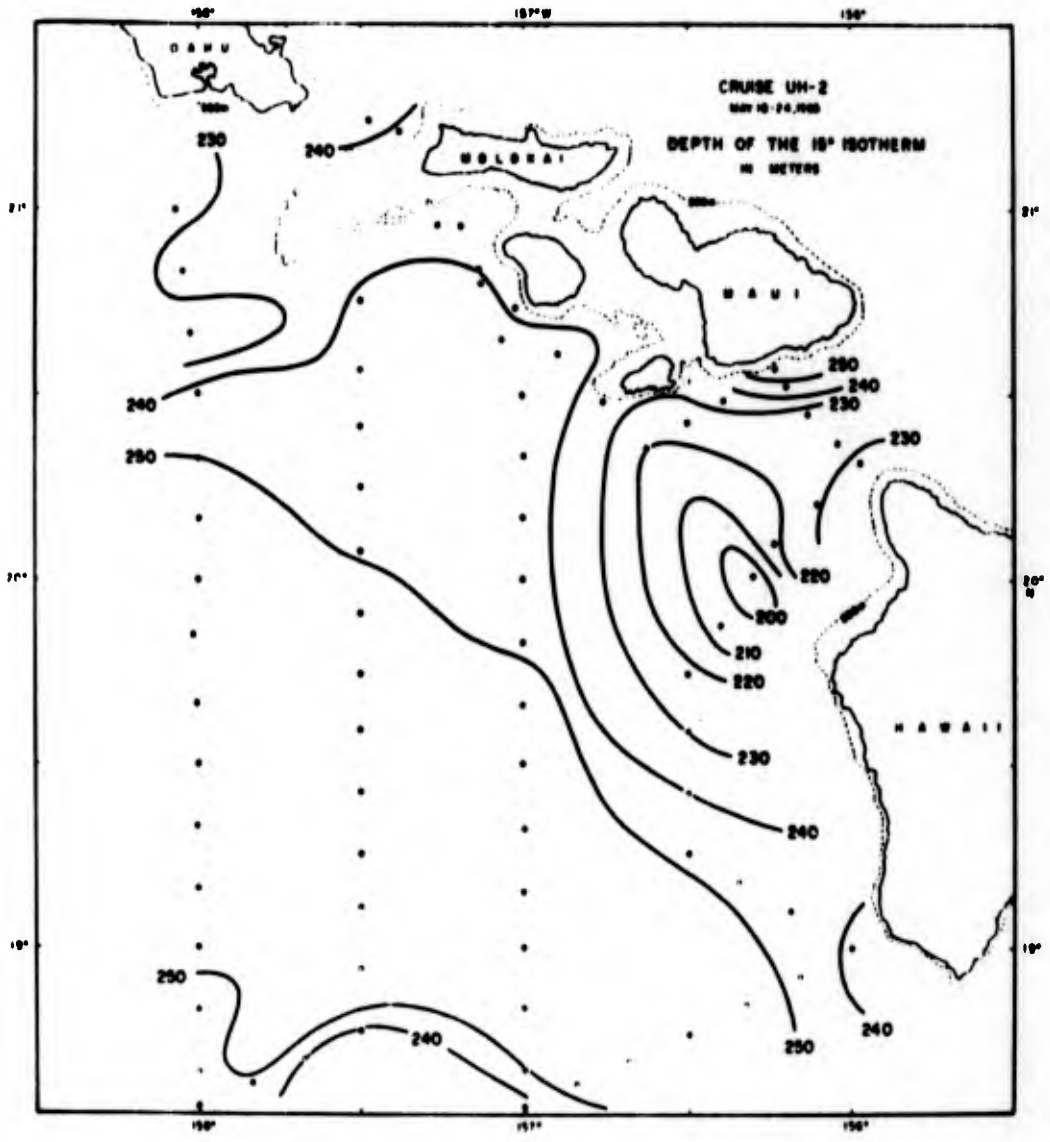

Figure 17. Depth of the 15°C isotherm from Cruise UH-2, May 18 - 24, 1965.

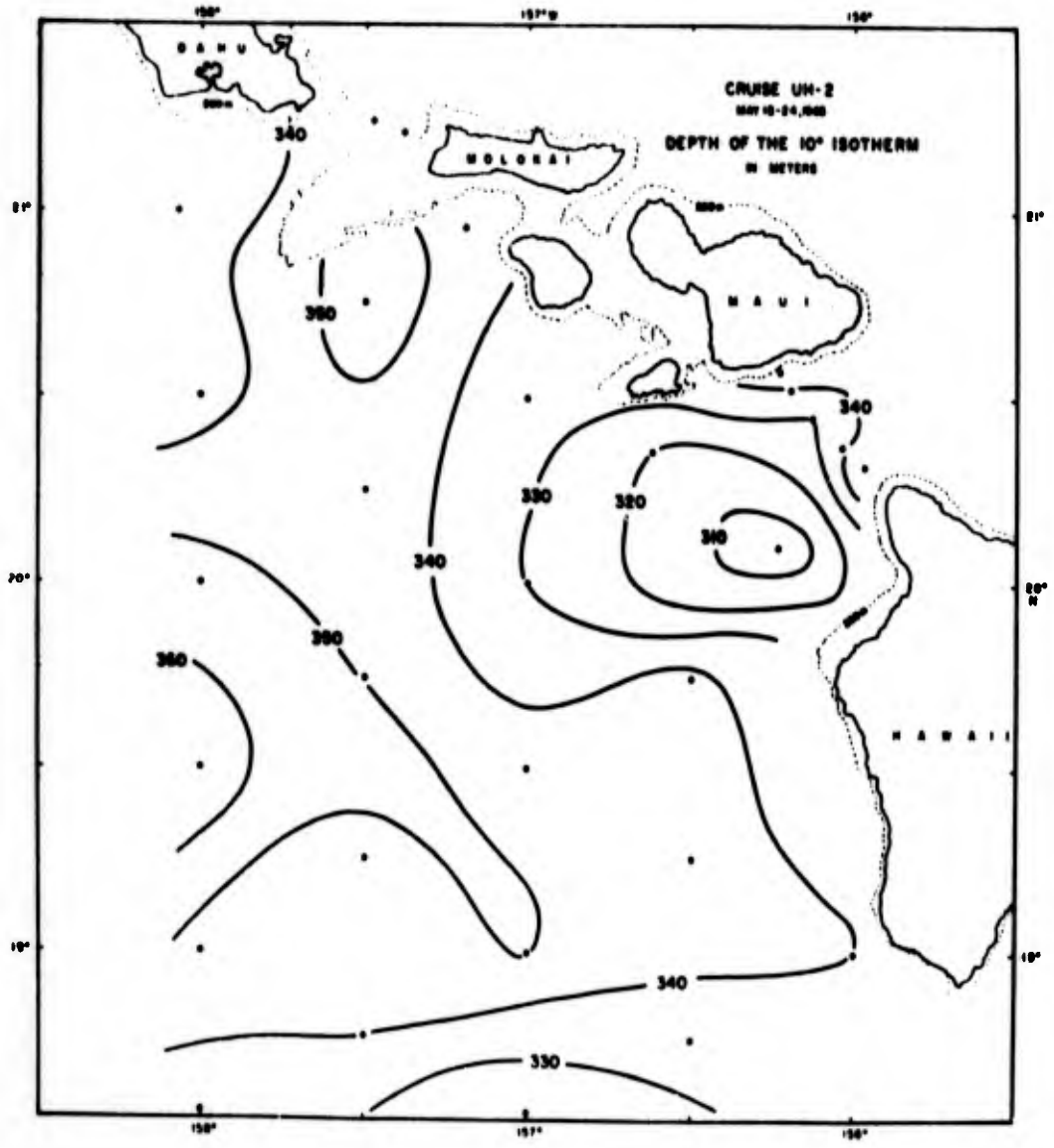

Figure 18. Depth of the 10°C isotherm from Cruise UH-2, May 18 - 24, 1965.

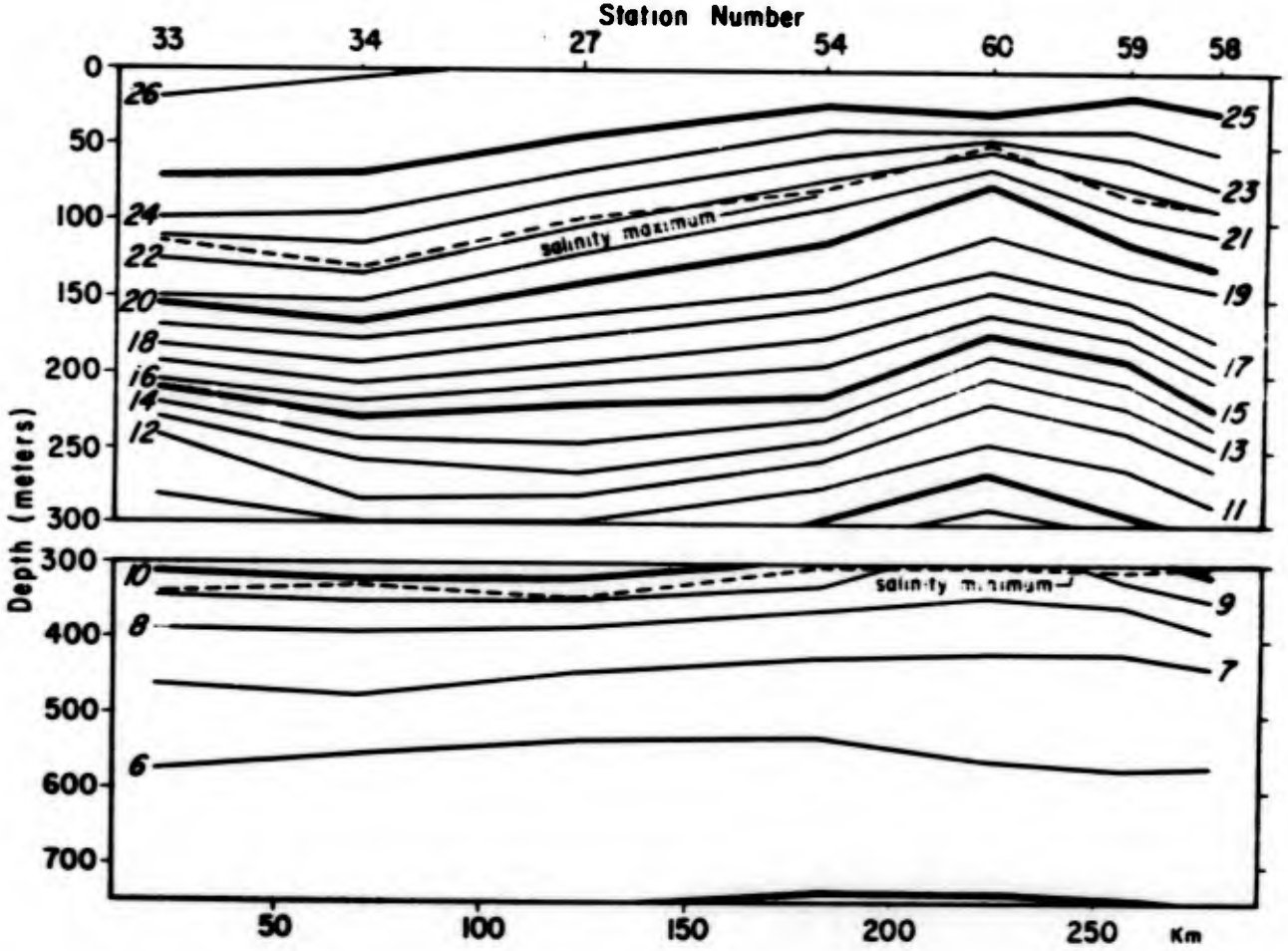

Figure 19. Temperature section across a small anti-cyclonic eddy (centered at station 34) and intense cyclonic eddy (centered at station 60) from Cruise UH-16, April 30 - May 6, 1967. Refer to Figure 7 for the positions of the stations.

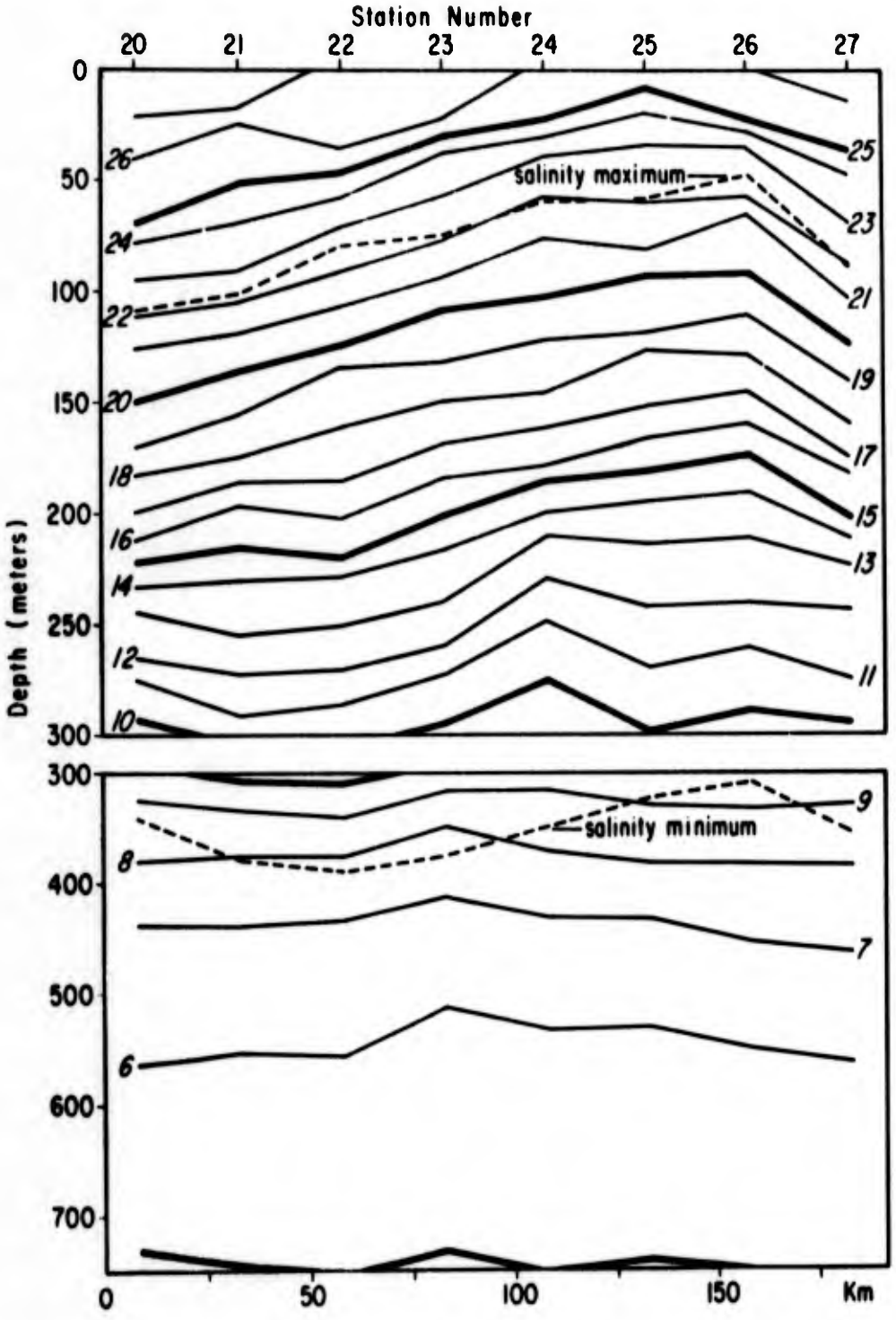

Figure 20. Temperature section across a cyclonic eddy from Cruise UH-17, June 12 - 20, 1967. Eddy centered at station 25.

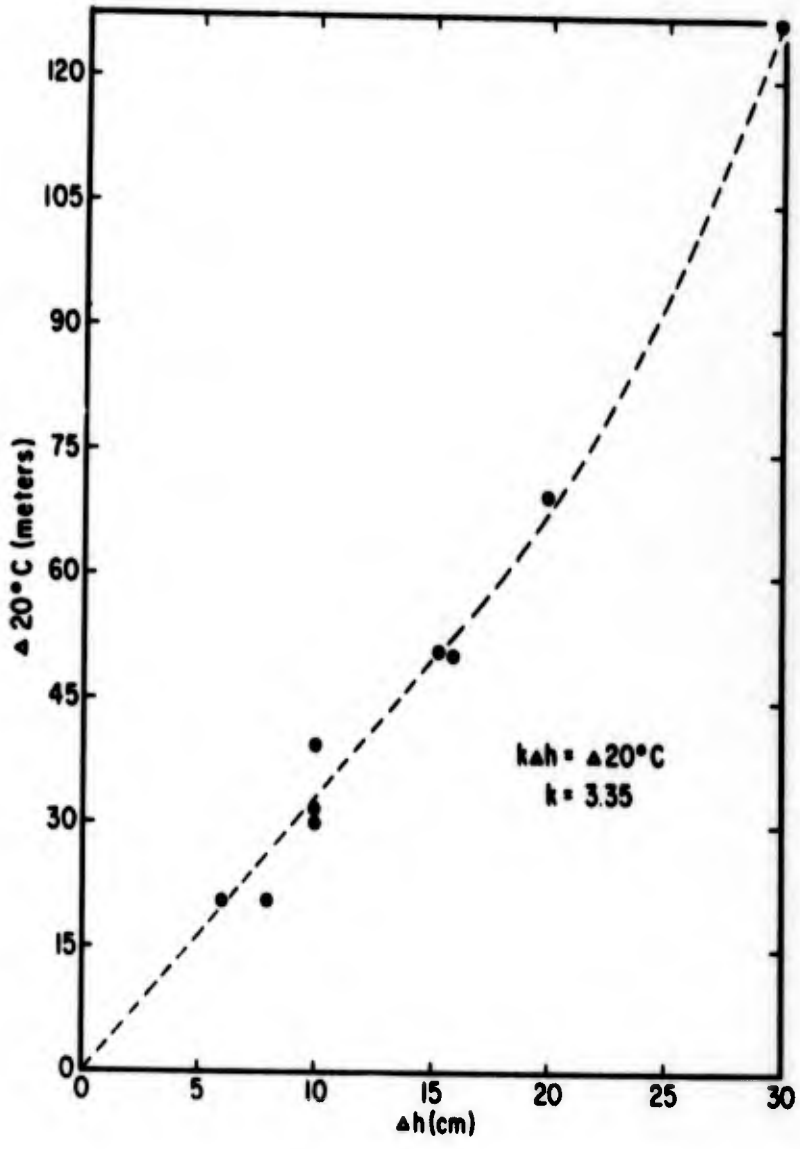

Figure 21. Observed change in the depth of the 20°C isotherm from the eddy center to periphery (Δ20°) versus the observed surface topography anomaly across the eddy (Δh) for the eddies observed during Cruises UH-2, UH-3, UH-12, UH-14, UH-16, and UH-17.

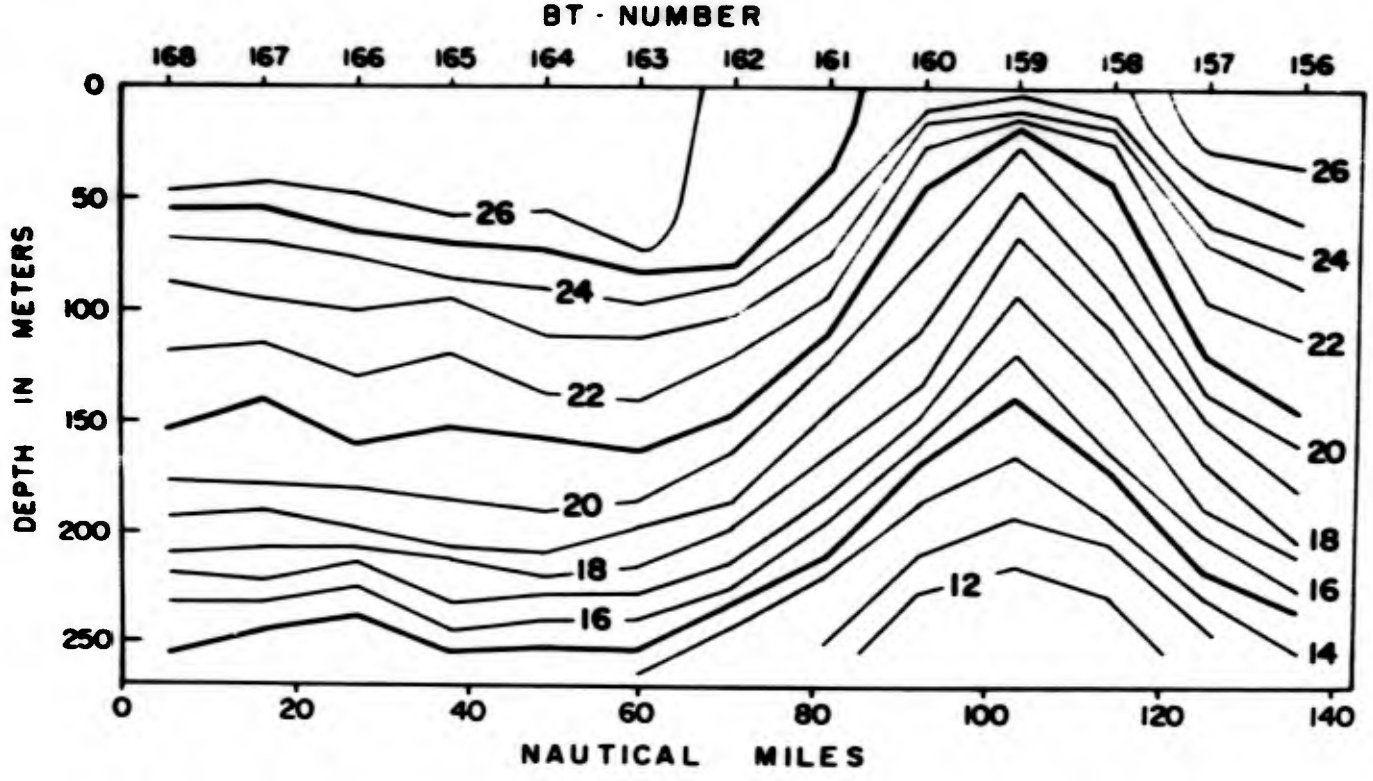

Figure 22. Temperature section (°C) across the intense cyclonic eddy observed during Cruise UH-3, July 19 - 23, 1965.

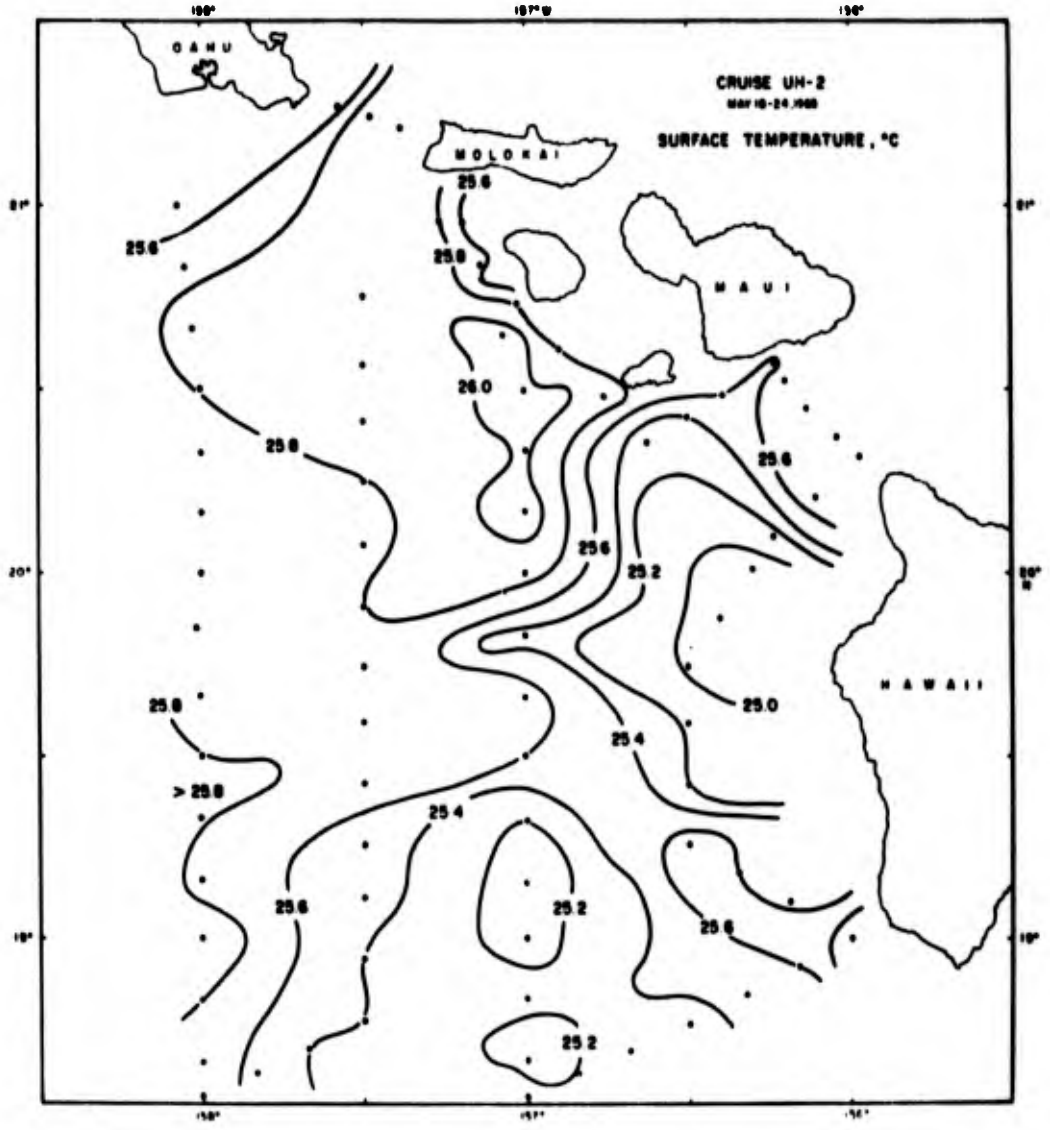

Figure 23. Surface temperature from Cruise UH-2, May 18 - 24, 1965.

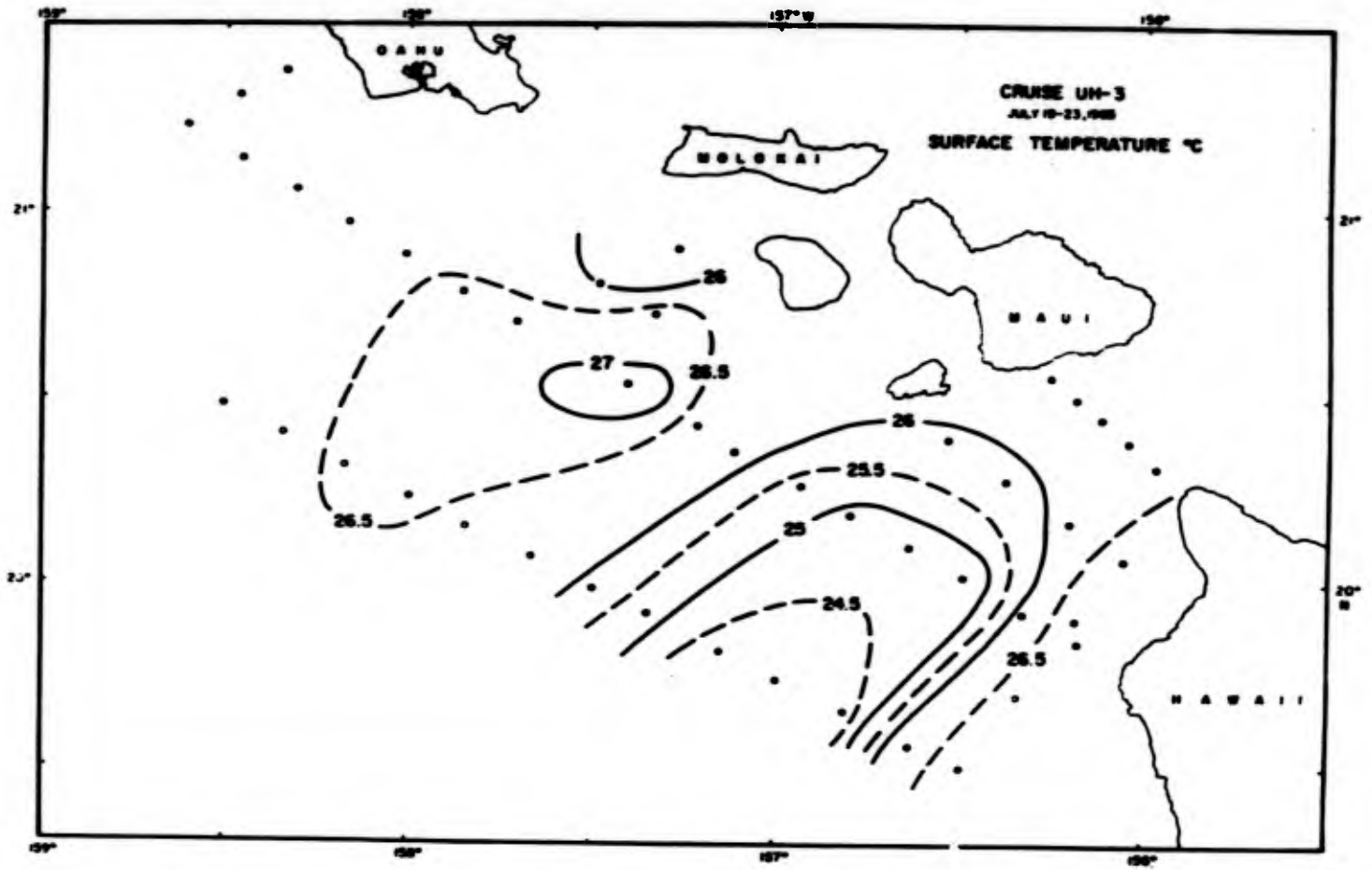

Figure 24. Surface temperature from Cruise UH-3, July 19 - 23, 1965.

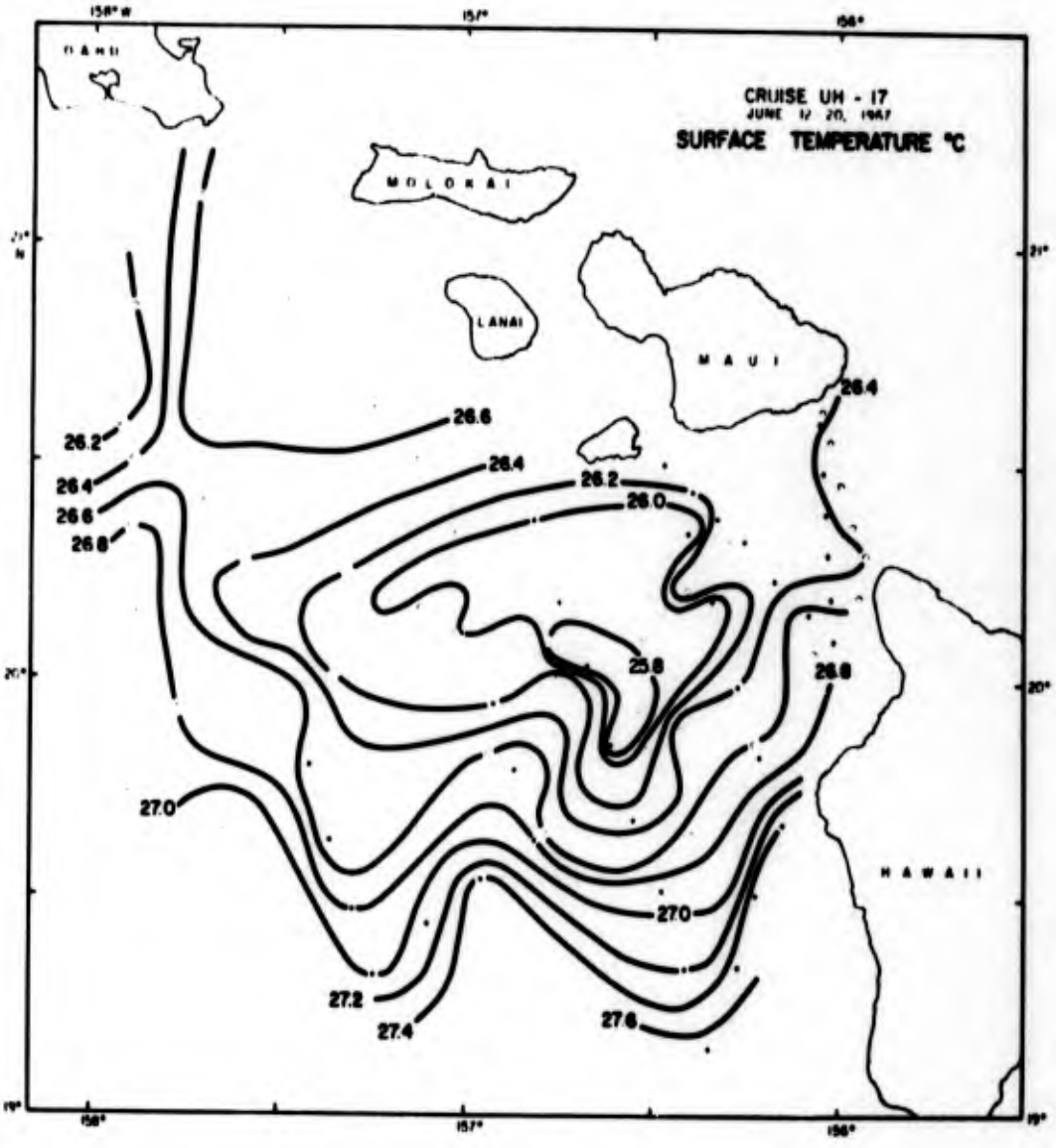

Figure 25. Surface temperature from Cruise UH-17, June 12 - 20, 1967.

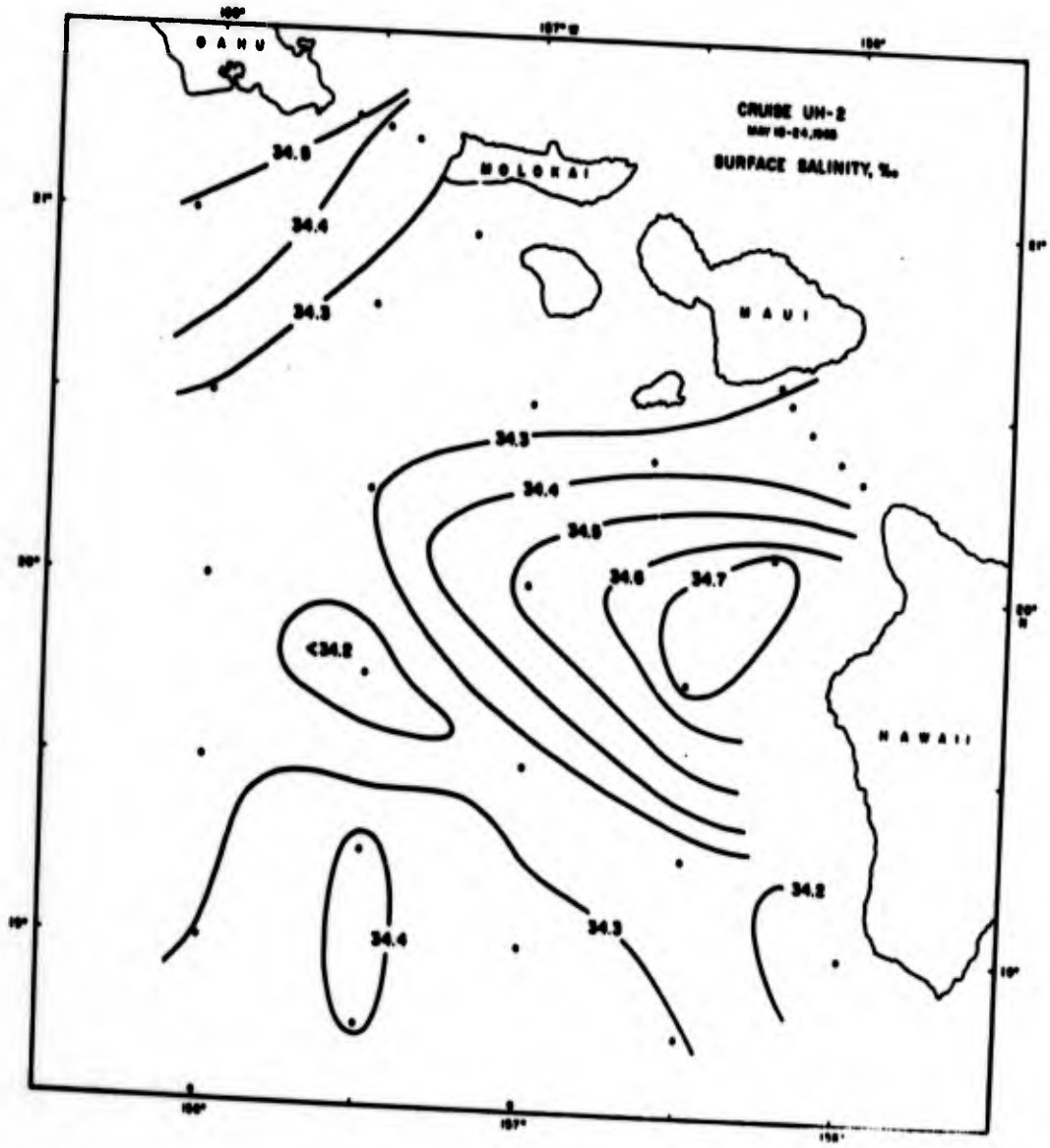

Figure 26. Surface salinity from Cruise UH-2, May 18 - 24, 1965.

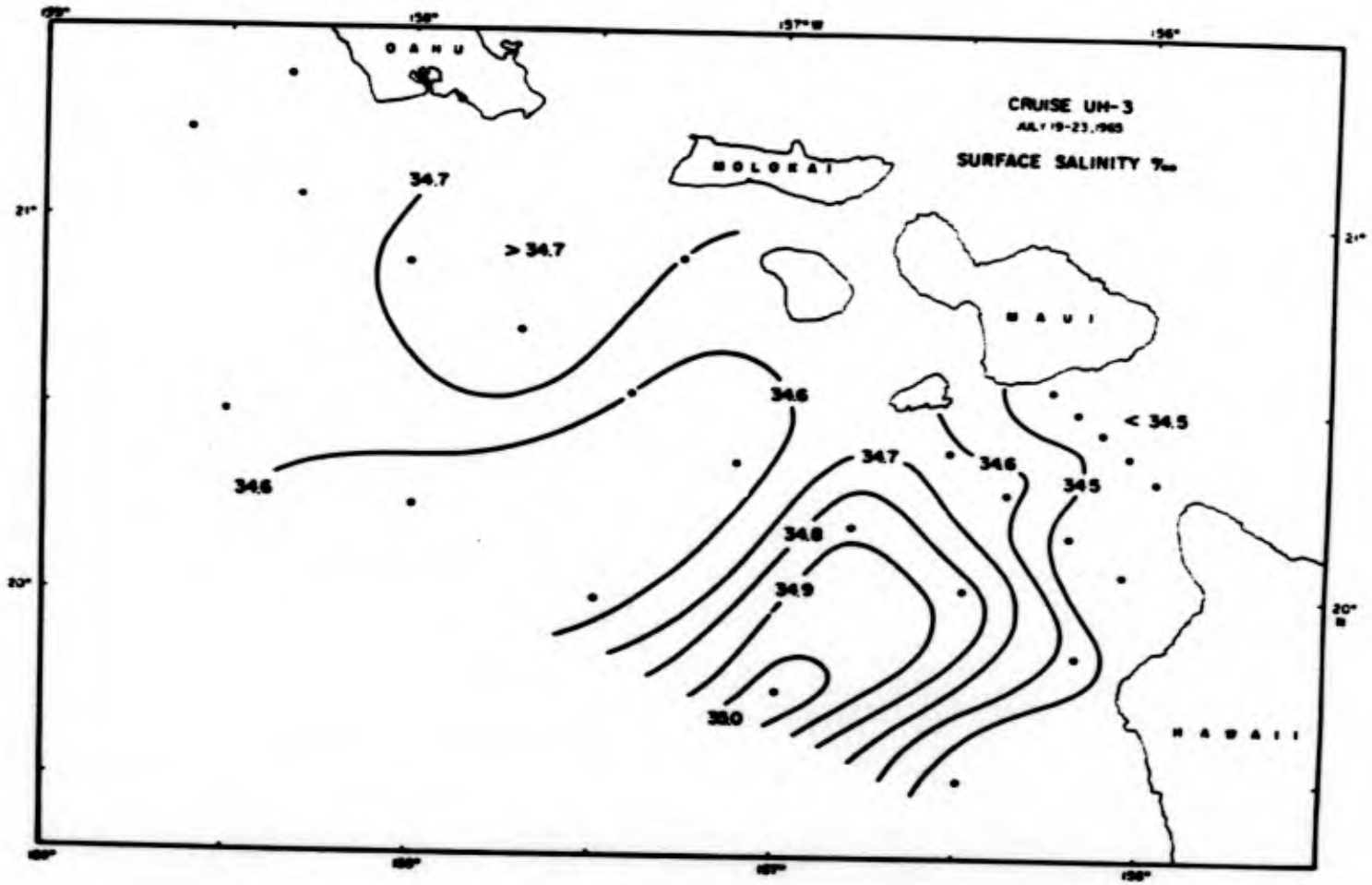

Figure 27. Surface salinity from Cruise UH-3, July 19 - 23, 1965.

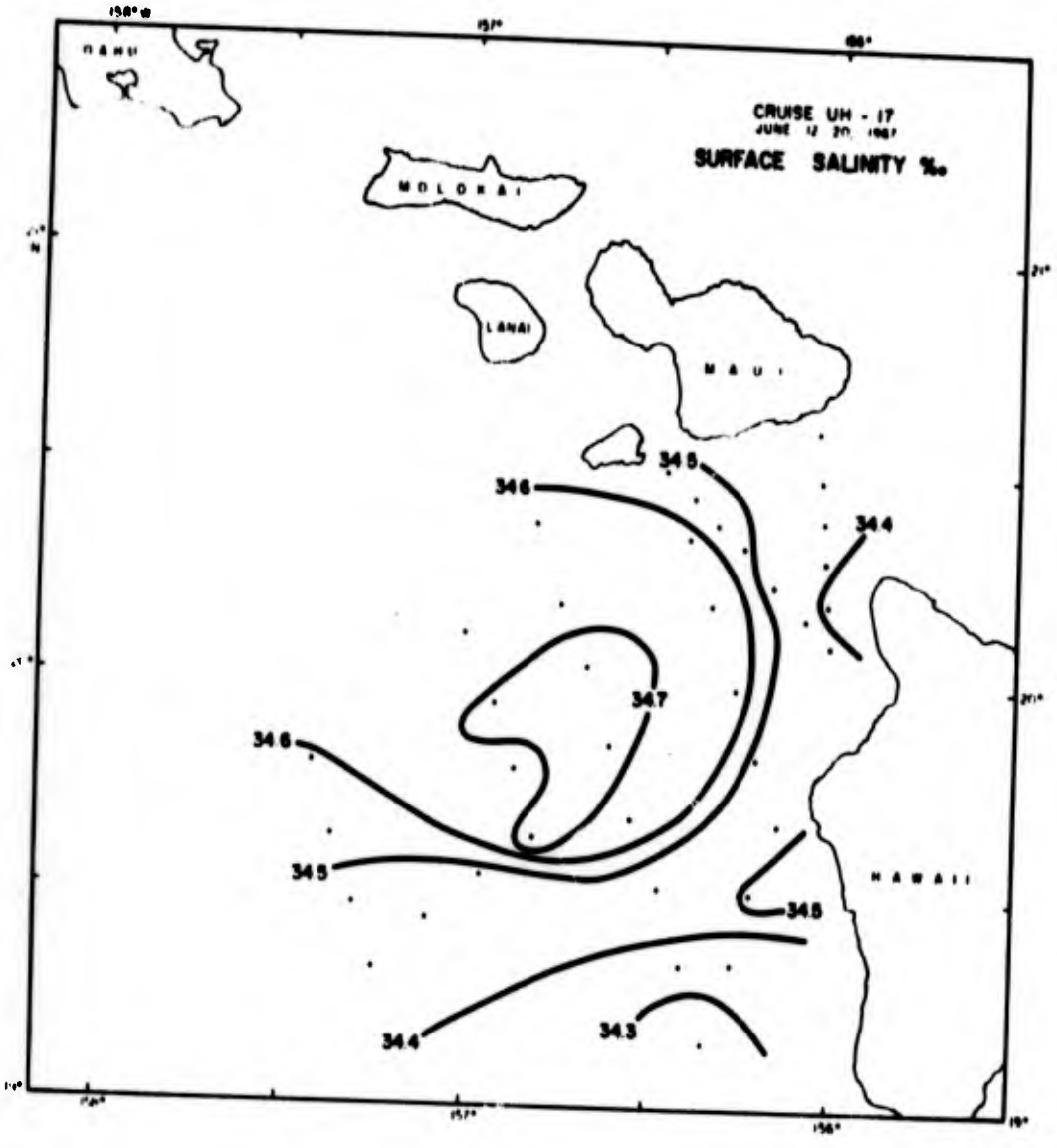

Figure 28. Surface salinity from Cruise UH-17, June 12 - 20, 1967.

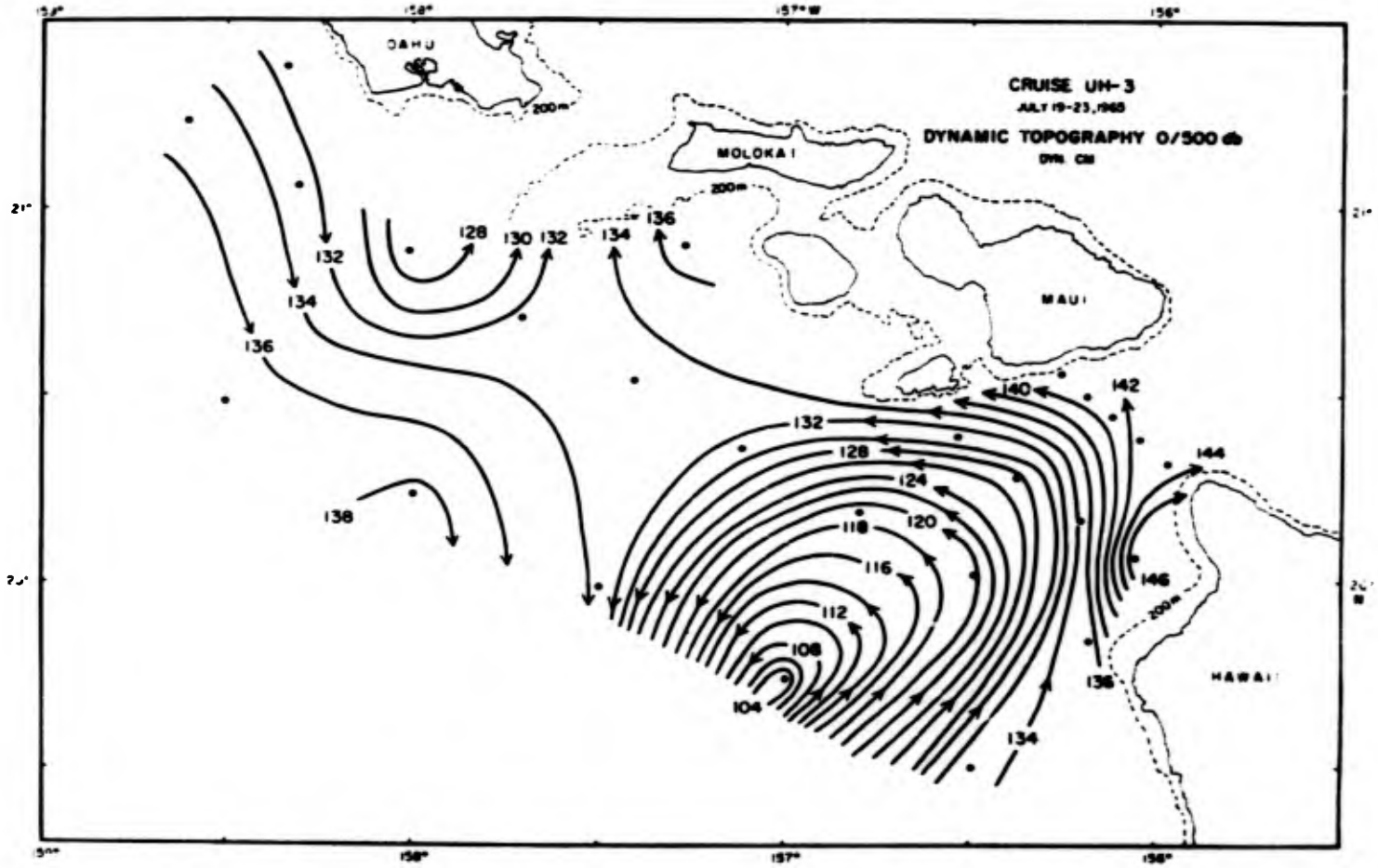

Figure 29. Dynamic topography 0/500 db from Cruise UH-3, July 19 - 23, 1965.

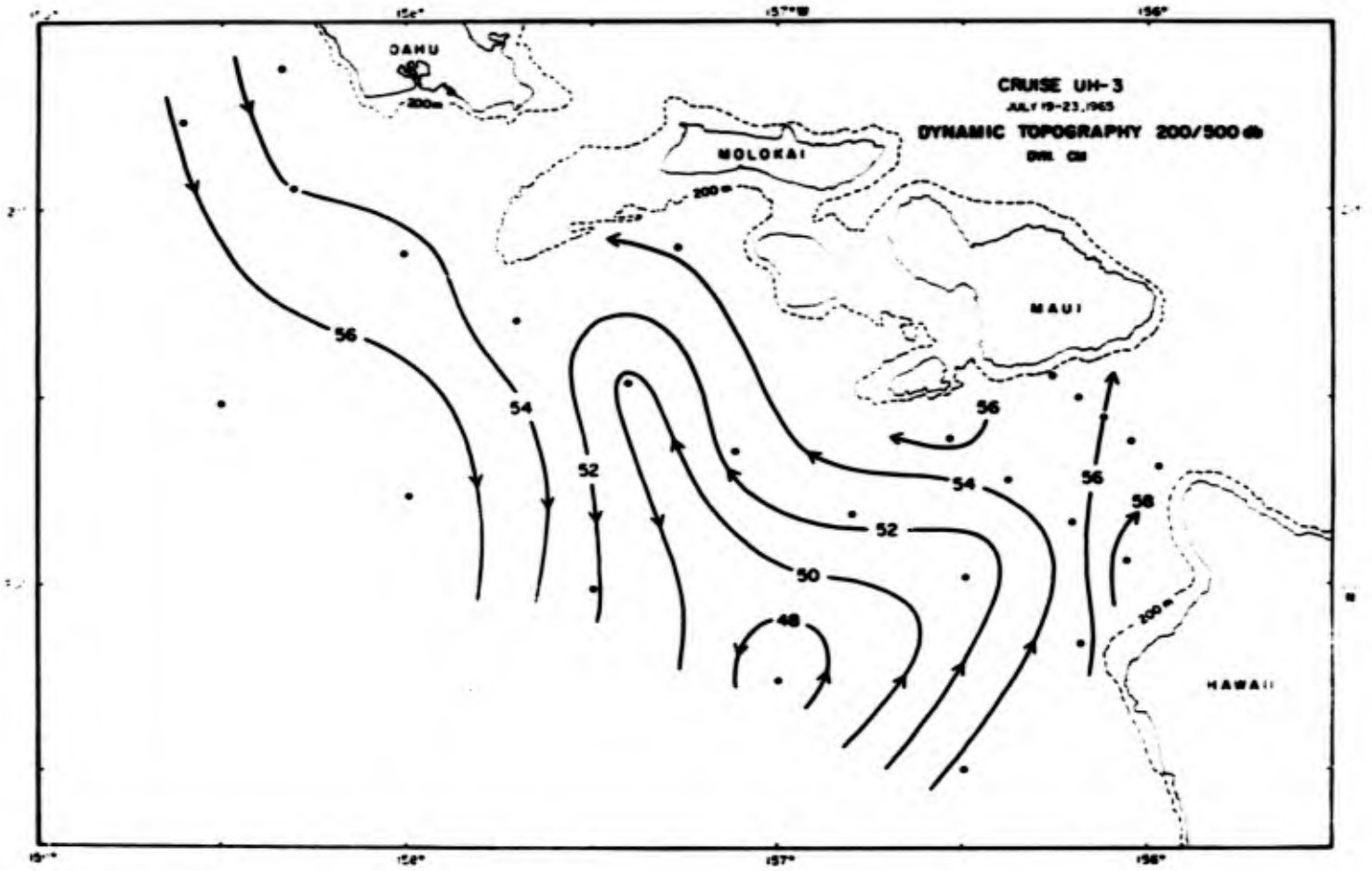

Figure 30. Dynamic topography 200/500 db from Cruise UH-3, July 19 - 23, 1965.

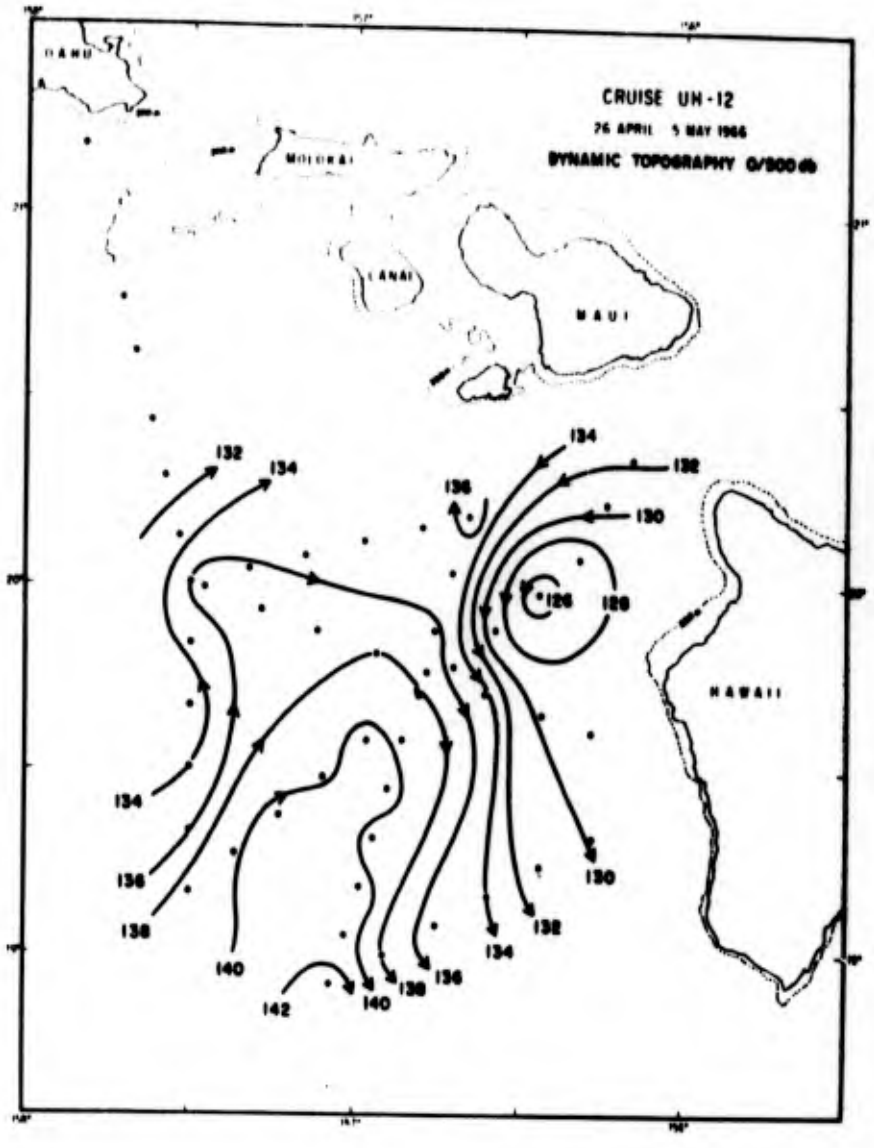

Figure 31. Dynamic topography (dyn cm) 0/500 db from Cruise UH-12, April 26 - May 5, 1966.

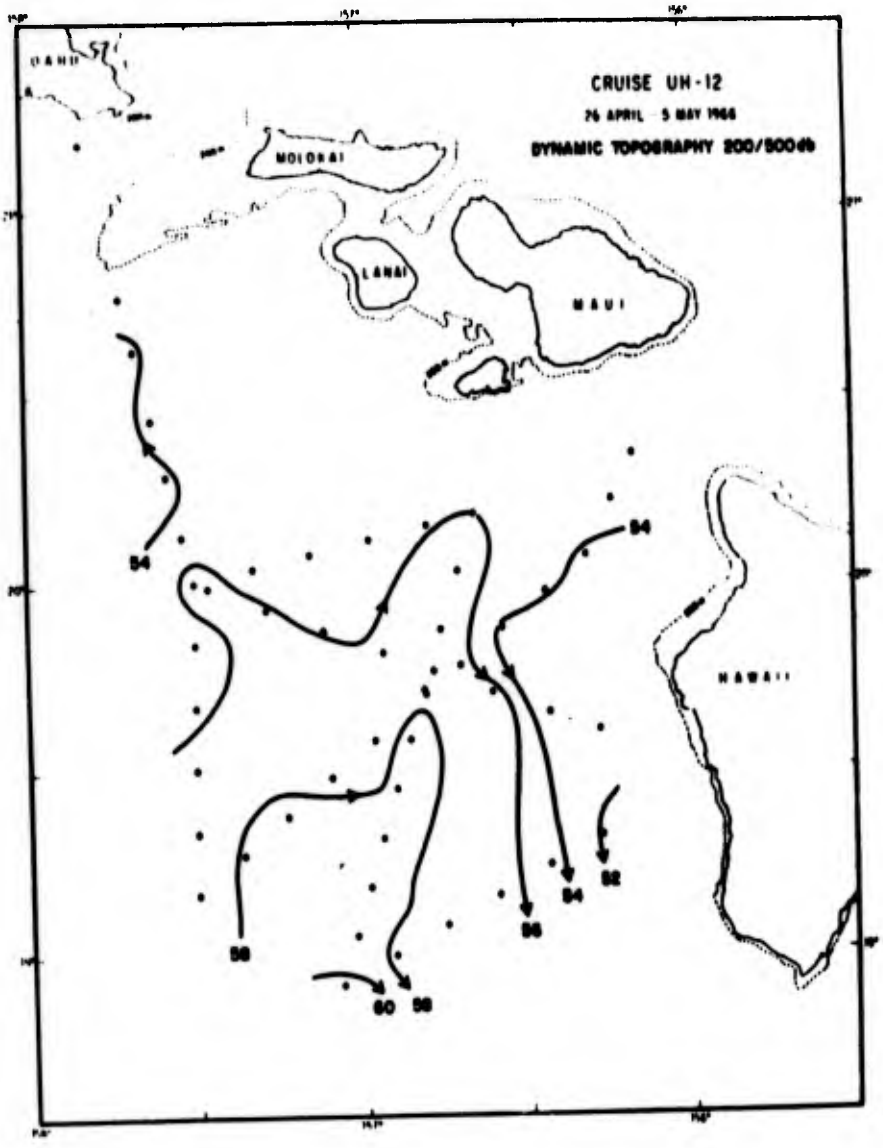

Figure 32. Dynamic topography (dyn cm) 200/500 db from Cruise UH-12, April 26 - May 5, 1966.

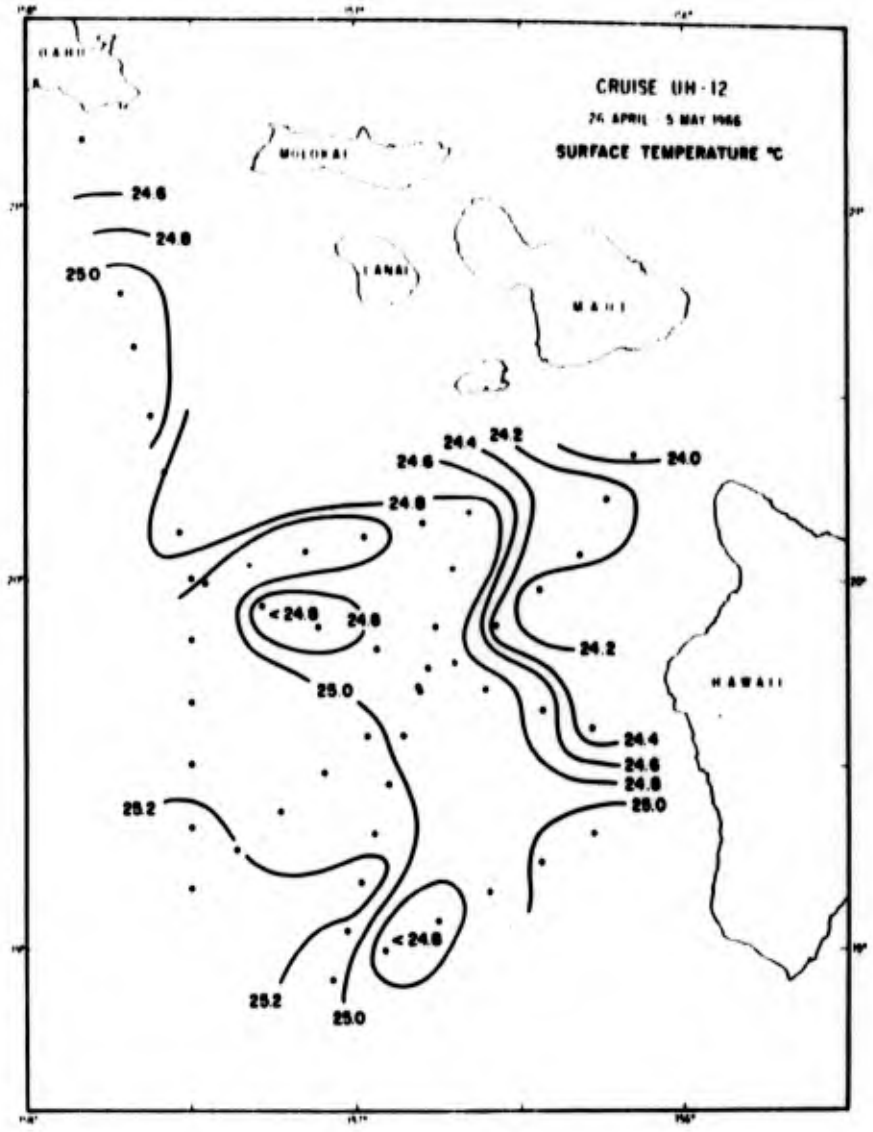

Figure 33. Surface temperature from Cruise UH-12, April 26 - May 5, 1966.

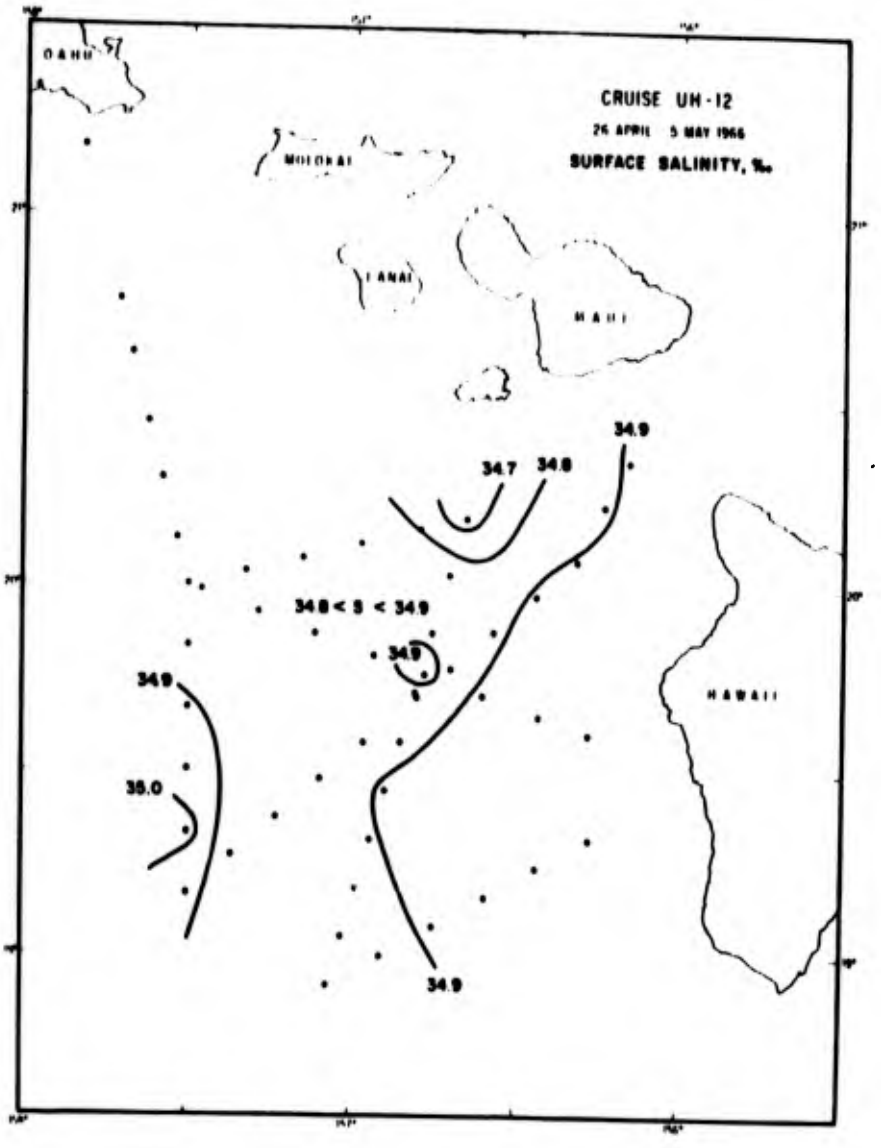

Figure 34. Surface salinity from Cruise UH-12, April 26 - May 5, 1966.

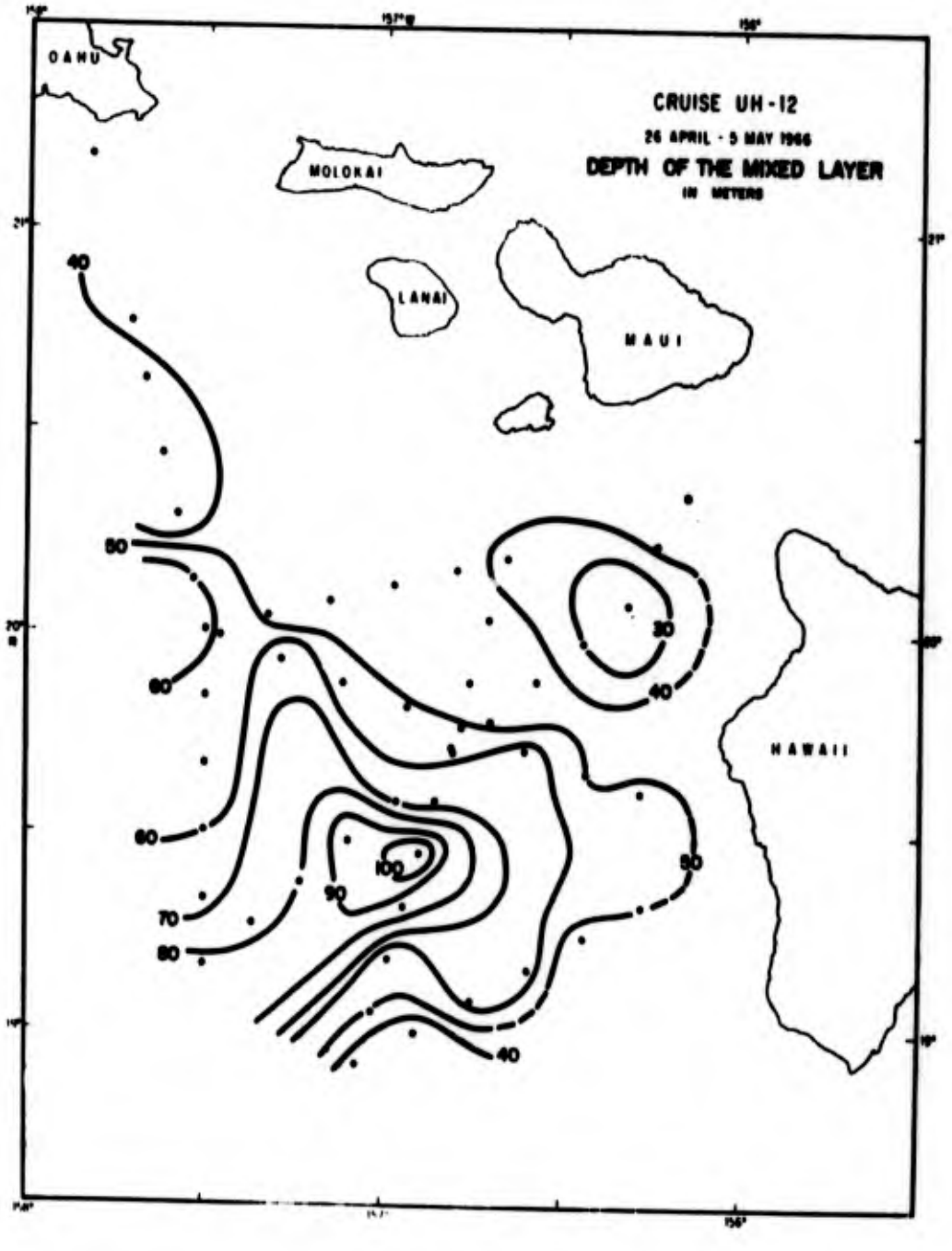

Figure 35. Depth of the mixed layer from Cruise UH-12, April 26 - May 5, 1966.

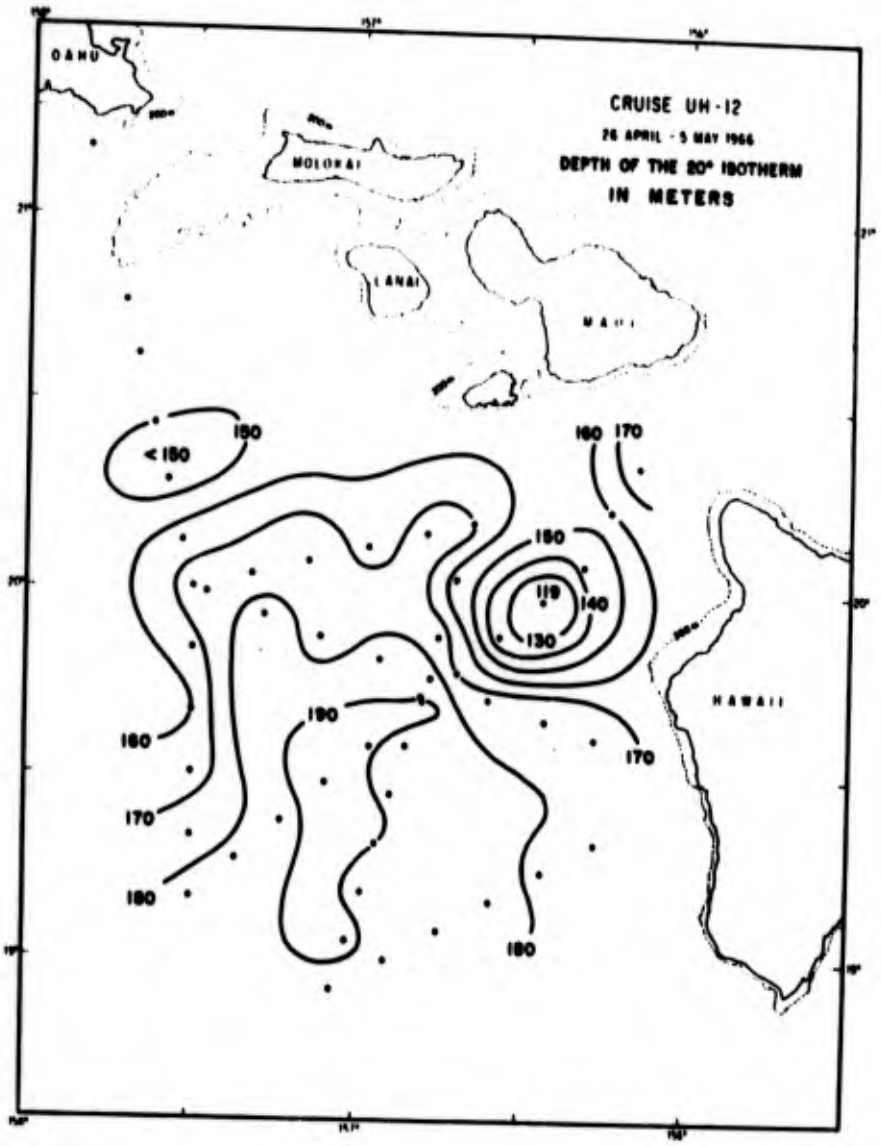

Figure 36. Depth of the 20°C isotherm from Cruise UH-12, April 26 - May 5, 1966.

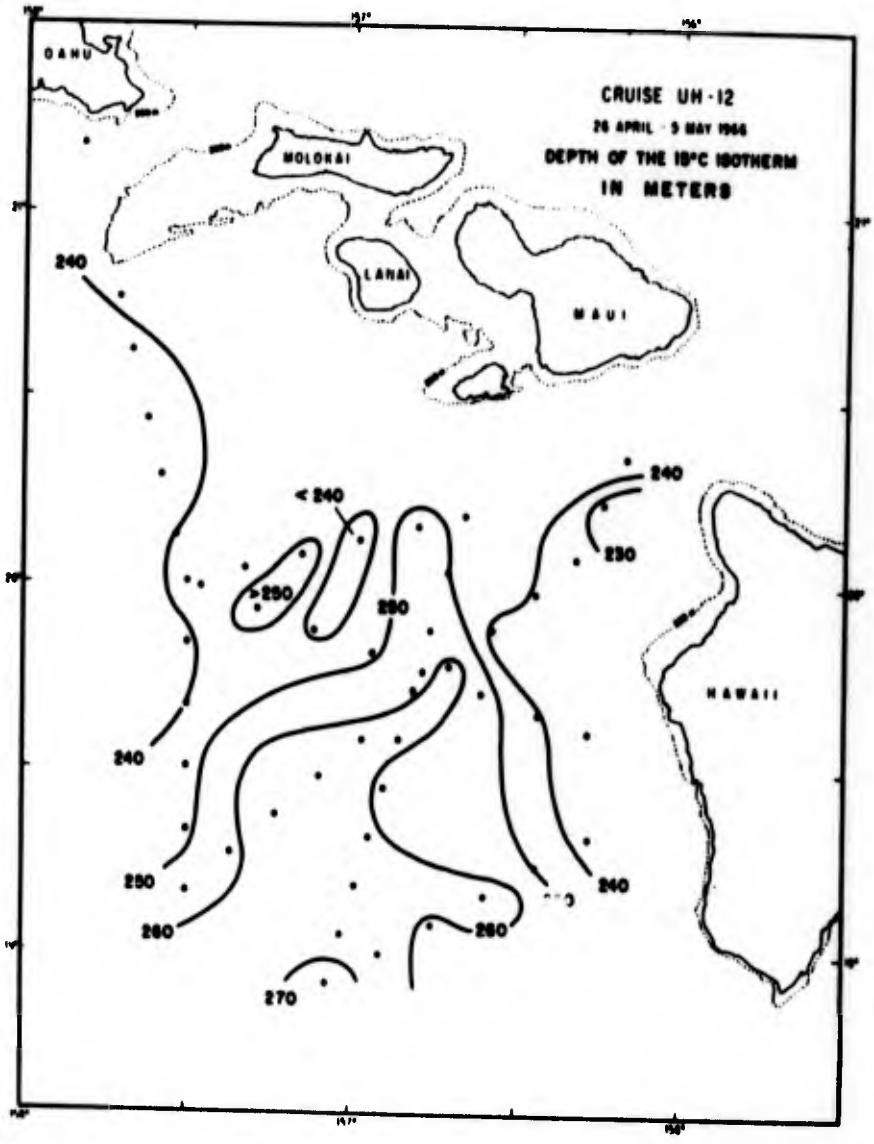

Figure 37. Depth of the 15°C isotherm from Cruise UH-12, April 26 - May 5, 1966.

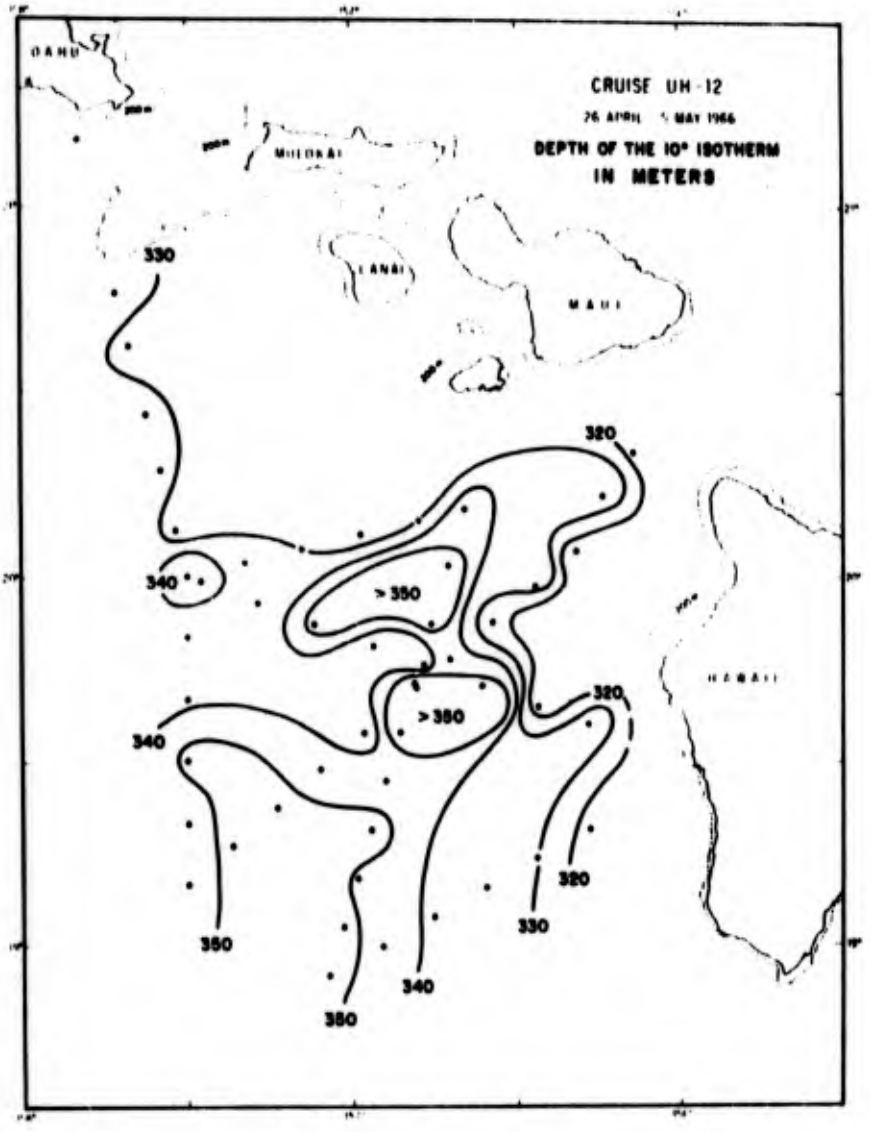

Figure 38. Depth of the 10°C isotherm from Cruise UH-12, April 26 - May 5, 1966.

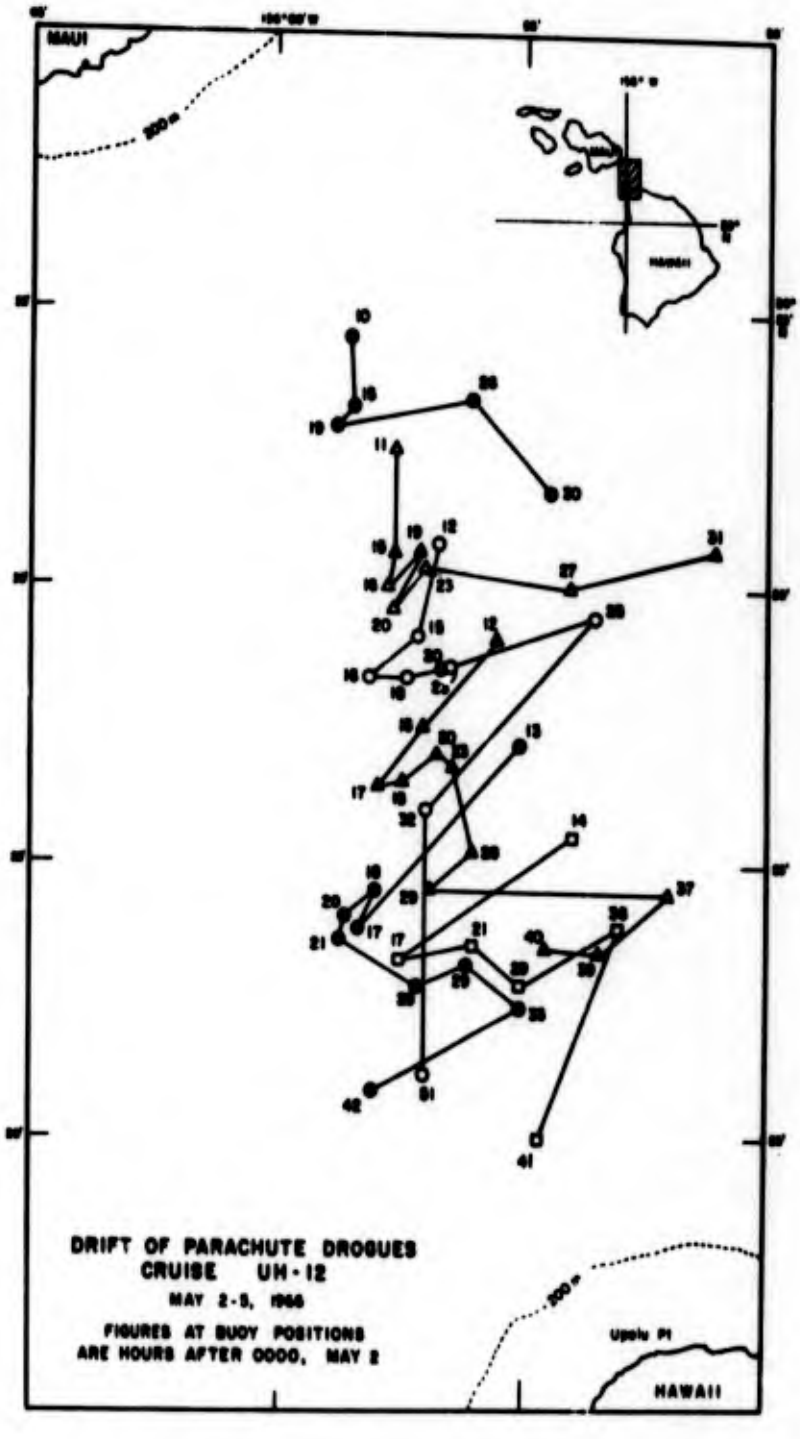

Figure 39. Drift of parachute drogues from Cruise UH-12, May 2 - 5, 1966. Figures at buoy positions are hours after 0000, May 2.

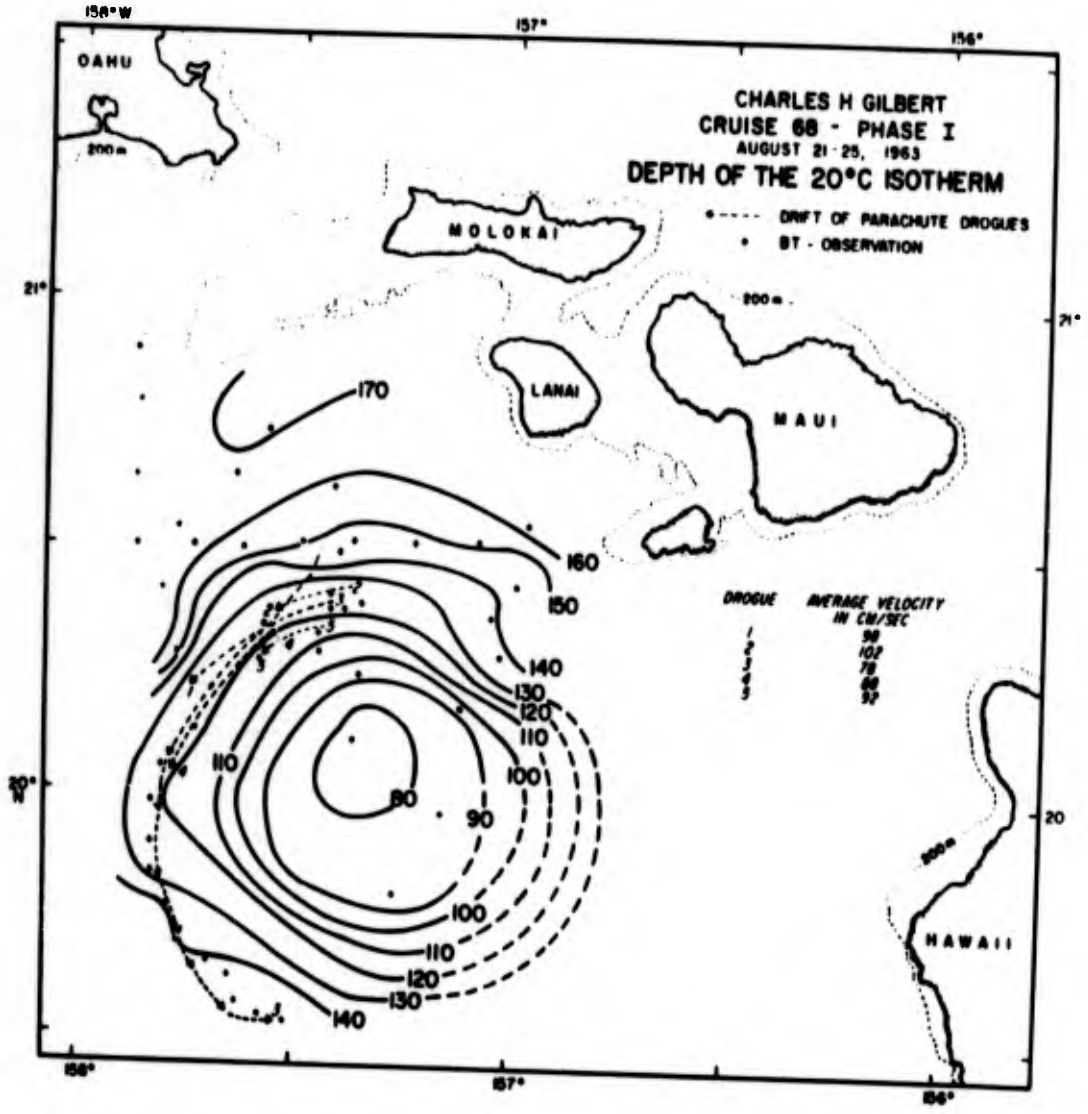

Figure 40. Depth of the 20°C isotherm (m) and drift of parachute drogues from CHARLES H. GILBERT Cruise 68, Phase I, August 21 - 25, 1963. The average velocities of drogues 1 - 5 are listed. The depth of the drogues was 15 meters.

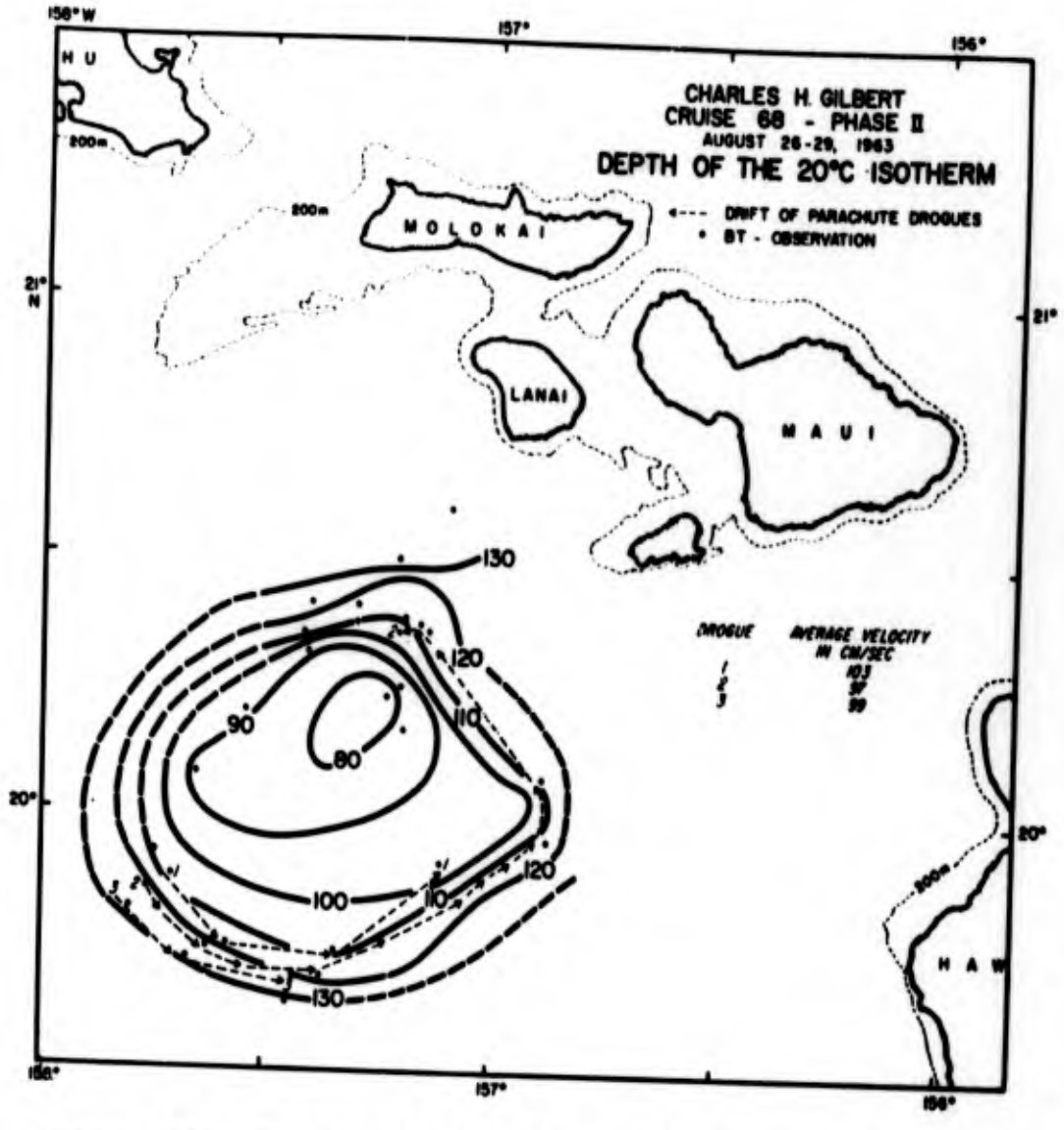

Figure 41. Depth of the 20°C isotherm (m) and drift of parachute drogues from CHARLES H. GILBERT Cruise 68, Phase II, August 26 - 29, 1963. The average velocities of drogues 1 - 3 are listed. The depth of the drogues was 15 meters.

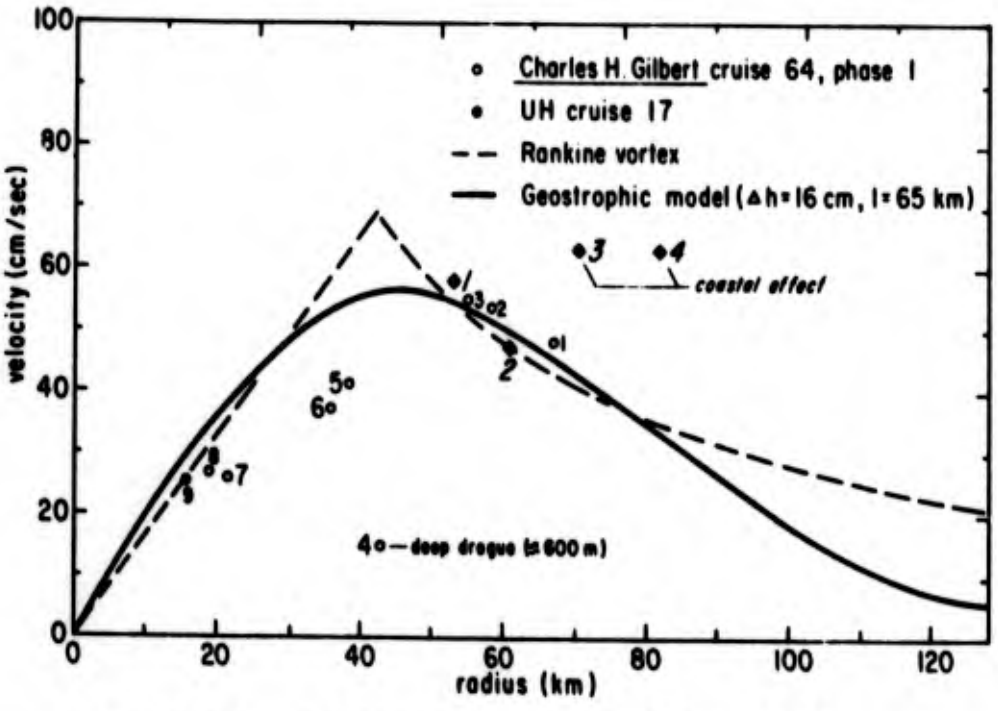

Figure 42. The average velocities of the drogues from CHARLES H. GILBERT Cruise 64, Phase I, and Cruise UH-17 versus the eddy radius. Drogue numbers correspond to the numbers shown in Figures 46 and 49. Also shown are the velocity distributions for the Rankine vortex and the geostrophic eddy model (Δh = 16 cm and ℓ = 65 km).

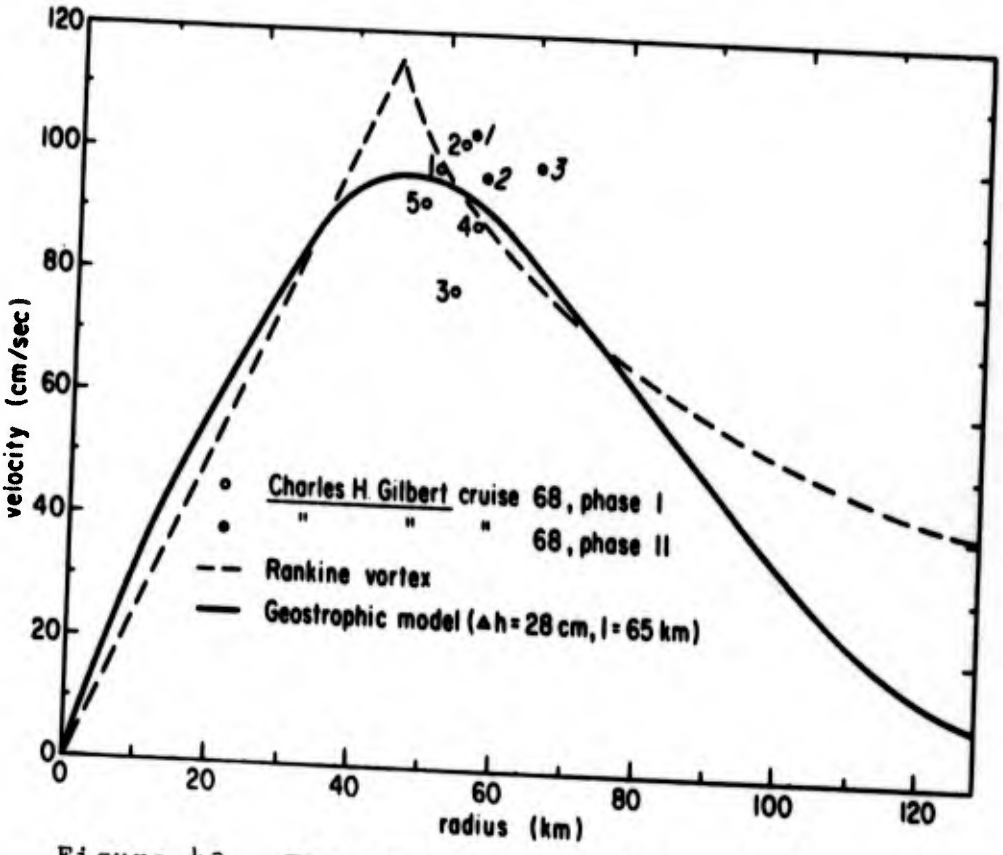

Figure 43. The average velocities of the drogues from CHARLES H. GILBERT Cruise 68, Phase I and II, versus the eddy radius. Drogue numbers correspond to the numbers shown in Figures 40 and 41. Also shown are the velocity distributions for the Rankine vortex and the geostrophic model (Δh = 28 cm and ℓ = 65 km).

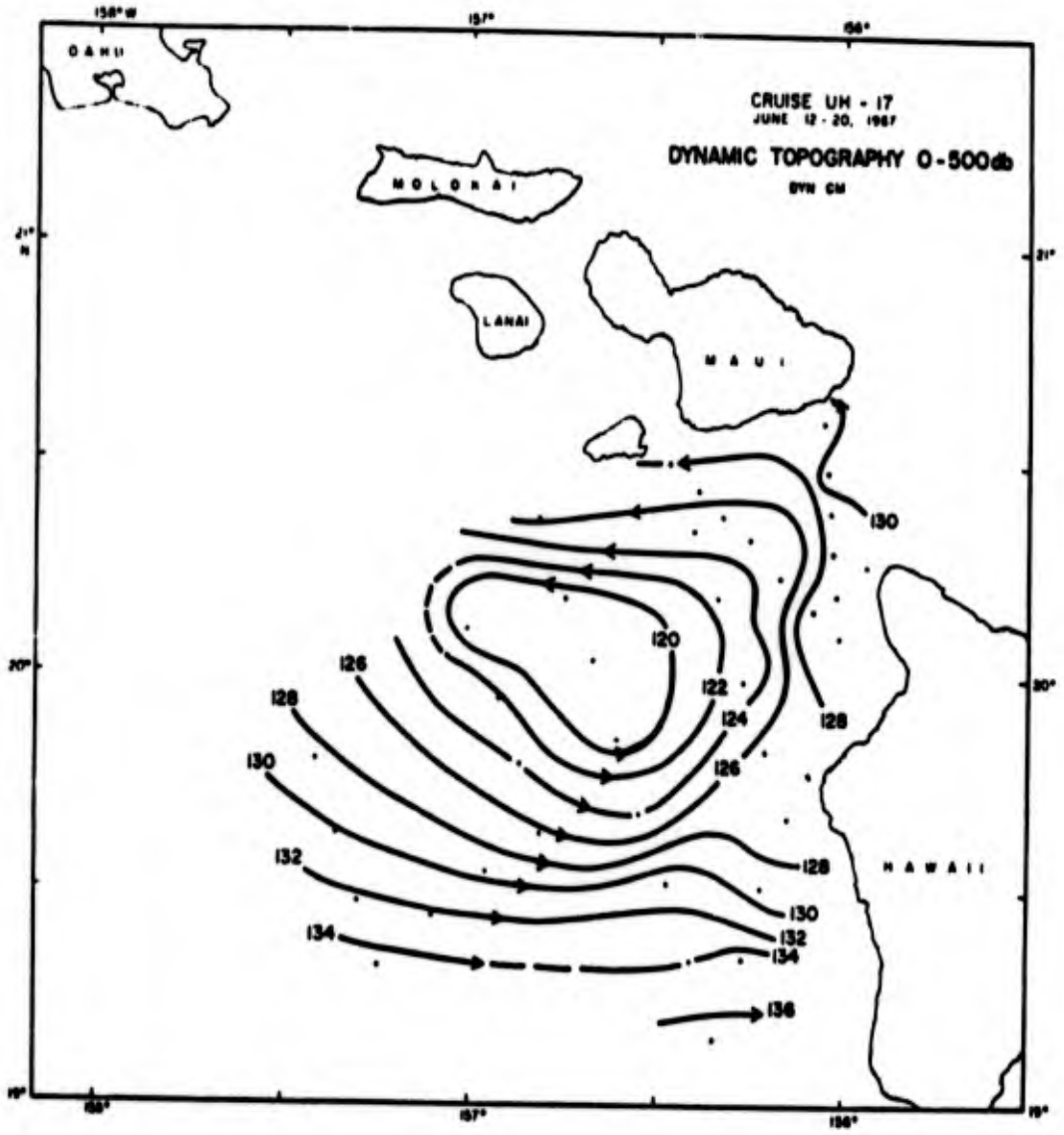

Figure 44. Dynamic topography 0/500 db from Cruise UH-17, June 12 - 20, 1967.

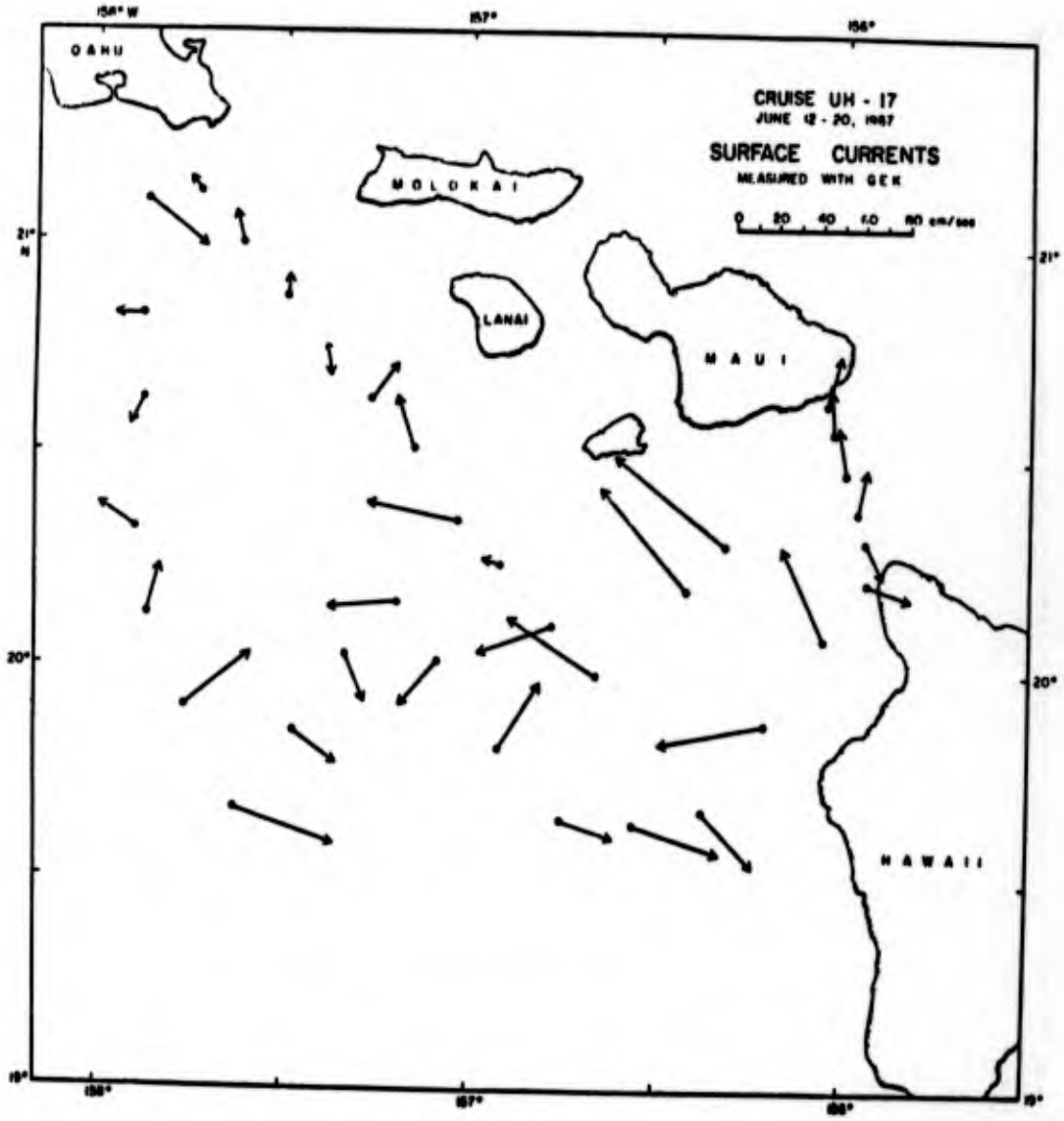

Figure 45. Surface currents as measured with GEK fixes from Cruise UH-17, June 12 - 20, 1967.

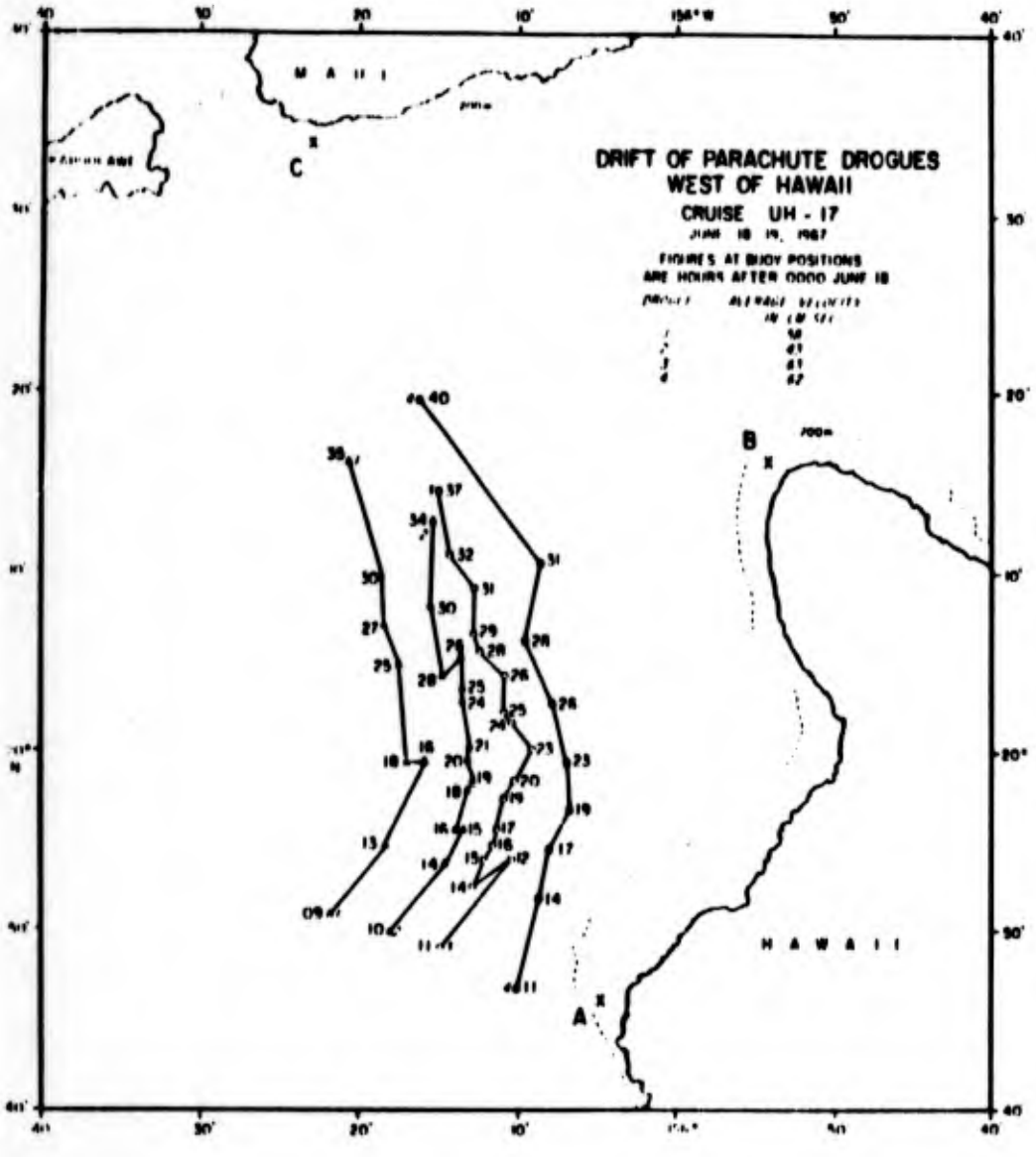

Figure 46. Drift of parachute drogues west of Hawaii from Cruise UH-17, June 18 - 19, 1967. Figures at buoy positions are hours after 0000, June 18. The average velocities of drogues 1 - 4 are listed. The depth of the drogues was 10 meters. Also shown are the locations of the moored current meters.

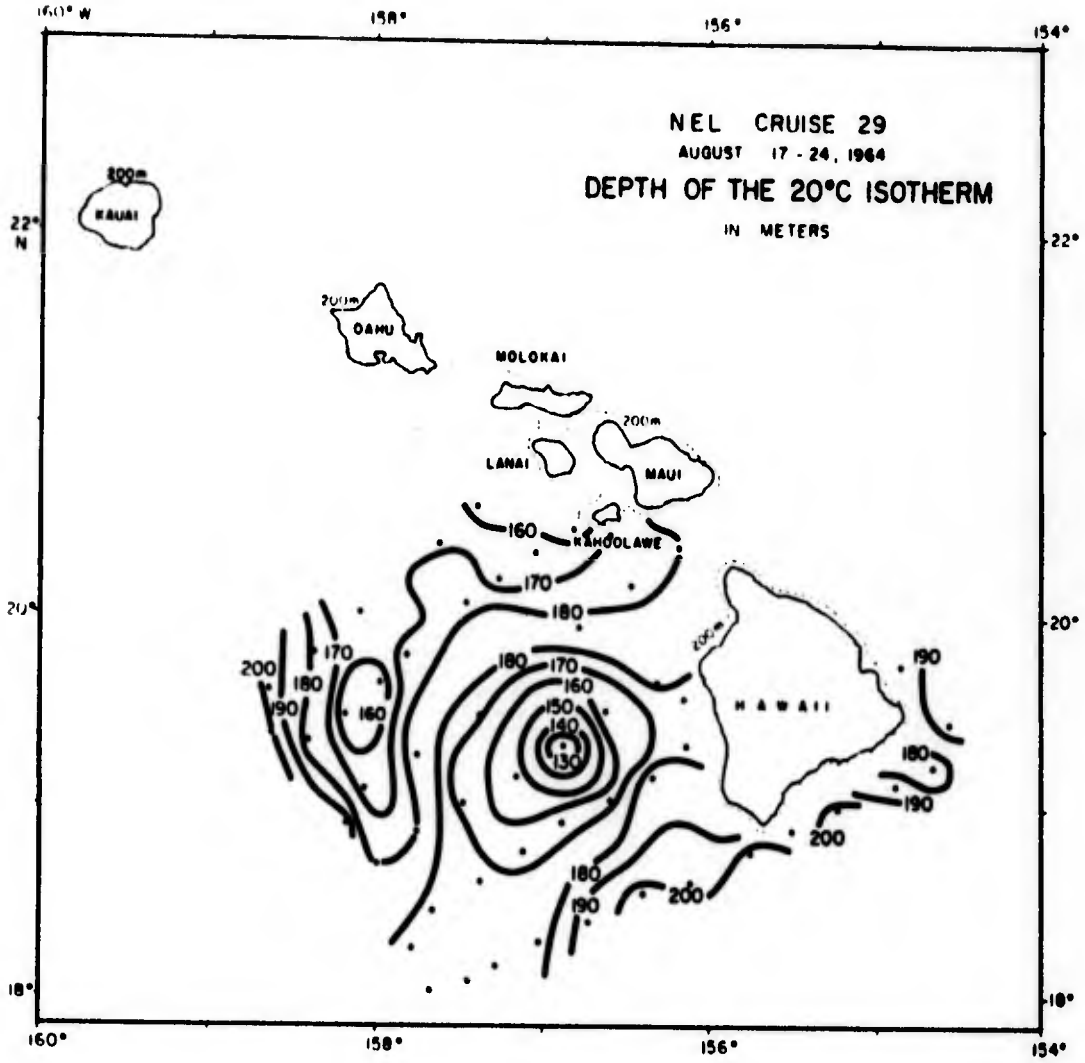

Figure 47. The depth of the 20°C isotherm from U.S.S. MARYSVILLE Cruise 29, August 17 - 24, 1964.

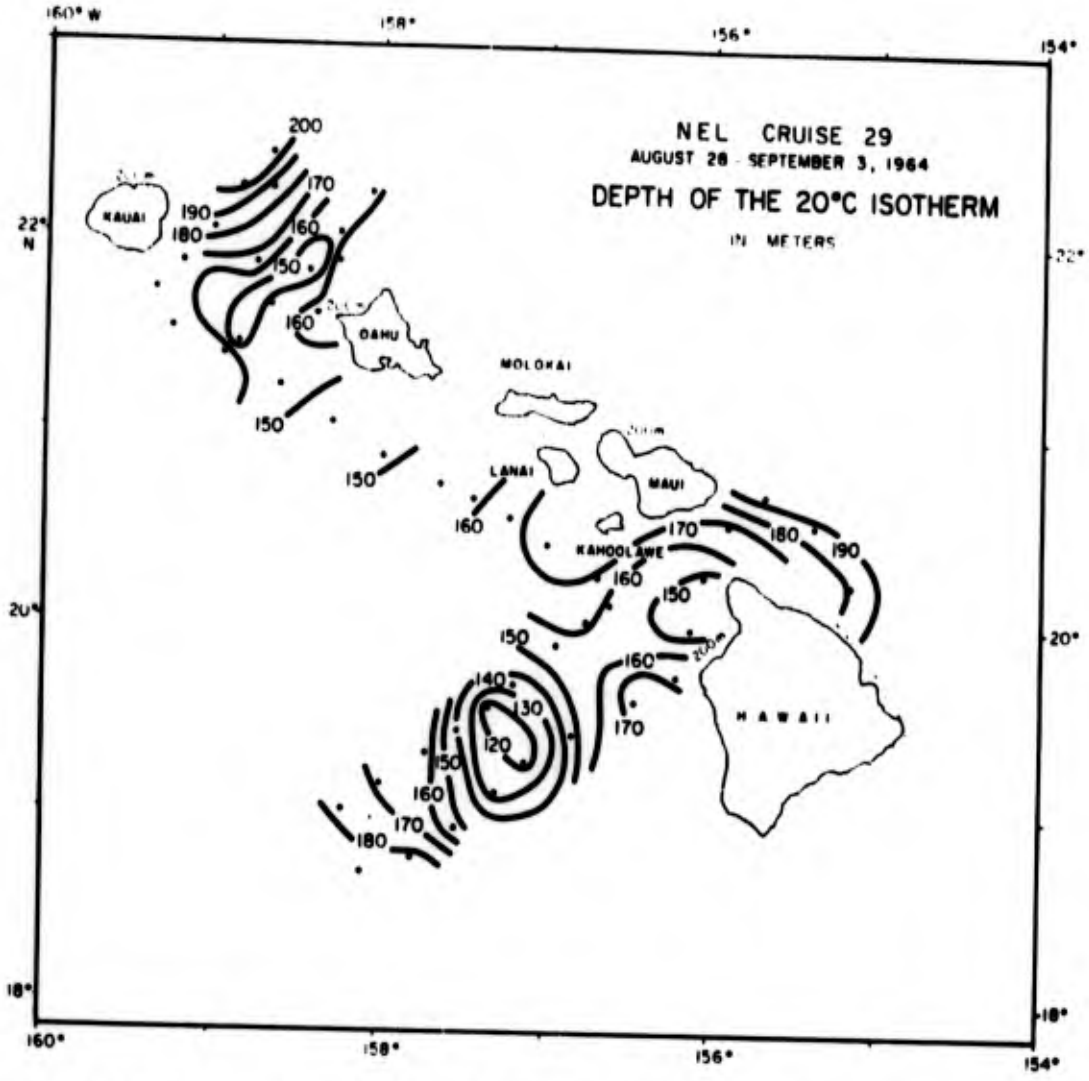

Figure 48. The depth of the 20°C isotherm from U.S.S. MARYSVILLE Cruise 29, August 28 - September 3, 1964.

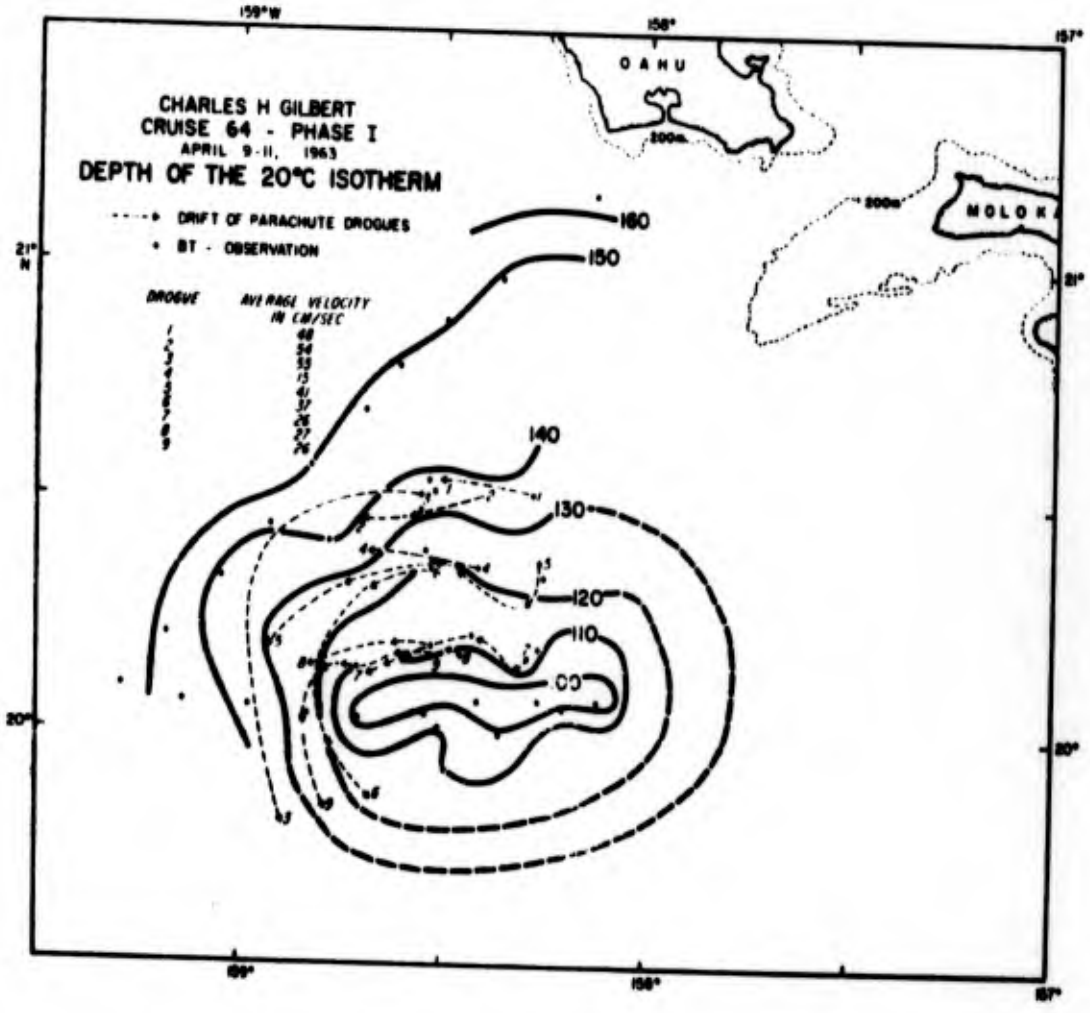

Figure 49. Depth of the 20°C isotherm (m) and drift of parachute drogues from CHARLES H. GILBERT Cruise 64, Phase I, April 9 - 11, 1963. The average velocities of drogues 1 - 9 are listed. The depth of the drogues was 15 meters.

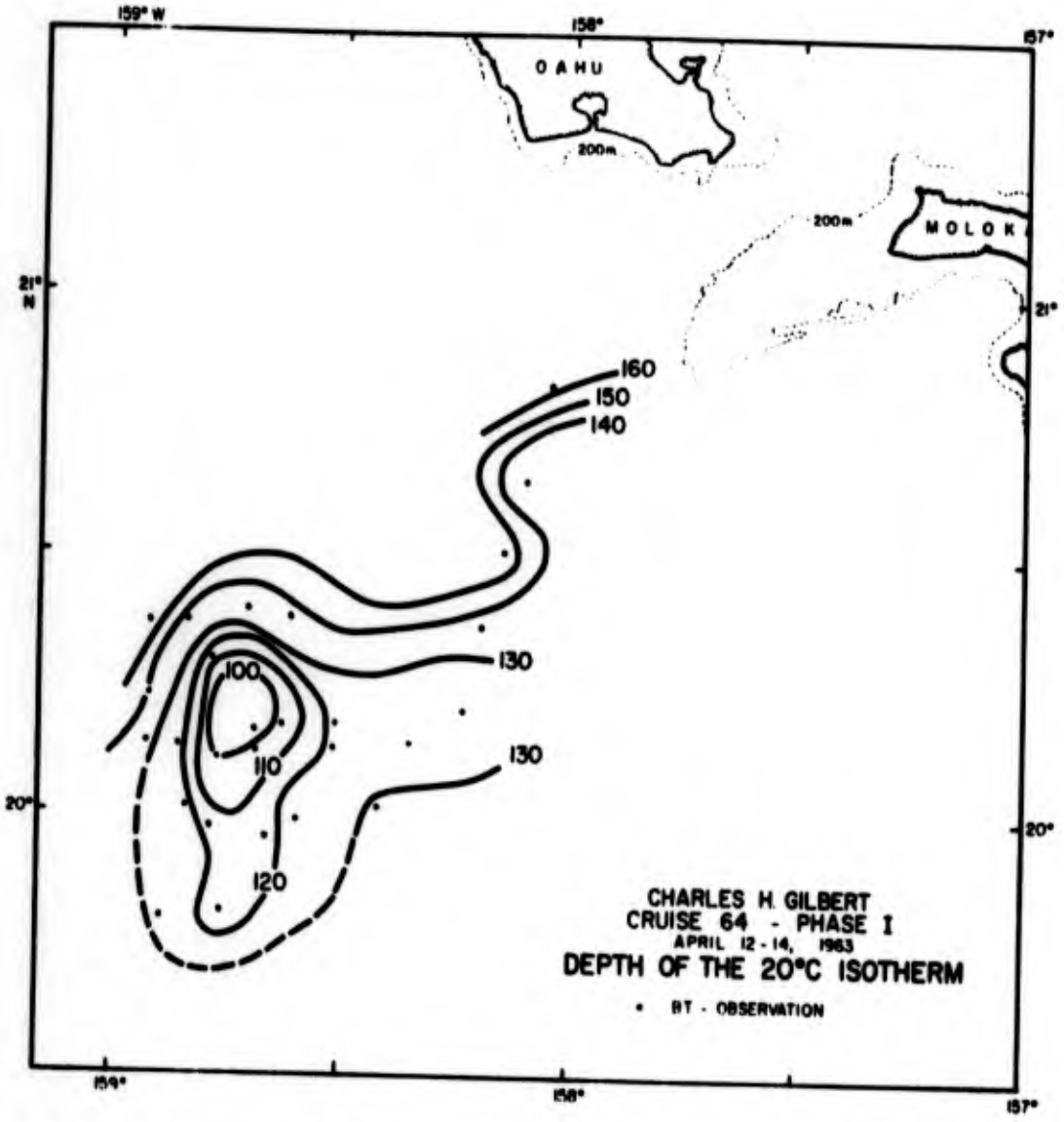

Figure 50. The depth of the 20°C isotherm (m) from CHARLES H. GILBERT Cruise 64, Phase I, April 12 - 14, 1963.

Figure 51. The depth of the 20°C isotherm (m) from CHARLES H. GILBERT Cruise 64, Phase II, April 24 - 29, 1963.

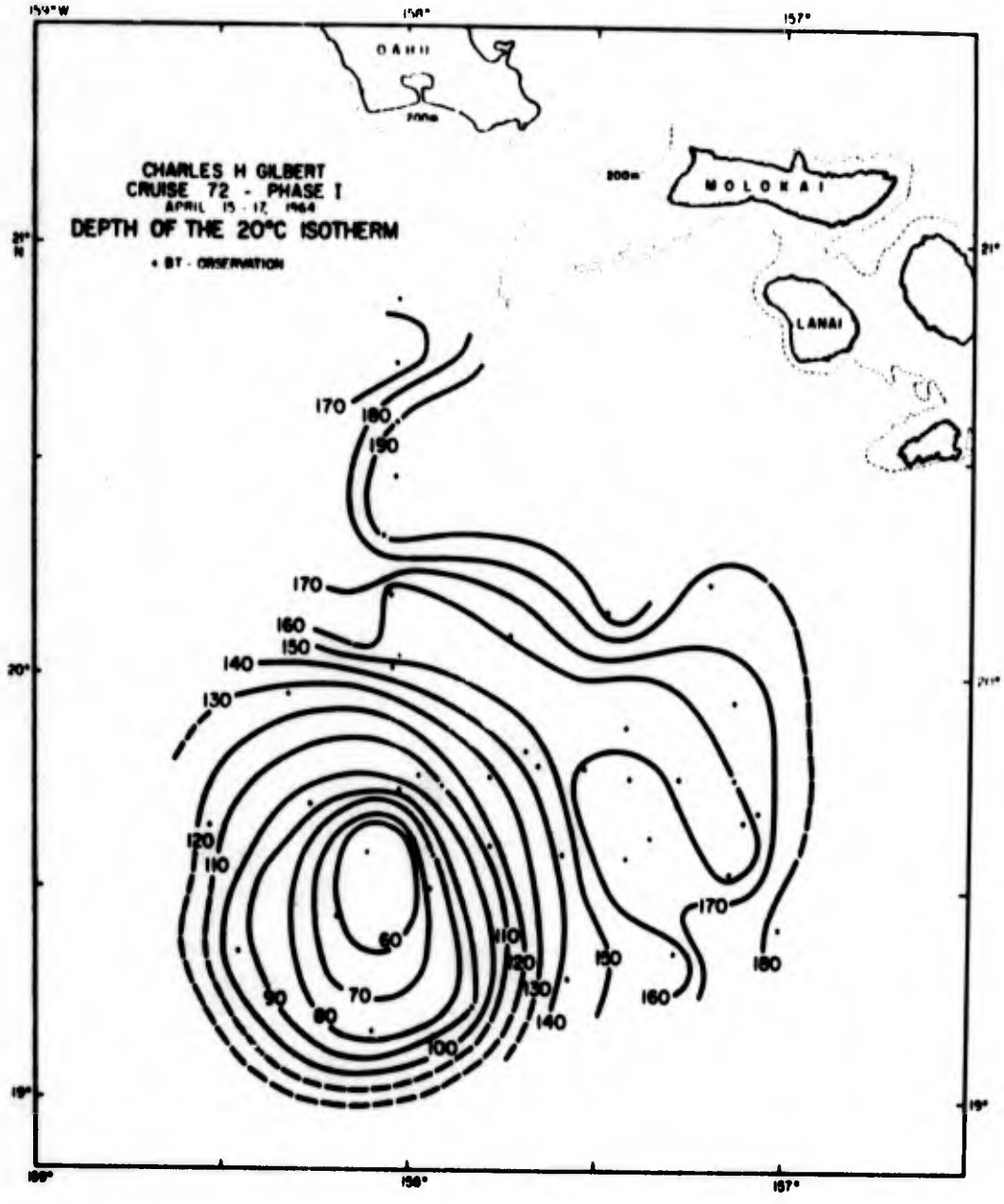

Figure 52. The depth of the 20°C isotherm (m) from CHARLES H. GILBERT Cruise 72, Phase I, April 15 - 17, 1964.

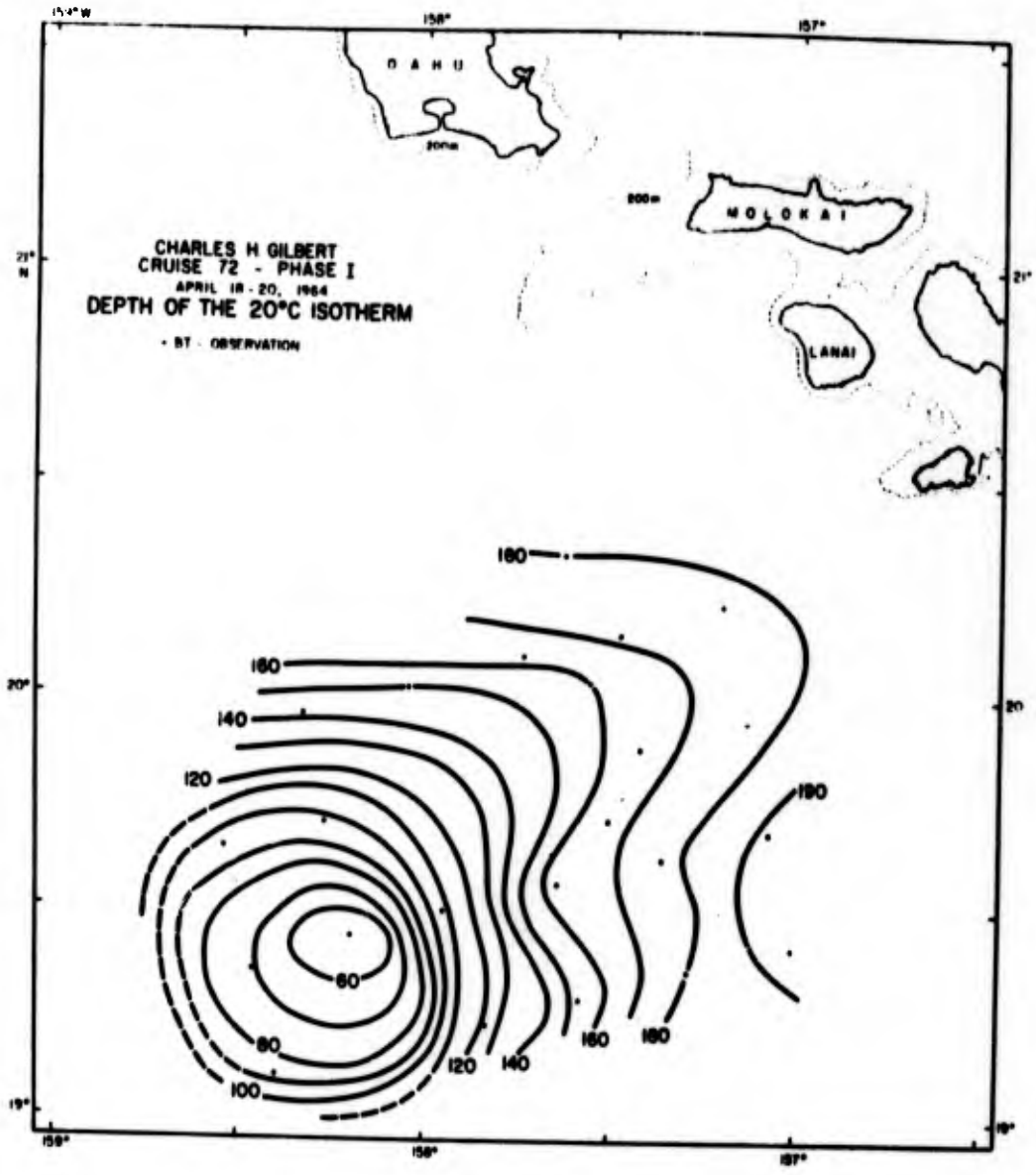

Figure 53. The depth of the 20°C isotherm (m) from CHARLES H. GILBERT Cruise 72, Phase I, April 18 - 20, 1964.

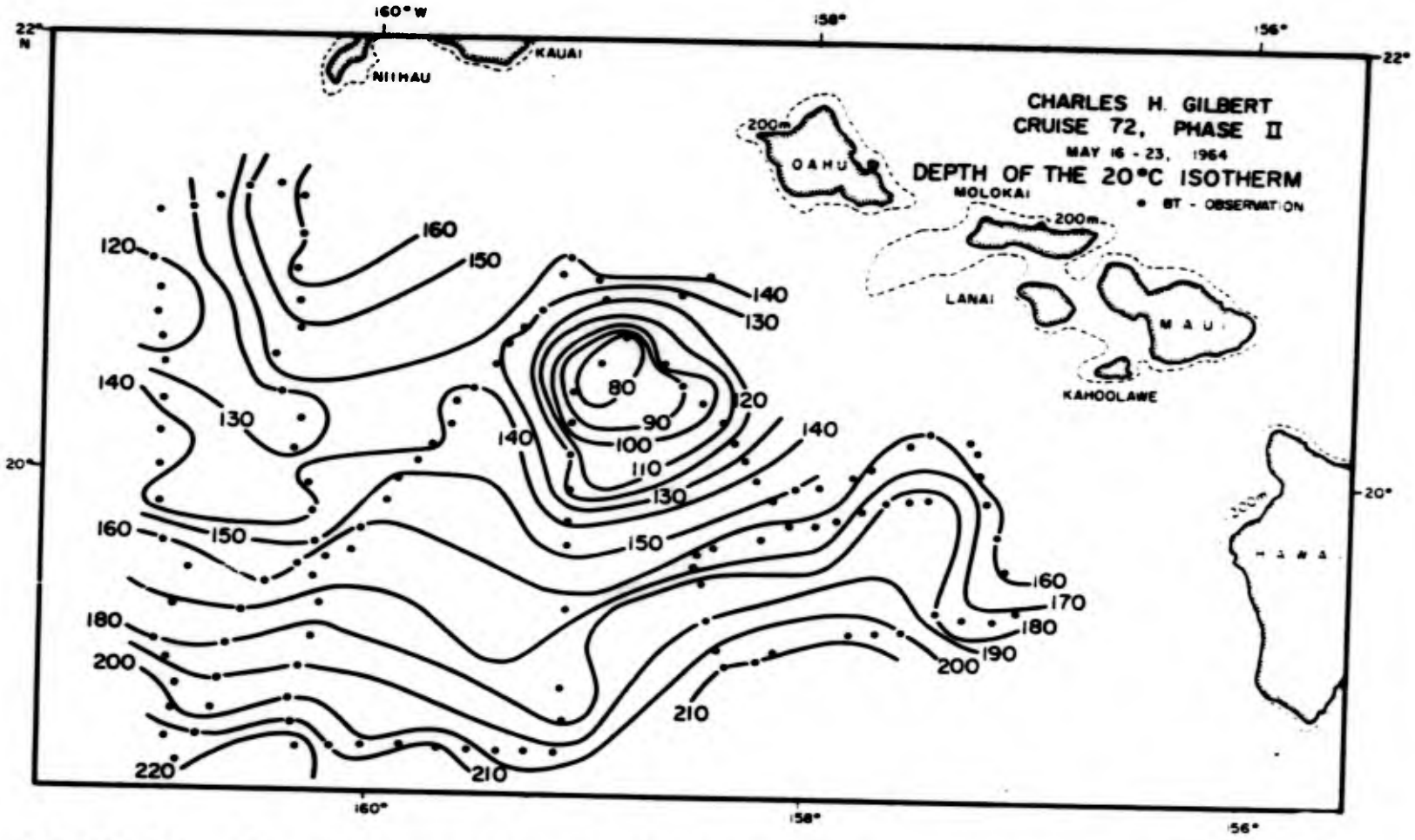

Figure 54. The depth of the 20°C isotherm (m) from CHARLES H. GILBERT Cruise 72, Phase II, May 16 - 23, 1964.

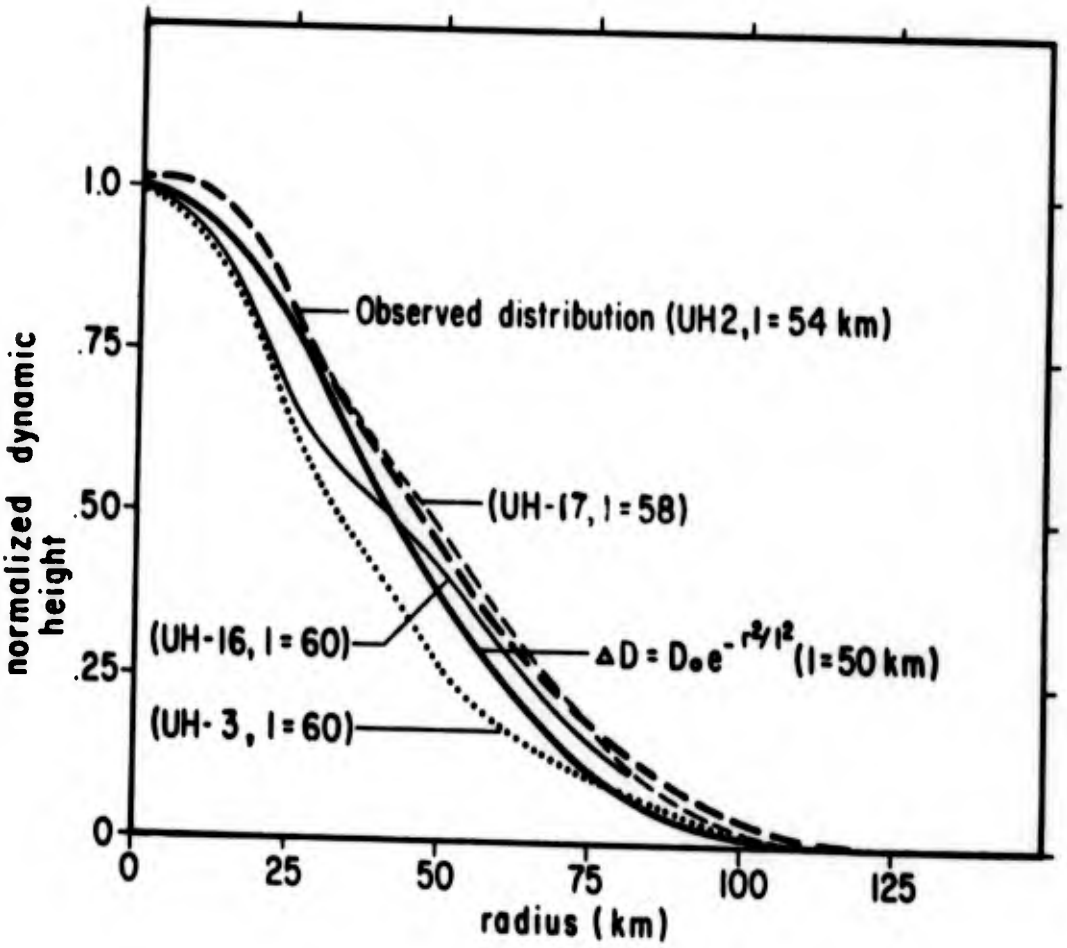

Figure 55. Observed normalized dynamic height for cyclonic eddies surveyed during Cruises UH-2, 3, 16, and 17 plotted as a function of eddy radius. Also shown is the assumed Gaussian distribution ($\Delta D = Doe^{-r^2/\ell^2}$).

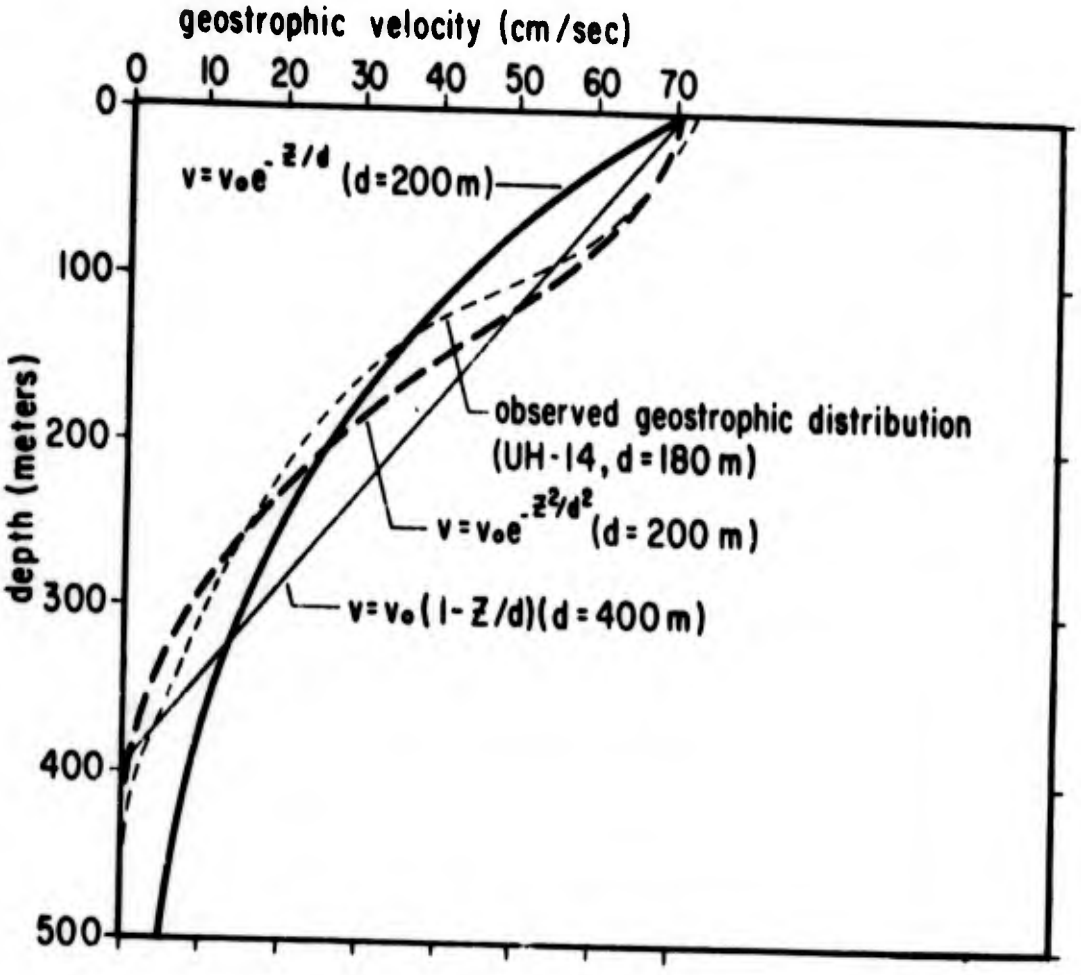

Figure 56. Observed geostrophic velocity distribution with depth between stations 70 and 71, Cruise UH-14 compared with three assumed distributions: linear, exponential, and Gaussian.

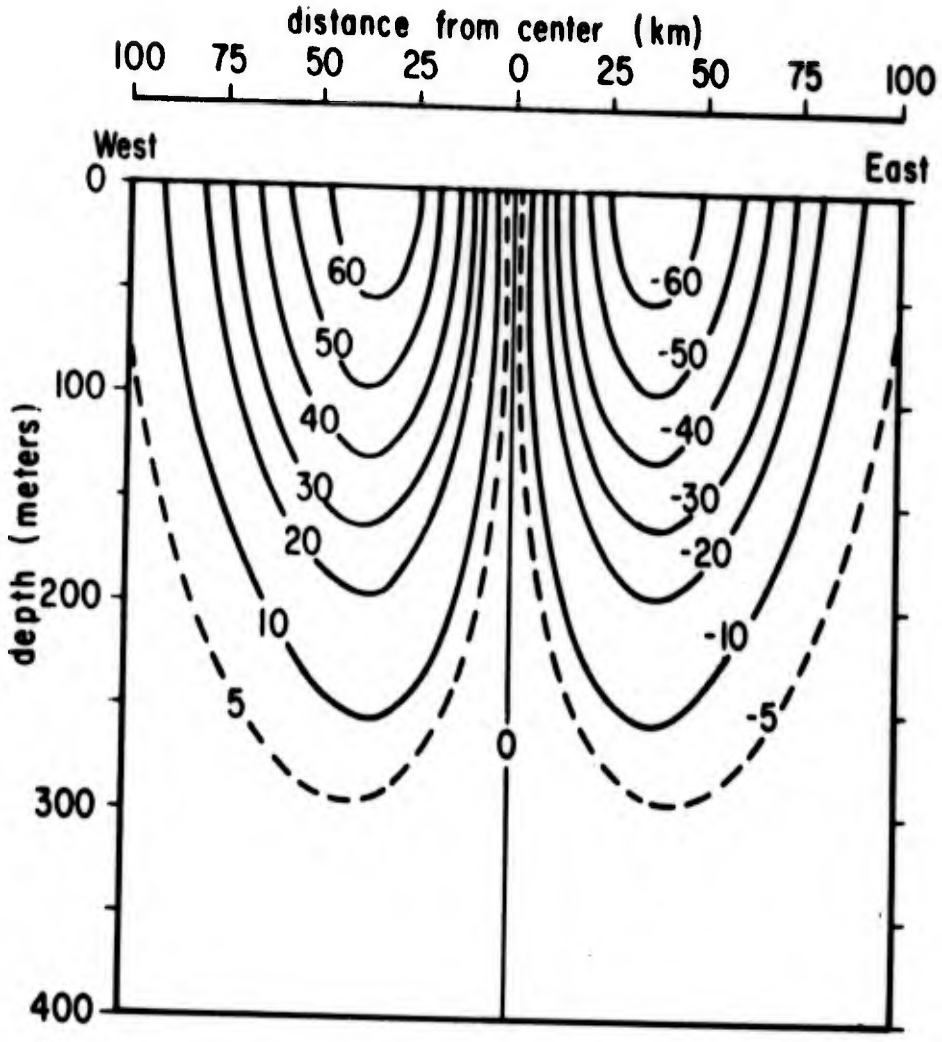

Figure 57. Plot of the geostrophic velocity distribution in cm/sec with depth and radius (distance from center). The parameters used to calculate the flow,

$$c = \frac{2\, g\Delta h\, r}{f\, \ell^2}\, e^{-r^2/\ell^2}\, e^{-z^2/d^2},$$

are Δh = 20 cm, $f = 5 \times 10^{-5}$ sec^{-1}, ℓ = 50 km, d = 175 m, and g = acceleration of gravity.

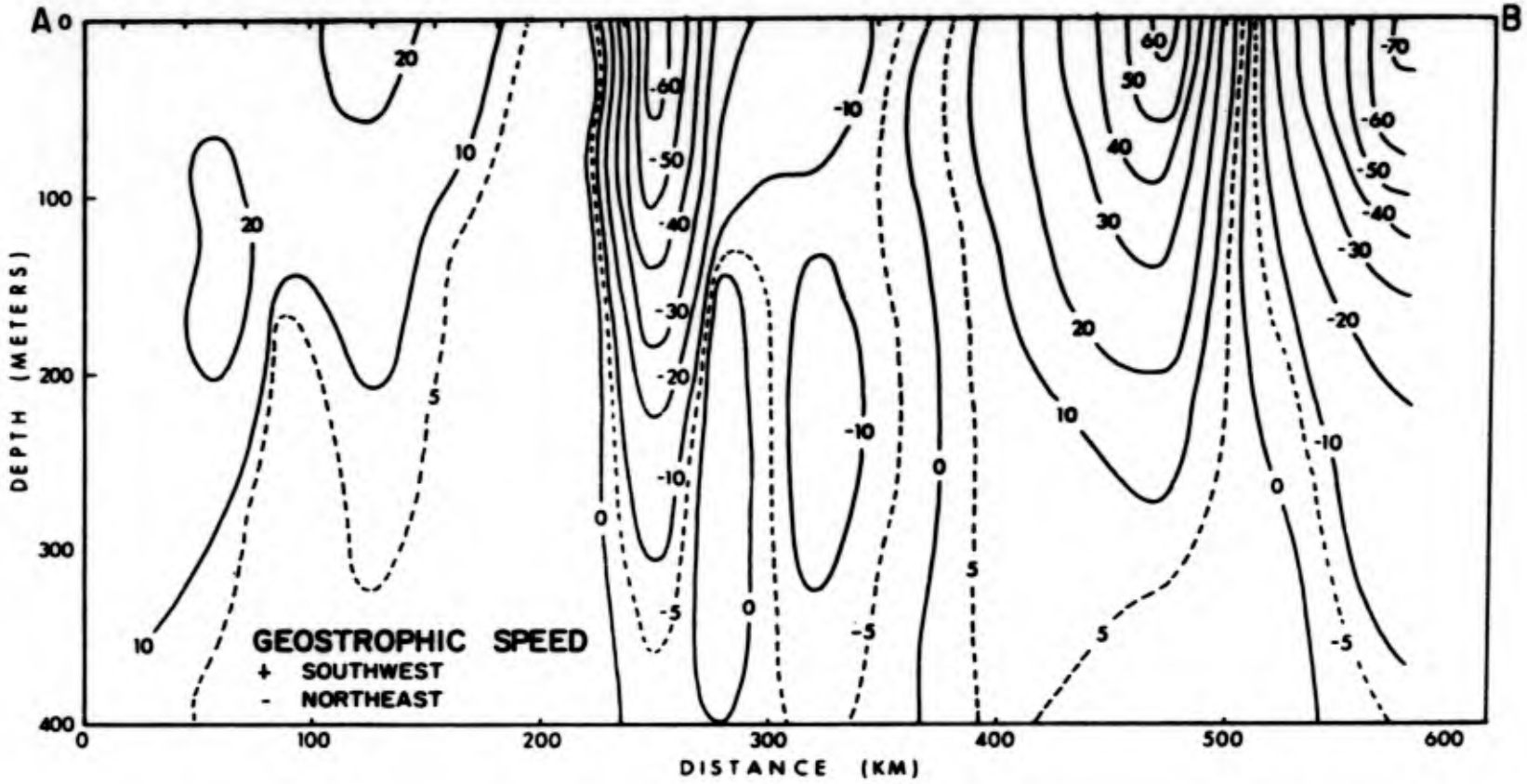

Figure 58. The geostrophic velocity distribution calculated from the observed mass distribution along the line AB (refer to Figure 59) from Cruise UH-14, July 26 - August 6, 1966. A cyclonic eddy is located on the right side of the section.

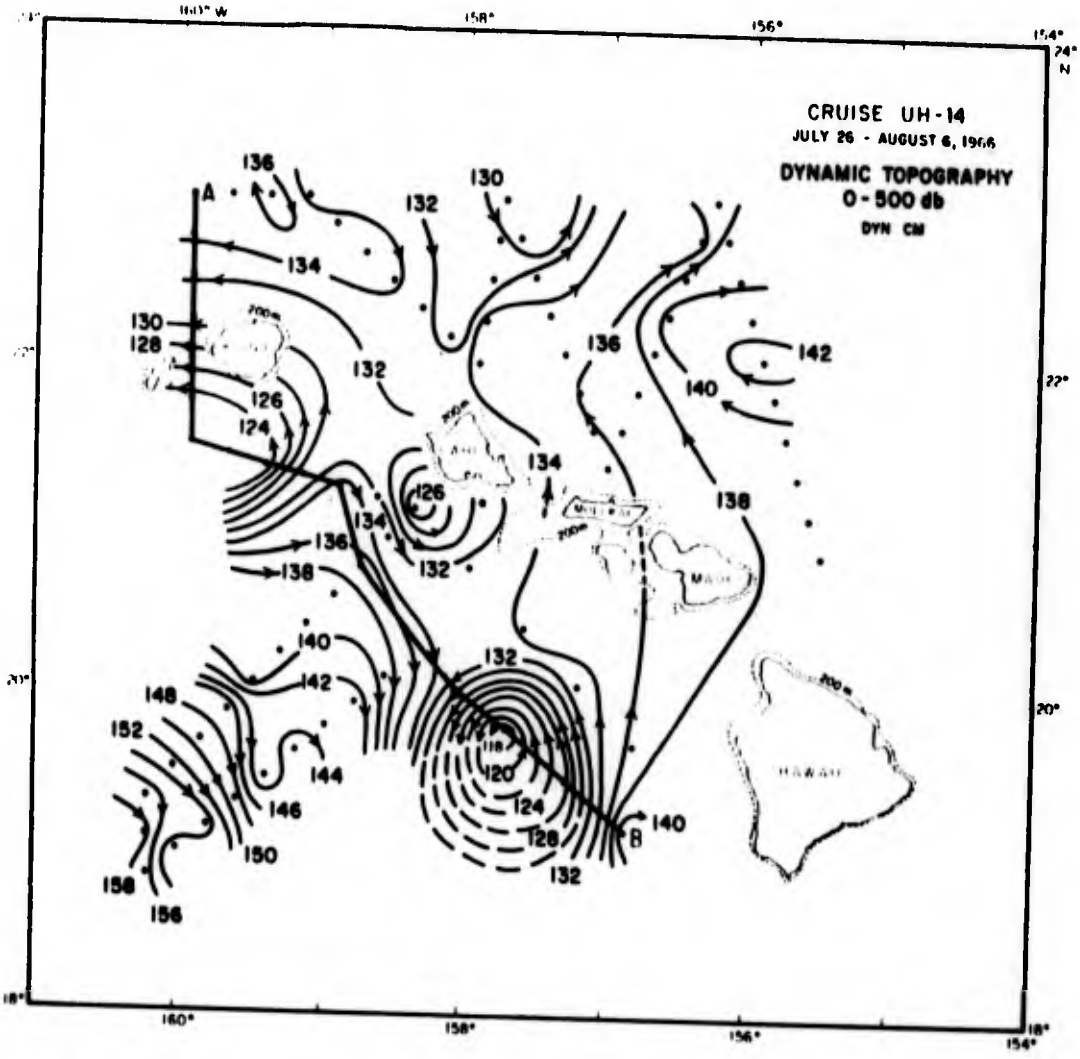

Figure 59. Dynamic topography 0/500 db from Cruise UH-14, July 26 - August 6, 1966. The line AB is referred to in Figure 58 which shows a section of the calculated geostrophic velocity.

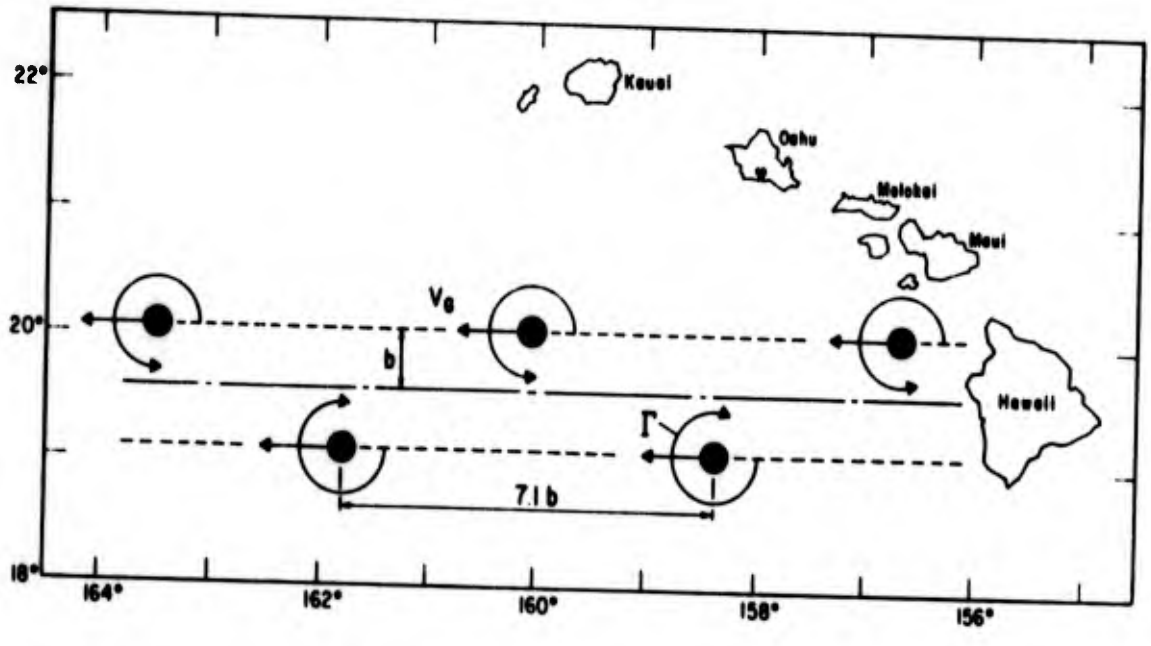

Figure 60. Characteristics of the Karman vortex trail. V_g is the group velocity or the speed that the eddies move to the west. Γ is the circulation. The lateral spacing between cyclonic and anticyclonic eddies is 2b. The longitudinal spacing between eddies of the same type is 7.1b.

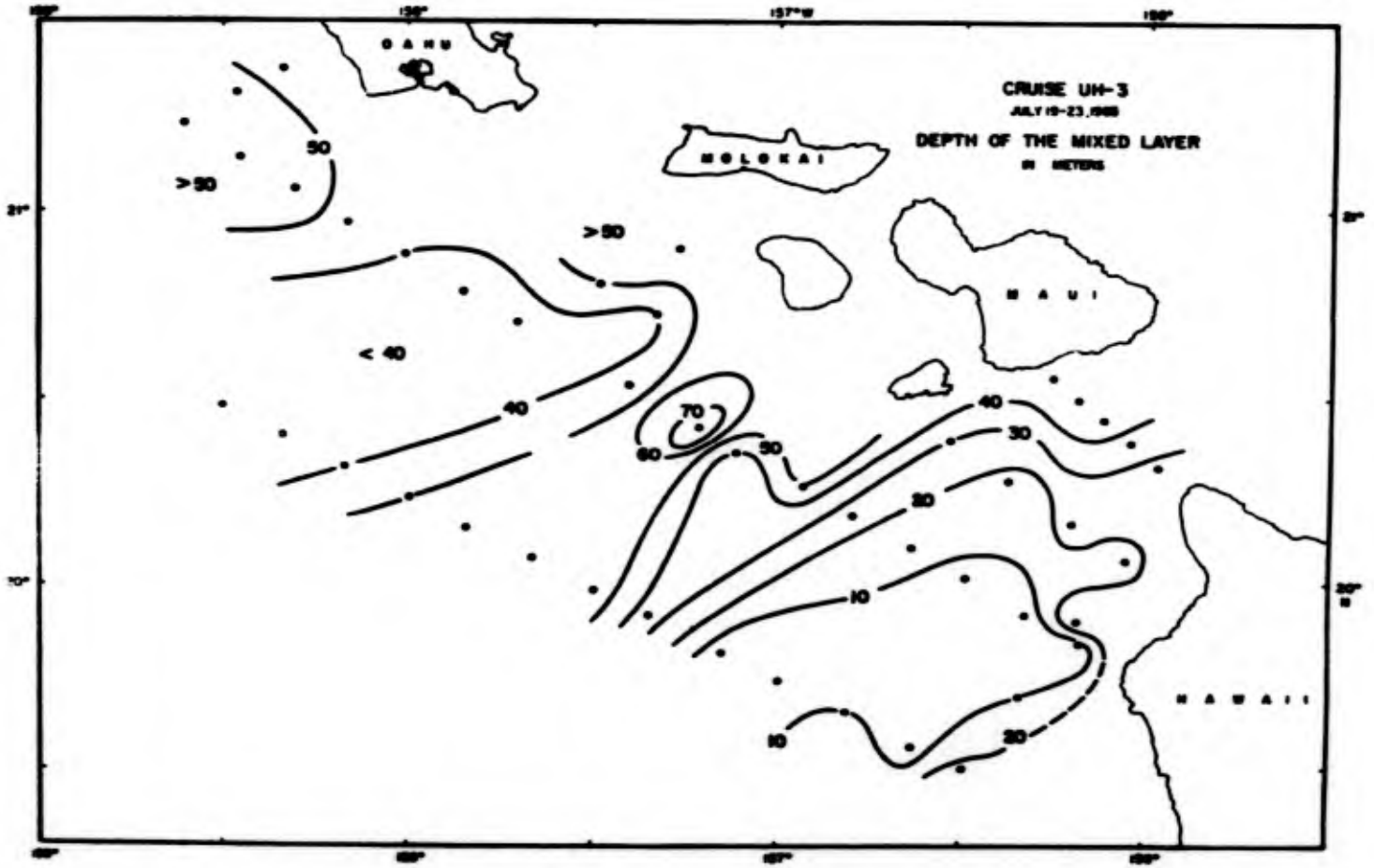

Figure 61. Depth of the mixed layer from Cruise UH-3, July 19 - 23, 1965.

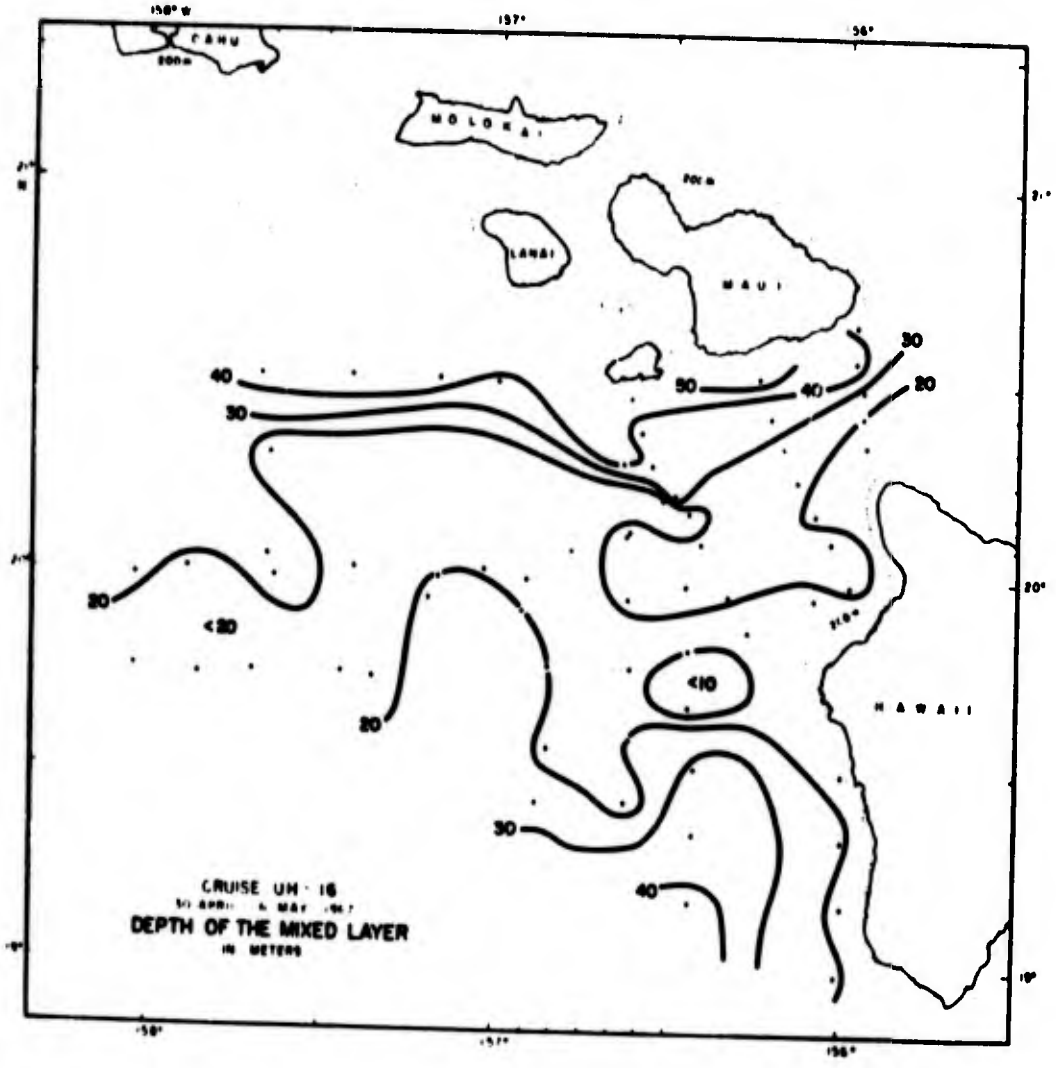

Figure 62. Depth of the mixed layer from Cruise UH-16, April 30 - May 6, 1967.

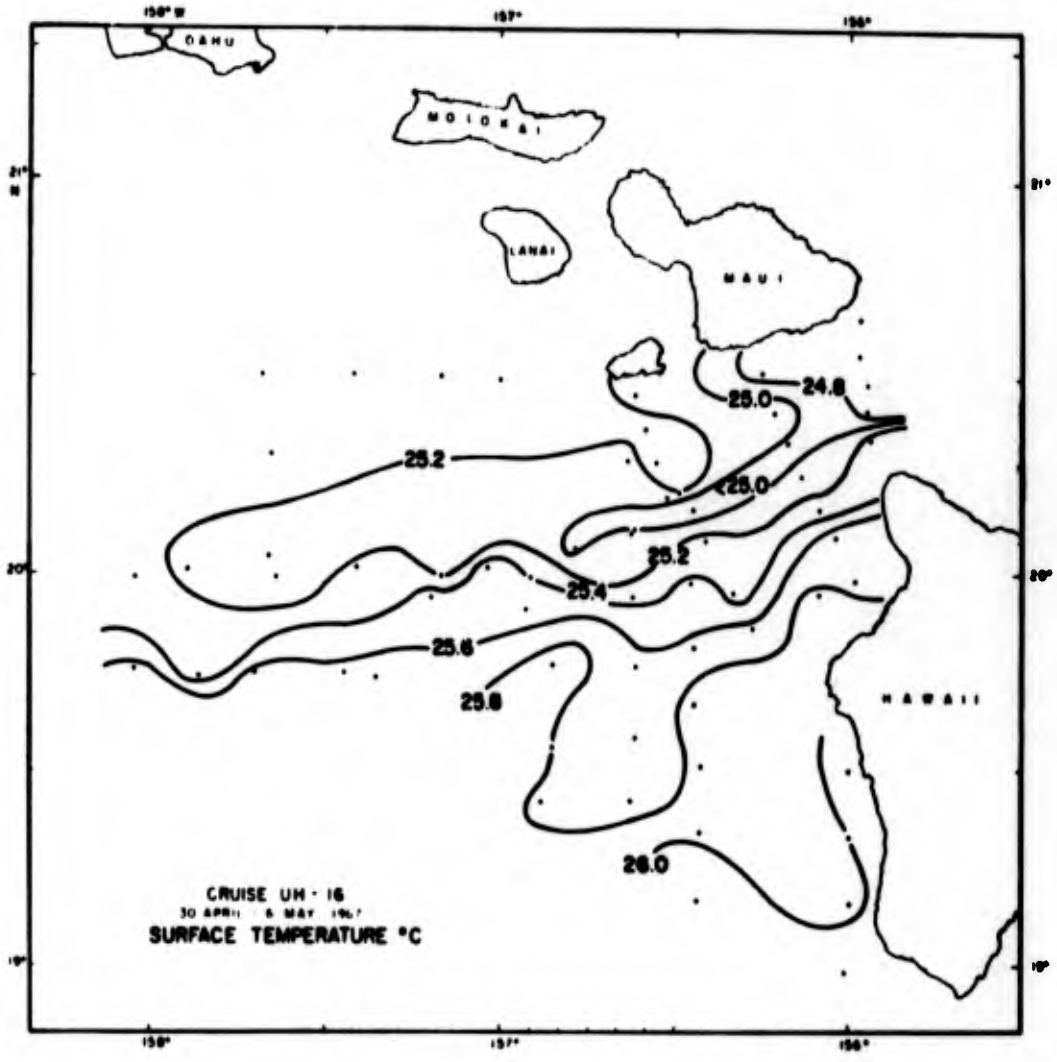

Figure 63. Surface temperature from Cruise UH-16, April 30 - May 6, 1967.

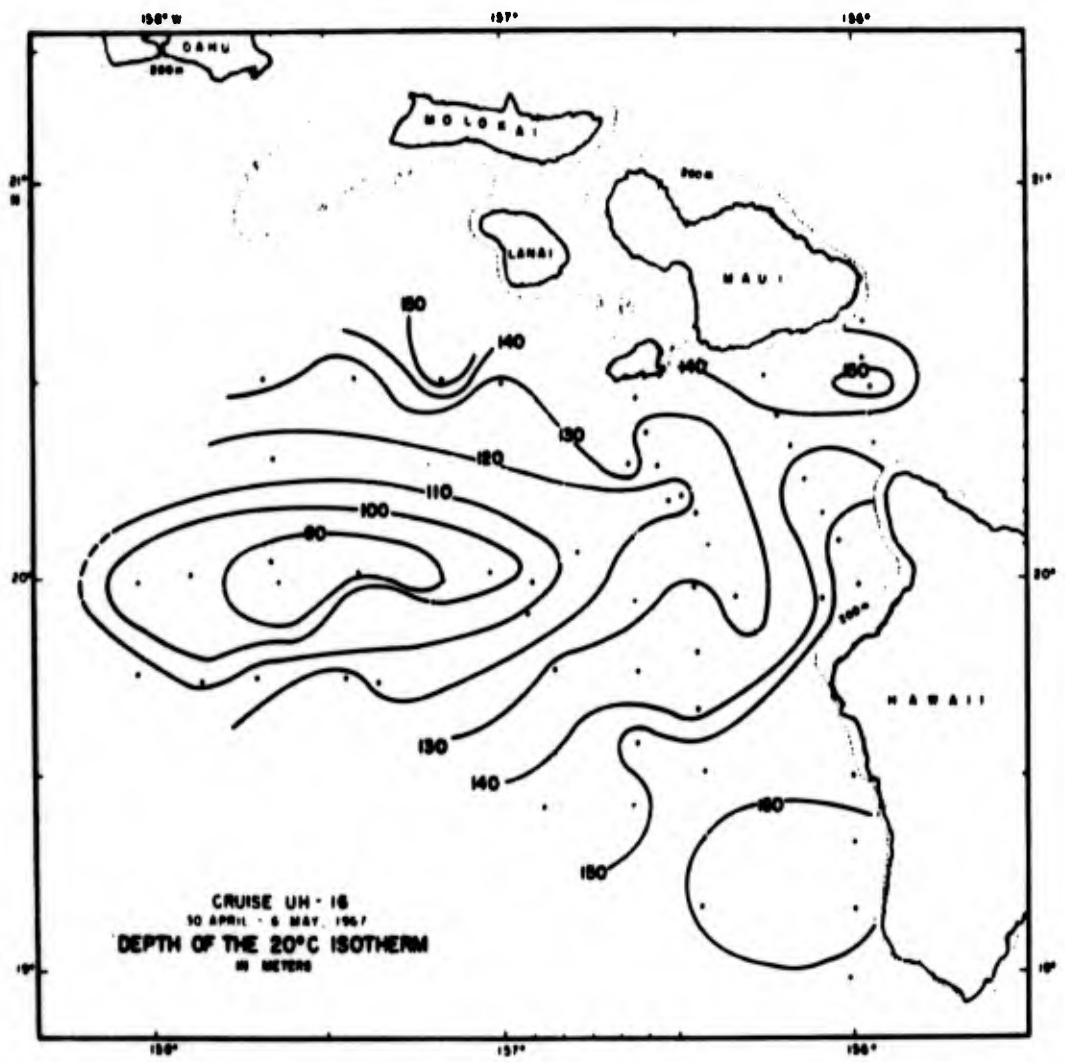

Figure 64. Depth of the 20°C isotherm from Cruise UH-16, April 30 - May 6, 1967.

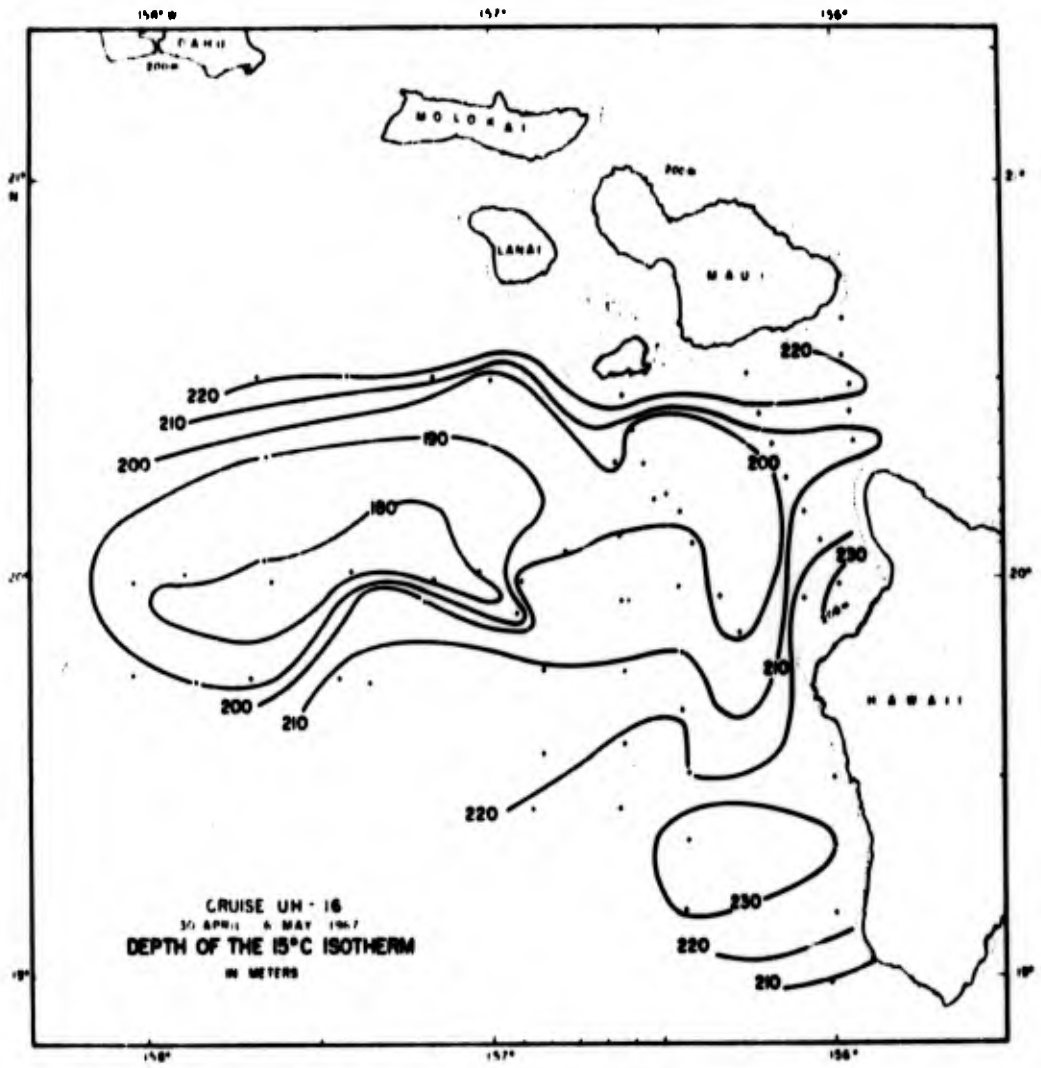

Figure 65. Depth of the 15°C isotherm from Cruise UH-16, April 30 - May 6, 1967.

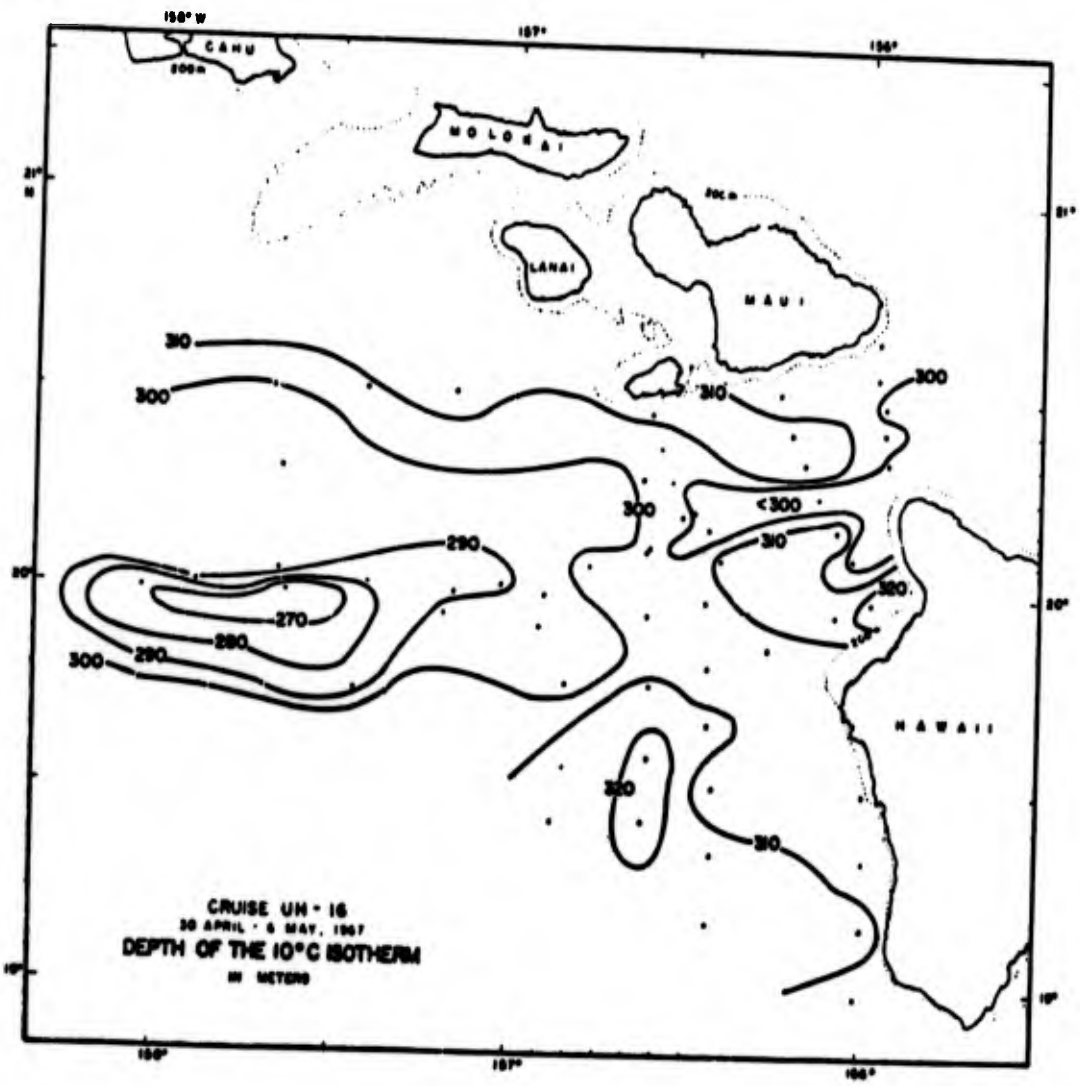

Figure 66. Depth of the 10°C isotherm from Cruise UH-16, April 30 - May 6, 1967.

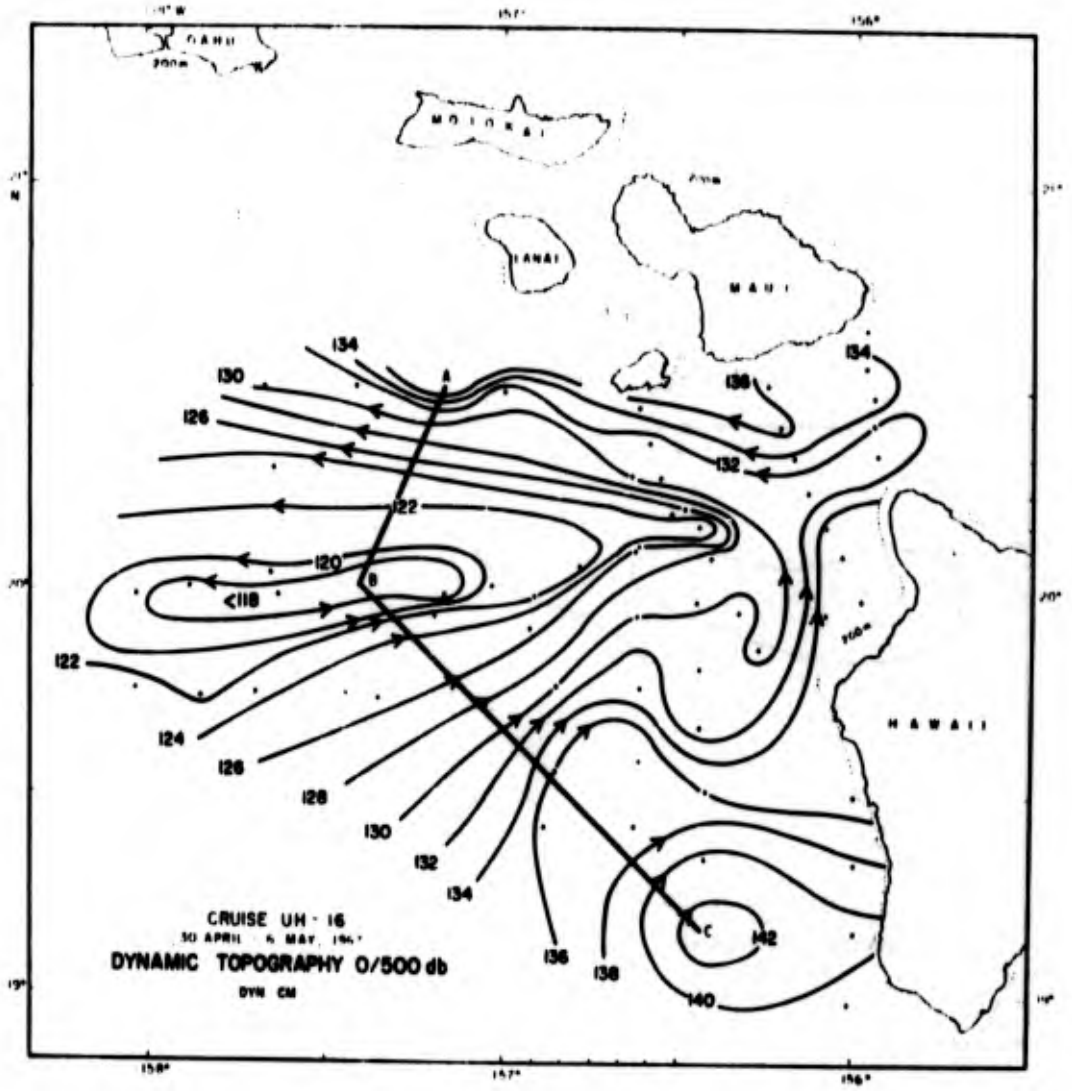

Figure 67. Dynamic topography 0/500 db from Cruise UH-16, April 30 - May 6, 1967.

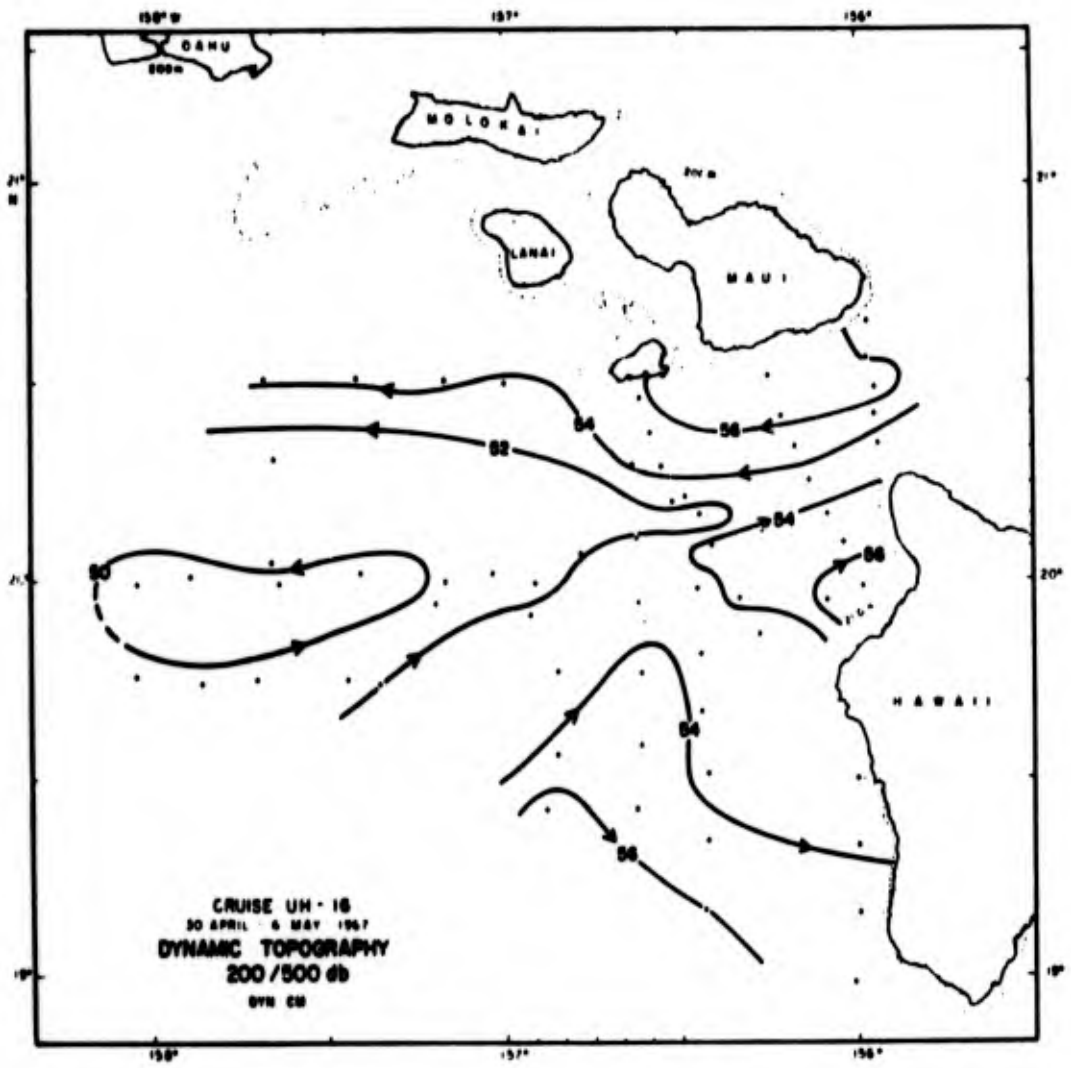

Figure 68. Dynamic topography 200/500 db from Cruise UH-16, April 30 - May 6, 1967.

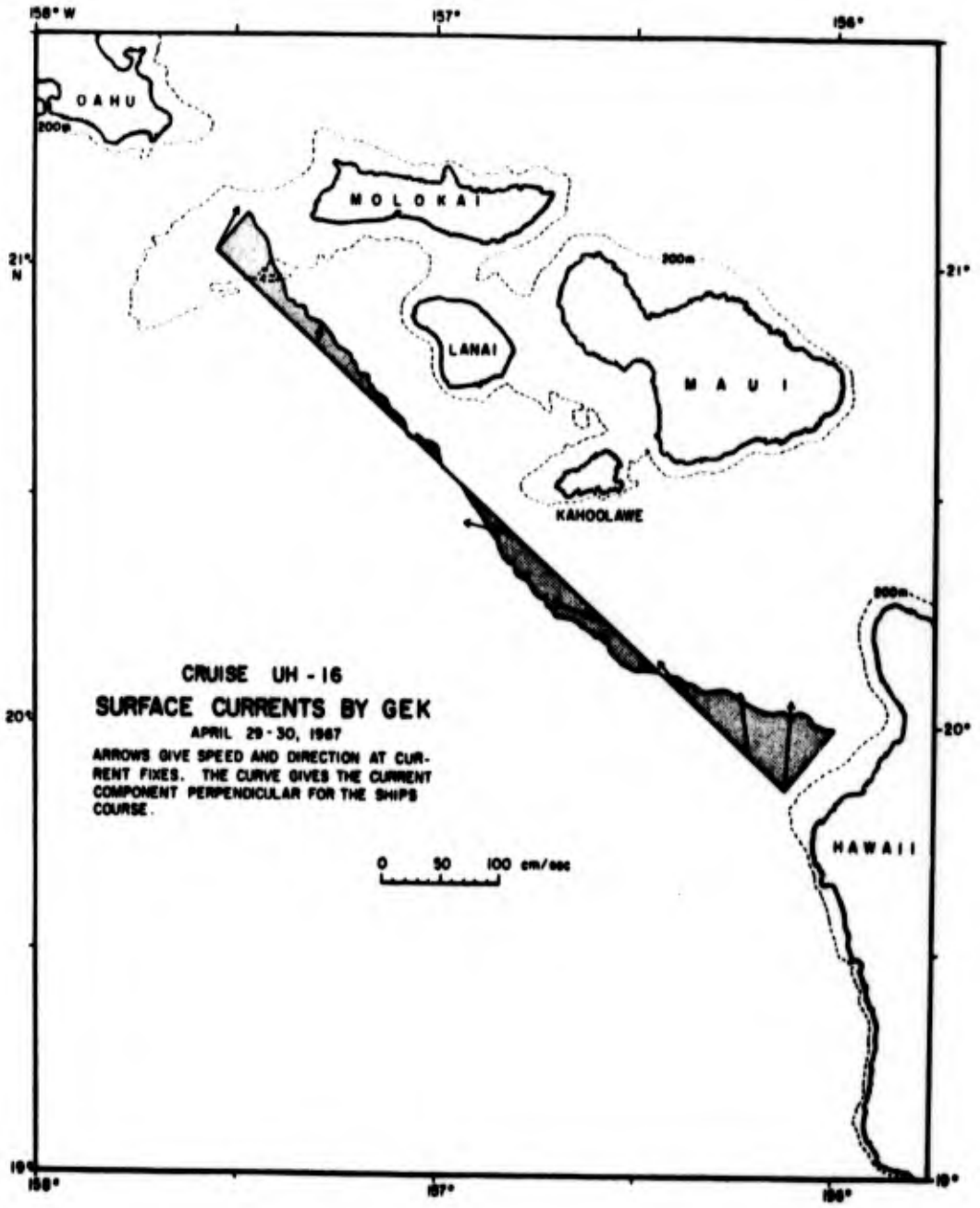

Figure 69. Surface currents as measured with GEK fixes from Cruise UH-16, April 29 - 30, 1967. Arrows give speed and direction at current fixes. The curve gives the current component perpendicular for the ship's course.

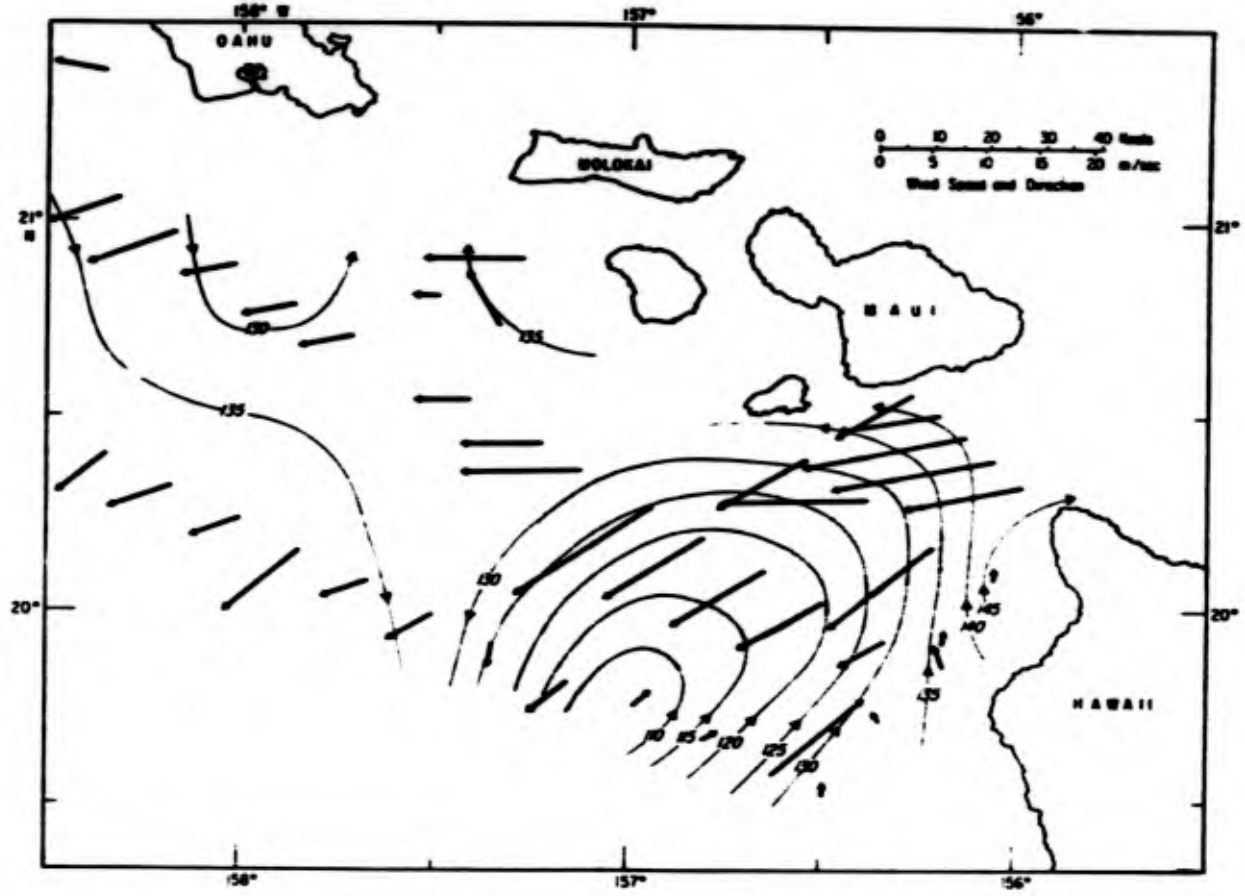

Figure 70. Wind speed and direction plotted with dynamic topography 0/500 db (dyn cm) from Cruise UH-3, July 19 - 23, 1965. The shaded region is the area where the wind stress is considered to add energy to the ocean eddy in equation 24.

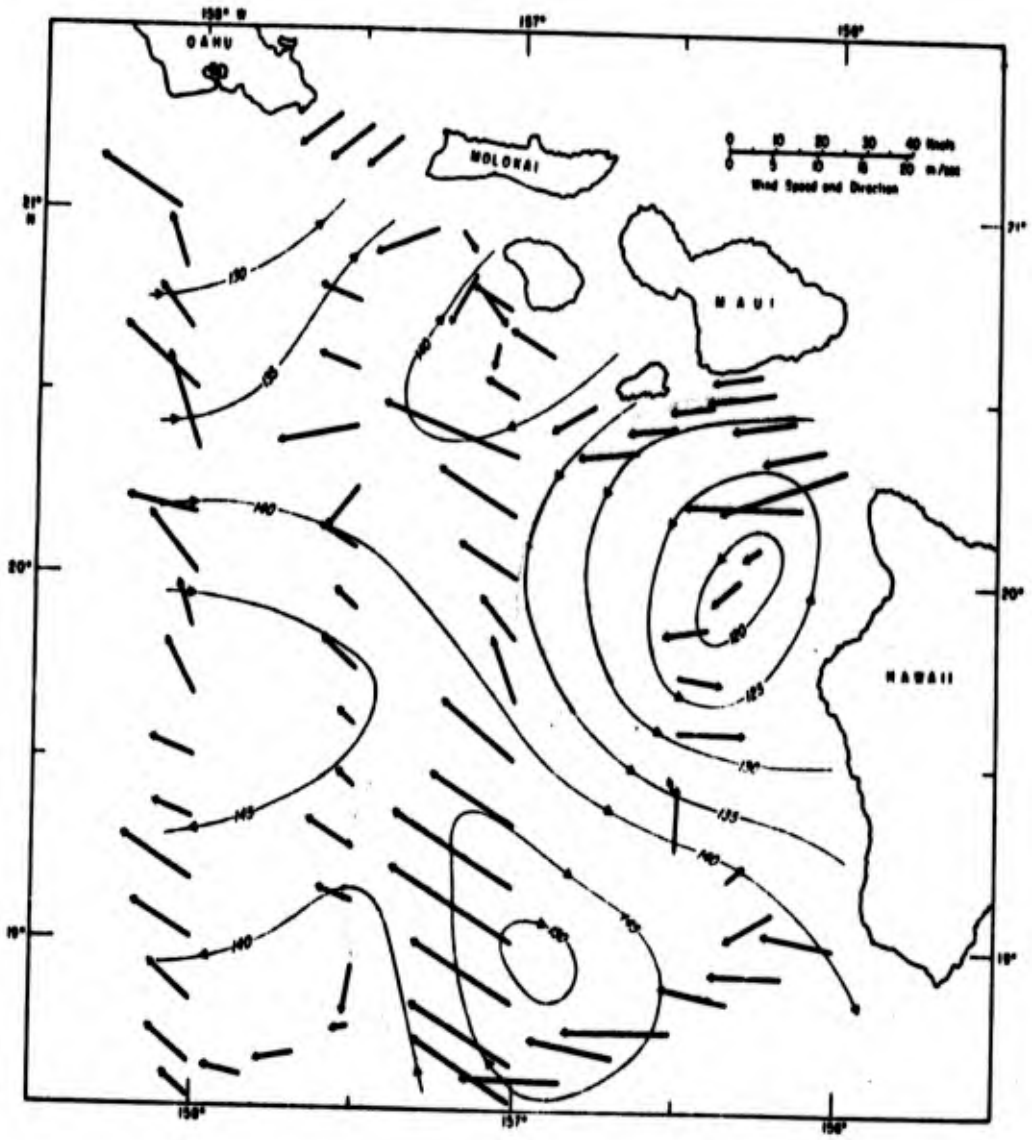

Figure 71. Wind speed and direction plotted with dynamic topography 0/500 db (dyn cm) from Cruise UH-2, May 18 - 24, 1965. The shaded region is the area where the wind stress is considered to add energy to the ocean eddy in equation 24.

Unclassified

Security Classification

DOCUMENT CONTROL DATA · R&D

(Security classification of title, body of abstract and indexing annotation must be entered when the overall report is classified)

1 ORIGINATING ACTIVITY (Corporate author)

Hawaii Institute of Geophysics
University of Hawaii
Honolulu, Hawaii 96822

2a REPORT SECURITY CLASSIFICATION

Unclassified

2b GROUP

3 REPORT TITLE

Eddies in Hawaiian Waters

4 DESCRIPTIVE NOTES (Type of report and inclusive dates)

5 AUTHOR(S) (Last name, first name, initial)

Patzert, William C.

6 REPORT DATE	7a TOTAL NO OF PAGES	7b NO OF REFS
April 1969	51 pages, 71 figs.	31

8a CONTRACT OR GRANT NO

ONR Contract Nonr-3748(06)

b PROJECT NO

c

d

9a ORIGINATOR'S REPORT NUMBER(S)

HIG-69-8

9b OTHER REPORT NO(S) (Any other numbers that may be assigned this report)

None

10 AVAILABILITY/LIMITATION NOTICES

no limitation

11 SUPPLEMENTARY NOTES

none

12 SPONSORING MILITARY ACTIVITY

Office of Naval Research

13 ABSTRACT

Oceanographic observations near the Hawaiian Islands demonstrate that ocean circulation is extremely variable and is dominated by eddies with diameters ranging from 50 to 150 kilometers. The data from 20 cruises that describe these eddies have been analyzed. Most of the eddies are cyclonic, and have been observed during all seasons. Observations show that the flow in them is nearly geostrophic and volume transports can be as large as 8 million m^3/sec. Although surface flow around them can be in excess of 100 cm/sec, the eddies are relatively shallow in depth and most of the horizontal flow is concentrated in the upper 150 m, above the 20°C isothermal surface. Near the center of the cyclonic eddies, doming of isothermal layers and upwelling take place. The energies of the eddies have been calculated, using a simplified geostrophic model, and the total of individual eddy energies is found to vary from 1×10^{22} ergs for a weak eddy to 5×10^{22} ergs for an intense eddy.

Calculations show that the eddies are not generated by the large-scale flow through the Hawaiian Islands—in the sense of a Kármán vortex stream behind an obstacle. Energy calculations indicate rather that the eddies are driven by strong, local winds blowing through the restricted passage between the islands of Maui and Hawaii. The calculations show that the eddies have a formation time of between 2 and 6 weeks, a value consistent with observations.

DD FORM 1 JAN 64 1473

Unclassified

Security Classification

14 KEY WORDS	LINK A		LINK B		LINK C	
	ROLE	WT	ROLE	WT	ROLE	WT
North Pacific Ocean Hawaiian Islands Oceanographic observations Geostrophic eddies Ocean circulation						

INSTRUCTIONS

1. **ORIGINATING ACTIVITY:** Enter the name and address of the contractor, subcontractor, grantee, Department of Defense activity or other organization *(corporate author)* issuing the report.

2*a*. **REPORT SECURITY CLASSIFICATION:** Enter the overall security classification of the report. Indicate whether "Restricted Data" is included. Marking is to be in accordance with appropriate security regulations.

2*b*. **GROUP:** Automatic downgrading is specified in DoD Directive 5200.10 and Armed Forces Industrial Manual. Enter the group number. Also, when applicable, show that optional markings have been used for Group 3 and Group 4 as authorized.

3. **REPORT TITLE:** Enter the complete report title in all capital letters. Titles in all cases should be unclassified. If a meaningful title cannot be selected without classification, show title classification in all capitals in parenthesis immediately following the title.

4. **DESCRIPTIVE NOTES:** If appropriate, enter the type of report, e.g., interim, progress, summary, annual, or final. Give the inclusive dates when a specific reporting period is covered.

5. **AUTHOR(S):** Enter the name(s) of author(s) as shown on or in the report. Enter last name, first name, middle initial. If military, show rank and branch of service. The name of the principal author is an absolute minimum requirement.

6. **REPORT DATE:** Enter the date of the report as day, month, year; or month, year. If more than one date appears on the report, use date of publication.

7*a*. **TOTAL NUMBER OF PAGES:** The total page count should follow normal pagination procedures, i.e., enter the number of pages containing information.

7*b*. **NUMBER OF REFERENCES:** Enter the total number of references cited in the report.

8*a*. **CONTRACT OR GRANT NUMBER:** If appropriate, enter the applicable number of the contract or grant under which the report was written.

8*b*, 8*c*, & 8*d*. **PROJECT NUMBER:** Enter the appropriate military department identification, such as project number, subproject number, system numbers, task number, etc.

9*a*. **ORIGINATOR'S REPORT NUMBER(S):** Enter the official report number by which the document will be identified and controlled by the originating activity. This number must be unique to this report.

9*b*. **OTHER REPORT NUMBER(S):** If the report has been assigned any other report numbers *(either by the originator or by the sponsor)*, also enter this number(s).

10. **AVAILABILITY/LIMITATION NOTICES:** Enter any limitations on further dissemination of the report, other than those imposed by security classification, using standard statements such as:

(1) "Qualified requesters may obtain copies of this report from DDC."

(2) "Foreign announcement and dissemination of this report by DDC is not authorized."

(3) "U. S. Government agencies may obtain copies of this report directly from DDC. Other qualified DDC users shall request through

_____."

(4) "U. S. military agencies may obtain copies of this report directly from DDC. Other qualified users shall request through

_____."

(5) "All distribution of this report is controlled. Qualified DDC users shall request through

_____."

If the report has been furnished to the Office of Technical Services, Department of Commerce, for sale to the public, indicate this fact and enter the price, if known.

11. **SUPPLEMENTARY NOTES:** Use for additional explanatory notes.

12. **SPONSORING MILITARY ACTIVITY:** Enter the name of the departmental project office or laboratory sponsoring *(paying for)* the research and development. Include address.

13. **ABSTRACT:** Enter an abstract giving a brief and factual summary of the document indicative of the report, even though it may also appear elsewhere in the body of the technical report. If additional space is required, a continuation sheet shall be attached.

It is highly desirable that the abstract of classified reports be unclassified. Each paragraph of the abstract shall end with an indication of the military security classification of the information in the paragraph, represented as *(TS), (S), (C), or (U)*

There is no limitation on the length of the abstract. However, the suggested length is from 150 to 225 words.

14. **KEY WORDS:** Key words are technically meaningful terms or short phrases that characterize a report and may be used as index entries for cataloging the report. Key words must be selected so that no security classification is required. Identifiers, such as equipment model designation, trade name, military project code name, geographic location, may be used as key words but will be followed by an indication of technical context. The assignment of links, roles, and weights is optional.